

The Effect of Loading Conditions
on a Kennedy Class I Implant-Assisted
Removable Partial Denture

By

Reza Shahmiri

A thesis submitted for the degree of

Master of Dental Technology

University of Otago

Date: Tuesday, 1 Nov 2011

ABSTRACT

Objective: To evaluate the strain behaviour of the Kennedy Class I implant-assisted removable partial denture (IARPD) distal extension area under various loading conditions to better understand the strain pattern.

Method: A mandibular Kennedy Class I was selected with natural teeth from the 34 to 44. A duplicated model was made out of polyurethane and a conventional removable partial denture was fabricated with a cobalt chromium metal framework and acrylic base. Strain gauges were placed on the fitting side of the acrylic and metal framework to measure the strain in the partial denture structure. Two Straumann® implants were then placed in the second molar regions and the removable partial denture was modified to accommodate ball attachments. The model was loaded to 120N unilaterally and bilaterally, with three different loading areas; premolar, molar and uniform.

Results: In all loading conditions the maximum micro-strains were in a bucco-lingual direction. In all loading conditions tension micro-strains were most common, except on the metal surface in the unilateral loading condition, which showed mainly compression micro-strains.

Conclusions: This research highlights that lateral movement/displacement was evident during bilateral and unilateral loading of the IARPD. Molar bilateral loading showed favourable strain behaviour during bilateral loading conditions whereas uniform unilateral loading showed less destructive strain behaviour during the unilateral loading conditions.

ACKNOWLEDGMENTS

I would like to thank my primary supervisor, John Aarts, for his continuous support throughout my research. His help, guidance and invaluable assistance in writing never stopped despite his busy schedule. I would like to thank Dr. Vincent Bennani for his vital advice in terms of the clinical aspect of my research. I would like to extend the deepest debt of gratitude to Professor Michael Swain for his unlimited support and utmost motivation and encouragement during my entire research.

I would like to express my greatest appreciation to my family and friends for their unbelievable encouragement. My sincere gratitude goes to my parents and brother and sisters for their magnificent support throughout my Master study and research.

I would like to thank John Aarts for providing the funding for my research from his personal research fund. I would like to thank Peter Fleury for the strain gauge set up, the Department of Oral Rehabilitation for a travel grant to the IADR conference, Professor Jules Kieser for the testing equipment and Neil Waddell for his assistance.

Last, but not least, I would like to thank Ms. Gretchen Kivell, Head of Abbey College, Mr. John Seaton, Deputy Head of Abbey College, and Mrs. Suzanne Schofield receptionist of Abbey College and all Abbey College residents for providing the best environment, putting up with me and taking care of me.

TABLE OF CONTENTS

ABSTRACT	iv
ACKNOWLEDGMENTS.....	v
LIST OF FIGURES	ix
LIST OF TABLES	xiii
Chapter One	1
Introduction	1
Chapter Two	9
Literature review	9
Non-clinical studies	13
Chapter Three	17
Method and Materials	17
Method	17
Model fabrication	17
Strain gauges.....	19
Strain measurement	23
Implant placement into model	24
Loading of the prosthesis.....	26
Converting the data to micro-strain values.....	28
Materials	32
Implants	32
Model.....	32
Alloy	33
Attachments	34
Strain gauges.....	34

Silicone	35
Acrylic	35
Die stone.....	35
Refractory material.....	36
Chapter Four	37
Results	37
Bilateral loading conditions.....	38
Micro-strain measurements at the acrylic base.....	38
Bilateral uniform loading.....	38
Bilateral premolar loading.....	39
Bilateral molar loading	40
Micro-strain measurements at the metal framework.....	41
Bilateral uniform loading.....	41
Bilateral premolar loading.....	42
Bilateral molar loading	43
Unilateral loading conditions.....	44
Micro-strain measurements at the acrylic base.....	44
Unilateral uniform loading.....	44
Unilateral premolar loading.....	45
Unilateral molar loading.....	46
Micro-strain measurements at the metal framework.....	47
Unilateral uniform loading.....	47
Unilateral premolar loading.....	48
Unilateral molar loading.....	49

The differences in micro-strain values under different loading conditions.....	50
Micro-strain behaviour of acrylic base	
(bilateral loading conditions)	51
Micro-strain behaviour of metal framework	
(bilateral loading conditions)	54
Micro-strain behaviour of acrylic base	
(unilateral loading conditions)	56
Micro-strain behaviour of metal framework	
(unilateral loading conditions)	59
Micro-strain behaviour of metal framework and acrylic base	
(bilateral loading conditions)	62
Micro-strain behaviour of metal framework and acrylic base	
(unilateral loading conditions)	63
Chapter Five	64
Discussion	64
Bilateral loading of metal and acrylic.....	66
Unilateral loading of the metal and acrylic.....	79
Chapter Six	86
Summary	86
Conclusions	88
Recommendations	89
References	90
Appendix 1	99
Appendix 2	109
Appendix 3	110
Appendix 4	116
Appendix 5	117
Appendix 6	149

LIST OF FIGURES

Figure 1:	(a) Fabricated model of polyurethane resin (Easycast®)	
	(b) Soft tissue simulated with silicone (Deguform®).....	17
Figure 2:	Fabricated metal framework	18
Figure 3:	Numbered strain gauges and their placement	19
Figure 4:	Placement positions of the strain gauges in: (a) Radial orientation;	
	(b) Mesio-distal direction; (c) Mesio-distal bucco-lingual.....	20
Figure 5:	Strain gauges attached to the terminals and channel layout.....	22
Figure 6:	Placement of strain gauges on the acrylic surface.....	23
Figure 7:	Prepared holes in the model for implant placement.....	24
Figure 8:	Completed RPD with retentive caps and strain gauges in place	25
Figure 9:	Colour coded wires attached to channels	25
Figure 10:	Bilateral loading; (a) Uniform (b) Premolar (c) Molar.....	26
Figure 11:	Unilateral loading; (a) Uniform (b) Premolar (c) Molar	26
Figure 12:	Bilateral loading of premolar region in	
	Instron universal testing machine	27
Figure 13:	Wheatstone bridge arrangement. (R=resistors, V=voltage)	30
Figure 14:	Strain gauge placement	37
Figure 15:	Maximum mean micro-strain measured on the acrylic base	
	(bilateral uniform loading)	38
Figure 16:	Maximum mean micro-strain measured on the acrylic base	
	(bilateral premolar loading).....	39
Figure 17:	Maximum mean micro-strain measured on the acrylic base	
	(bilateral molar loading)	40
Figure 18:	Maximum mean micro-strain measured on the metal framework	
	(bilateral uniform loading)	41
Figure 19:	Maximum mean micro-strain measured on the metal framework	
	(bilateral premolar loading).....	42

Figure 20:	Maximum mean micro-strain measured on metal framework (bilateral molar loading)	43
Figure 21:	Maximum mean micro-strain measured on the acrylic base (unilateral uniform loading)	44
Figure 22:	Maximum mean micro-strain measured on the acrylic base (unilateral premolar loading)	45
Figure 23:	Maximum mean micro-strain measured on the acrylic base (unilateral molar loading)	46
Figure 24:	Maximum mean micro-strain measured on the metal framework (unilateral uniform loading)	47
Figure 25:	Maximum micro-strain measured on the metal framework (unilateral premolar loading)	48
Figure 26:	Maximum micro-strain measured on the metal framework (unilateral molar loading)	49
Figure 27:	Micro-strain values for acrylic base (bilateral loading conditions)	51
Figure 28:	An inverse correlation between maximum micro-strain in bucco-lingual direction in mesial area of the distal extension versus around the implant as the loading point moves forward.	53
Figure 29:	Maximum mean micro-strain values of metal surface for all three bilateral loading conditions	54
Figure 30:	Maximum mean micro-strain values (gauge 6) of metal surface for all three bilateral loading conditions	55
Figure 31:	Micro-strain values for acrylic base (unilateral loading conditions)	56
Figure 32:	Direct correlation between movement of the loading point forward and location of maximum micro-strain	58
Figure 33:	Micro-strain values for metal framework (unilateral loading conditions)	59

Figure 34:	Direct correlation for the value and location of the maximum micro-strain upon moving the loading point forward	61
Figure 35:	Comparison of micro-strain values in both metal framework and acrylic base (bilateral loading conditions)	62
Figure 36:	Comparison of micro-strain values in both metal framework and acrylic base (unilateral loading conditions)	63
Figure 37:	Cross-section illustration of the areas around the implants in coronal plane, showing the locations of the micro-strain gauges on the acrylic and metal structures	66
Figure 38:	Highest micro-strain value acrylic base recorded on labial side of left implant during bilateral uniform loading	67
Figure 39:	Micro-strain-time plot of gauge 1 on buccal side of right implant during bilateral uniform loading	68
Figure 40:	Micro-strain-time plot of gauge 10 on buccal side of left implant during bilateral uniform loading	68
Figure 41:	Micro-strain-time plot illustrating pre-loading, loading and unloading micro-strain behaviour during a bilateral uniform loading cycle	69
Figure 42:	Micro-strain value on acrylic base around the implant in mesio-distal direction (bilateral uniform loading)	70
Figure 43:	Implant acting as the primary load support point during bilateral uniform loading	71
Figure 44:	A simplified schematic image of IARPD subjected to bilateral uniform loading	72
Figure 45:	Simplified schematic illustrating the molar (broken) and premolar (solid) loading conditions showing the loading forces are now medially placed relative to the rigid implant support locations	73
Figure 46:	Schematic illustration indicating that premolar loading generates greater off-axis lever arm distance from the line between supporting structures	74

Figure 47:	Cross-sectional image of area around the mesial area of the distal extension in coronal plane with bilateral premolar loading.....	75
Figure 48:	Moving the loading point forward will increase the ratio of the effort arm to resistance arm.....	76
Figure 49:	Highest micro-strain values were recorded in the mesial area of the distal extension on the acrylic base under bilateral premolar loading	77
Figure 50:	Highest micro-strain values were recorded in the mesial area of the distal extension on the metal framework for all three bilateral loading conditions.....	77
Figure 51:	Bilateral molar loading; (a) Micro-strain values around the implants and mesial areas of the distal extensions on acrylic base (b) Micro-strain values around the mesial areas of the distal extension on the metal framework	78
Figure 52:	A simplified schematic image of IARPD subjected to unilateral uniform loading.....	80
Figure 53:	Highest micro-strain value in acrylic base; (a) Unilateral uniform loading (b) Unilateral molar loading (c) Unilateral premolar loading	81
Figure 54:	Simplified schematic illustrating the molar and premolar loading condition showing the loading forces are now medially positioned relative to the rigid implant support.	82
Figure 55:	Highest micro-strain value area on metal framework; (a) Unilateral uniform loading (b) Unilateral molar loading (c) Unilateral premolar loading	82
Figure 56:	Effect of unilateral loading conditions on metal framework	83
Figure 57:	Micro-strain values of unilateral molar loadings on; (a) acrylic and (b) metal framework.....	84

LIST OF TABLES

Table 1:	Chemical and mechanical properties of Straumann dental implant.....	32
Table 2:	Physical and handling properties of Easycast®.....	33
Table 3:	Composition, mechanical and physical properties of Wironit®.....	33
Table 4:	Vishay strain gauge properties (Vishay technical manual).....	34
Table 5:	Vertex™ Castapress technical specification (Vertex™ Dental webpage).....	35
Table 6:	Statistical comparison of maximum micro-strain values of three loading conditions.....	52
Table 7:	Statistical analysis of gauge 6 maximum mean micro-strain values for all three bilateral loading condition.....	55
Table 8:	Statistical analysis of maximum mean micro-strain of all three loading conditions.....	57
Table 9:	Significant differences in mean maximum micro-strain exhibited between all three loading conditions.....	60

Chapter One

Introduction

The percentage of fully edentulous adults in the population has been reported to be decreasing, so more people will have more teeth when they get older (Douglass and Watson, 2002). As a result, demands for replacement of missing teeth, to serve functional and social roles are increasing. The options to restore the partially edentulous patients are fixed partial dentures, removable partial dentures and implant-retained fixed prostheses. However, anatomical changes due to the loss of teeth and supporting structures can present challenges and limitations to the fixed prosthetic options. Loss of ridge volume is a major consequence of losing teeth. In general, bone loss is greater in the mandible than the maxilla, and is more severe in the posterior region. The mandibular arch broadens as it resorbs, while the maxillary arch narrows. These anatomical changes can create many challenges for implant-supported prostheses and removable partial dentures (RPD)(Carr *et al.*, 2011).

In a patient with no molar teeth, only RPD and implant-retained fixed prostheses options are available as treatment modalities, since there is a lack of distal tooth support (Carr *et al.*, 2011). The ideal treatment for these patients, if possible, is an implant-retained fixed prosthesis. When such treatment options are not possible or are too expensive for the patient, a RPD is considered to be a cost effective option to treat partially edentulous patients (Bergman *et al.*, 1982; Douglass and Watson, 2002). A well constructed RPD can be an adequate treatment option

(Kapur, 1991; Rissin *et al.*, 1985). A distal extension RPD needs to be accurately designed to provide dual support. Support should be provided by the framework via teeth contact and by the distal extension base. Distal extension tissue provides vertical and lateral support for the distal extension base of the RPD. However, distal extension tissue support changes with time and can compromise support for the prosthesis during function. In addition, distal extension tissue has a different resiliency to abutment teeth. The differences in the characteristics of RPD supporting structures (teeth and soft tissue) will cause rotation in relation to three cranial planes (Carr *et al.*, 2011).

Placing two implant abutments distally in the mandible has been recommended to transform a bilateral distal extension (Kennedy Class I) RPD to a tooth and implant-supported/assisted RPD (a pseudo Kennedy Class III) (Orr *et al.*, 1992). The pseudo Kennedy Class III design will improve the support, stability and retention of a distal extension RPD (Mijiritsky, 2007; Tolstunov, 2007). This could be seen as a cost effective alternative compared with implant-retained fixed prosthetic options.

An implant in conjunction with an RPD was used in the treatment of the bilateral distal extension for the first time in the early 1970s (Fields and Campfield, 1974) and since then several clinical trials have shown good survival rates (Chikunov *et al.*, 2008; Grossmann *et al.*, 2009; Mijiritsky *et al.*, 2005). However, fracturing of the acrylic base was reported when resilient attachments were used in this design (Payne *et al.*, 2006).

The type of resilient attachment usually used in implant-assisted removable partial dentures (IARPD) is an extra-coral resilient attachment (ERA), o-ring system, or a similar attachment system. Locator® abutments have also been recommended because they can be easily repaired or replaced and have good resiliency and retention. They also have a straight profile and are available in different heights, making them ideal for areas with limited space. The term IARPD is used when resilient attachments are placed. Implants, incorporated into RPDs provide support through the use of healing caps, hence the term *implant-supported* RPD (ISRPD) (Shahmiri and Atieh, 2010).

The mandibular bilateral distal extension situation will be discussed to better understand the limitations of conventional RPDs and how converting a RPD into an IARPD/ISRPD improves its outcomes. Despite the RPD being a reasonable option for the patient without molars, it has limited success and it is not easy to achieve patient satisfaction (Jepson *et al.*, 1995). A survey by Wetherell and Smales (1980) showed that one RPD (bilateral distal extension) out of 150 survived over a 10-year period. The term “failure” was defined as partial dentures which had been replaced or which could not be worn at all. The failures identified were; (1) discarded by the patient, (2) need replacement regularly, (3) did not improve eating, (4) had poor retention, and (5) had poor stability.

The distal extension area of the mandibular offers little support in comparison with the distal extension area of the maxilla (Carr *et al.*, 2011). In addition, the mandibular bilateral distal extension RPD is supported by two different structures, the edentulous ridges and abutment teeth. These two different

structures have different resiliency and viscoelastic responses to loading. The soft tissue under loading has a displacement range of 350-500 μ m, whereas a sound tooth (not periodontally compromised) has a displacement of 20 μ m under the same load (Manderson *et al.*, 1979). This mismatch of support will result in the transmission of torque forces to the abutment teeth via a rotational movement of the RPD (Monteith, 1984). In 1984 Watt and MacGregor linked tooth mobility to the torque forces that are developed against the abutment teeth. In addition, the rotational movement of the RPD is directed towards the underlying soft tissue, and as a result the torque force in the soft tissue is then transmitted as a shearing force, which progressively causes resorption of residual ridges (Witter *et al.*, 1994).

It has been suggested that a specific clasp design for a mandibular bilateral distal extension RPD must be incorporated to provide stress relief for the abutment teeth. As a consequence various retentive units were designed that incorporate a stress relief component. The RPI (R = mesial rest, P = proximal plate, I = I-bar retentive arm), RPA (rest, proximal plate, Akers clasp), RPL clasp (mesial rest, proximal plate, L-bar) and Equipoise back action clasp systems were designed to compensate for the torque induced by the mismatch in different types of support available to the RPD (Eliason, 1983; Goodman, 1963; Krol, 1973).

On the contrary, Igarashi *et al.*, (1999) argued that flexible retainers can cause more damage to the abutment than a more rigid design. They evaluated the mobility of abutments when loading the distal extension of the RPDs. They assessed three different types of retainers; wrought wire clasps, Akers cast clasps and conical telescopic crowns. Maximum tooth mobility was observed with the wrought wire

clasps, which represented the least rigid retainer design in this study. However, Mizuuchi *et al.*, (2002) revealed that a distal rest produced greater distal torque on the abutment tooth regardless of clasp design. They identified that the shorter the distance from the occlusal rest to the loading point, the smaller the resistance arm will be and as a result the magnitude of the distal torque on the abutment will decrease.

Another issue related to the support provided by soft tissue is a lack of resiliency throughout the mandibular distal extension. The tissue in the region of the retromolar pad is much more resilient than the tissue immediately adjacent to the last abutment tooth. The areas that are least resilient will bear most of the load. This can cause tissue creep in the limited contact area under the load and consequently damage to the underlying alveolar bone (Vahidi, 1978). Shortening the dental arch in the distal extension to the first molar could be a possible solution. A concern is that the potential loss of function may cause a temporomandibular joint problem. Witter *et al.*, (1994) compared shortened distal extension RPDs with lengthened distal extension RPDs. These authors established there was no significant difference in the oral functionality of either group.

A link between bone resorption and RPDs has been shown in a number of studies. There was a considerable difference in residual bone resorption between patients who had an RPD and those that did not wear one (Campbell, 1960; Imai *et al.*, 2002; Jozefowicz, 1970; Mijiritsky *et al.*, 2007). Mori *et al.*, (1997) and Ohara *et al.*, (2001) evaluated the effect of continuous pressure on RPD's support tissue. They

found that exceeding a threshold value range of 1.5KPa to 4.9KPa caused irreversible bone resorption, even after the discontinuation of the pressure.

One of the recurrent problems associated with a mandibular bilateral distal extension RPD stems from the loading of the edentulous ridge (Brudvik, 1999). Vertical compressive forces applied to a mandibular ridge are well tolerated (Kelly, 2003; Zarb, 1978). In the bilateral distal extension RPD, the situation of the occlusal rests on the distal abutments affects transmission of the load to the underlying tissue. The distal extension of the RPD can move freely which transmits the full masticatory load via a rotational movement, which in turn is transmitted to the distal end of the edentulous ridges as a shear force (Hindels, 2001; Monteith, 1984; Watt and MacGregor, 1984; Zarb, 1978). The shear force is not well tolerated by the edentulous ridges and can contribute to bone loss (Kelly, 2003; Renner, 1990). Different methods such as functional impression, one-stage impression, relining methods, mucostatic techniques and stress breakers have been suggested as solutions to minimize the effects of different resiliency of the two supporting structures (Hindels, 2001). Understanding how different designs transmit an occlusal load to the underlying structures may help limit the detrimental effects on the supporting tissues.

Another problem related to the mandibular bilateral distal extension RPD is combination syndrome or Kelly syndrome. This occurs when the RPD opposes a maxillary complete denture. It causes the downward growth of maxillary tuberosities, papillary hyperplasia (severe oedema and eventual inflammatory fibrosis of the connective tissue papillae between the rete processes of the palatal

epithelium), resorption of the pre-maxilla, over-eruption of the mandibular anterior teeth, and resorption of the posterior mandibular ridge (Kelly, 2003). However, there has been a lack of supporting evidence since the publication by Kelly on this phenomenon 25 years ago (Carlsson, 1998). Palmqvist *et al.*, (2003) also concluded that there is a lack of epidemiological studies and publications to be able to classify this combination syndrome as a medical syndrome. Salvador *et al.*, (2007) assessed the prevalence of combination syndrome and concluded an overall prevalence of 25%. In the same year, Tolstunov (2007) proposed a classification for combination syndrome and identified complications in each classification. It was concluded that using implant rehabilitation was the most promising treatment for these conditions.

Using roots to support a removable partial over-denture (RPOD) with bilateral distal extensions is promising. Compressive forces from the denture are transferred to tensile forces in the bone when passed through the roots and periodontal ligaments (PDL), rather than the mucoperiosteum and residual ridge. Therefore, hard and soft tissues under the distal extension area experience less stress (Renner, 1990). In addition, the PDL proprioceptors generate a signal against physiological overloading and prevent bone resorption (Crum and Rooney, 1978). However, RPODs require additional time and cost more, as well as requiring more sophisticated clinical and laboratory procedures (Renner and Boucher, 1987). Patient oral hygiene must also be kept to a high standard, otherwise the patient is susceptible to dental caries and periodontal disease which affect the overall prognosis of the RPOD (Ettinger *et al.*, 1984; Ettinger, 1988).

The mandibular bilateral distal extension RPDs have a number of complications. Stability of such a prosthesis predominantly depends on the shape and anatomy of the soft tissue on the distal extension area (Vahidi, 1978). The optimal type of retentive clasp design to achieve adequate retention and desirable aesthetics is still arguable (Igarashi *et al.*, 1999; Mizuuchi *et al.*, 2002). A link between bone resorption and RPDs due to the effect of continuous pressure on the support tissue was another identified complication of distal extension RPDs (Campbell, 1960; Imai *et al.*, 2002; Jozefowicz, 1970; Mijiritsky *et al.*, 2007).

All of the above issues associated with mandibular bilateral distal extension RPDs may be improved by implants. Placing two implant abutments distally in the mandible has been recommended to transform a bilateral distal extension RPD to a tooth-implant-supported/assisted RPD to help redistribute the heavy masticatory load posteriorly and improve the conventional RPD design (Mijiritsky, 2007; Orr *et al.*, 1992; Tolstunov, 2007).

Chapter Two

Literature review

Oral implants placed in posterior sites modify the Kennedy Classification of partially edentulous arches by converting a Class I (tooth- and tissue-supported) to a pseudo Class III (tooth- and implant-supported). ISRPD and IARPD seem to overcome the numerous problems associated with RPDs in addition to achieving a higher level of patient satisfaction. An improvement in function and stability has been demonstrated (Mijiritsky, 2007; Tolstunov, 2007). In addition, attachments can be added chair-side to an existing RPD after implants have been placed, reducing cost and simplifying the treatment (Shahmiri and Atieh, 2010). However, there is still no evidence that validates the use of such a treatment modality in managing bilateral distal partial edentulism, or supports the use of implants with healing abutments or resilient attachments as a means of providing extra support and retention to the RPD.

Placement of implants to stabilize and support the prosthesis can increase maximum muscular effort and occlusal forces (Bakke *et al.*, 2002; Ohkubo *et al.*, 2008; van Kampen *et al.*, 2002). The bite force generated by an edentulous person is approximately 11% of that of a dentate individual and a person with a RPD will generate a bite force equivalent to 35% of a dentate individual. This has been established to be in the range of 54N for the complete denture wearer and 173N for the RPD wearer (Miyaura *et al.*, 2000).

General bilateral balanced occlusion seems to be the most effective occlusal scheme for distal extension IARPDs; this is because it evenly distributes forces across the prosthesis. However, chewing patterns are unique to each individual and mastication usually takes place either on the right or left side, regardless (Pond *et al.*, 1986). There currently are no studies available that have investigated the influence of loading conditions on the RPD comparing bilateral with unilateral loading.

Fields and Campfield (1974) were the first to report the use of an implant in conjunction with a mandibular bilateral distal extension RPD. Although a 7-month follow-up study showed promising results, a longer follow-up study on ISRPD/IARPD was needed to determine the prognosis of this treatment modality. Several review papers have been published on the use of the ISRPD/IARPD with various recorded follow-up periods (Chikunov *et al.*, 2008; Grossmann *et al.*, 2009; Mijiritsky *et al.*, 2005; Payne *et al.*, 2006). Currently the longest follow-up study is published by Grossmann *et al.*, (2009). They carried out a retrospective study of 35 patients treated with either unilateral or bilateral distal extension ISRPDs/IARPDs with a survival rate of 97.1%.

The treatment paradigm of IARPD/ISRPD has been evaluated in terms of: bone loss, combination syndrome, aesthetics, position of implant, maintenance, soft tissue condition, chewing ability and patient satisfaction. An early study by Fields and Campfield (1974) reported no bone loss was detected around the implants of ISRPD cases during a 7-month follow-up period. However, Payne *et al.*, (2006) reported marginal bone loss with ISRPD/IARPD during a 12-month follow-up

period. A long term clinical study is required to evaluate bone condition around IARPD/ISRPD.

When posterior tooth support is lost or reduced, pathological changes of occlusion can happen in the form of loss of arch integrity, collapse of the occlusion or combination syndrome (Stern and Brayer, 1975). A study using healing caps in ISRPDs, showed a lower risk of occlusal collapse compared with RPDs (Halterman *et al.*, 1999). In the case of a mandibular bilateral distal extension RPD functioning against a maxillary complete denture, an IARPD/ISRPD can offer more even force distribution. The additional posterior support provided by ISRPD/IARPD prevents the resorption of the anterior maxilla and reduces the risk of combination syndrome (Keltjens *et al.*, 1993).

The position of the implant can have a significant effect on force distribution. Placement of implants in the second molar location provides the best support and stability (Grossmann *et al.*, 2009; Ohkubo *et al.*, 2008). In the case where there is insufficient bone in the second molar region, placement of the implant close to the adjacent abutment is recommended. This provides a future option for a fixed implant-supported prosthesis (Grossmann *et al.*, 2009). Further clinical studies are still needed to evaluate the most effective position of the implant (Shahmiri and Atieh, 2010).

Healthy soft tissue surrounding a dental implant gives protection to the osseous structure during the osseointegration of the implant (Geurs *et al.*, 2010). Therefore, it is important to evaluate the soft tissue condition around the implant in

IARPD/ISRPD. Fields and Campfield (1974) reported that tissue around the ISRPD remained healthy during the 7-month follow-up period. Mitrani *et al.*, (2003) evaluated peri-implant soft tissue conditions in both IARPD and ISRPD and reported that the soft tissue remained stable during the 12-48 month follow-up period. However, the complication of hyperplastic tissue was reported in the ISRPD patients during the follow up period.

The longevity of IARPD/ISRPD depends on prosthetic maintenance requirements as well as biological complications (Payne and Solomons, 2000). Fracturing of the acrylic base was observed when ball attachments (IARPD) were incorporated into existing partial dentures opposing a complete maxillary denture (Payne *et al.*, 2006). Several other studies also reported complications related to IARPD/ISRPD such as adjustment of the acrylic base, implant failure, repeated relining, rest rupture, pitting of the surface of the healing abutments, screw loosening, framework fracture, hyper-plastic tissue formation, loosening of healing cap and fracture of the acrylic denture base (Grossmann *et al.*, 2009; Keltjens *et al.*, 1993; Mijiritsky *et al.*, 2005; Mitrani *et al.*, 2003; Payne *et al.*, 2006).

Maintenance or renewal of attachments or healing caps was reported more frequently than any other complication with IARPD/ISRPD (Mitrani *et al.*, 2003; Payne *et al.*, 2006). Loosening of the healing cap (ISRPD) in 84% of cases was reported in 24 patients after a 12-month period in a randomized controlled study by Payne *et al.*, (2006). In the second component of the same study, resilient attachments were placed (IARPD) and 58.3% of patients reported complications.

Several clinical studies have reported improved chewing ability and patient satisfaction for IARPDs/ISRPDs compared to RPDs (Mijiritsky *et al.*, 2005; Mitrani *et al.*, 2003; Ohkubo *et al.*, 2008). Mitrani *et al.*, (2003) carried out a retrospective study of both IARPD and ISRPD and concluded that IARPD/ISRPD improved patient satisfaction. Mijiritsky *et al.*, (2005) reported improved chewing ability and patient satisfaction when wearing IARPD during a 24-48 month follow-up period. Ohkubo *et al.*, (2008) conducted a single blind randomized crossover study of five partially edentulous patients (Kennedy Class I). The study was designed to evaluate masticatory movements, occlusal forces and patient comfort following placement of an ISRPD. The study showed that the occlusal force and contact areas were greater and more distally located in the ISRPD than for a RPD.

The reviews of clinical studies and case reports on ISRPD/IARPD identified only two randomized trials Ohkubo *et al.*, (2008), Payne *et al.*, (2006) and three retrospective studies Grossmann *et al.*, (2009), Mijiritsky, (2007) and Mitrani *et al.*, (2003). All the studies had insufficient follow-up periods and were lacking in statistical power.

Non-clinical studies

Cho, (2002) studied the load transfer characteristics of IARPDs and showed that the use of resilient attachments with distal implants reduced the stress concentration around implants and abutment teeth. Although only resilient attachments (IARPD) were used in this study, the use of healing abutments

(ISRPD) in different studies showed a similar result. Itoh *et al.*, (2007) used a photo-elastic model of a mandibular bilateral distal extension implant-tooth borne RPD and found that both healing abutments and ball attachments provided support to the RPD with no difference in stress concentration.

Lacerda *et al.*, (2005) compared different connection designs for an IARPD. They compared various hinge and rigid connectors and evaluated the load on the abutment, alveolar ridge and implant. They found that ball, ring and magnet connectors behaved as hinges, preventing a bending moment on the implant. However, such a flexibility in the connection between the implant and RPD increased the load on the abutment teeth and IARPD structure. On the other hand, a ball attachment with adjustable resilient matrix design can reduce the amount of stress on the structure of the prosthesis (Shahmiri and Atieh, 2011). However, there is currently no available evidence to recommend one design over another in terms of retention and support.

With regard to implant location, Cunha *et al.*, (2008) used finite element analysis (FEA) to show that there is a greater tendency for displacement when implants are placed in the second molar position, and suggested that a more mesial position in the arch (i.e. first molar region) would reduce this. However, Ohkubo *et al.*, (2007) showed that implant placement in the second molar region reduced the distal displacement. In addition, an increase of the implant angle increased displacement and tension, which is considered harmful to the structure of the prosthesis (Santos *et al.*, 2006). Further studies are required to evaluate the most effective position of the implant.

Dissipation of the occlusal forces over an abundant surface of an implant can help maintain bone integrity (Lum, 1991). In a biomechanical study, Verri *et al.*, (2007) created six models and used FEA to evaluate the influence of length and diameter of implants on the design of a RPD. The authors showed that increasing both the length and diameter of implants was likely to reduce the tension values. Yet, it is expected that the ISRPD can be shorter if the implants are used for vertical support only (Brudvik, 1999). However, the optimal length and diameter of the implants for use with RPDs have not been determined.

An increase in the masticatory forces will have an influence on the prosthesis components and supporting structures. Rocha *et al.*, (2003) carried out a FEA study to evaluate behaviour of the support structure of a ISRPD compared to a RPD with the same loading conditions. It was concluded that the presence of a implant, supported the RPD and promoted smaller stress levels in alveolar bone.

The influence of the different loading conditions and retention systems were studied in three separate FEA studies by Pellizzer *et al.*, 2003, 2004 and 2010. In the 2003 study stress values were measured in an ISRPD support structure and prosthesis under four different loading schemes, with gradual vertical forces applied onto the first and second molars. It was concluded that stress values exceeded the ultimate stress value of the acrylic and a material with more resistance needed to be used for occlusal coverage (Pellizzer *et al.*, 2003).

In 2004 they evaluated the effect of vertical and oblique loads on a distal extension IARPD. Loads at 90° and 45° angles were applied in two directions, mesial to

distal and distal to mesial. It was found that 45° mesial to distal loading generated less tension than distal to mesial. Nevertheless, the tendency for more displacement and greater tension was observed for the 45° loads compared to the 90° loads (Pellizzer *et al.*, 2004).

Pellizzer *et al* (2010) third study compared biomechanical behaviour of IARPD and ISRPD with different retention systems. They evaluated the effect of axial and oblique loads on a conventional RPD, ISRPD, IARPD with ERA attachments, IARPD with O-ring attachments, single fixed implant (UCLA abutment) supporting a RPD. It was concluded that IARPD with ERA attachments displayed the best stress distribution in the supporting structure. The single fixed implant (UCLA abutment) supporting a RPD was a nonviable treatment option.

IARPD/ISRPD places more stress on the prosthesis components than a RPD, due to an increase in mastication forces (Cibirka *et al.*, 1992; Ohkubo *et al.*, 2008). Fracture of the acrylic base was reported when an existing RPD was fitted with implants in the distal of the distal extension, which was opposed by a maxillary complete denture (Payne *et al.*, 2006). Stability of the maxillary complete denture can be promoted by developing balanced loading to minimize tipping stress when the mandibular Kennedy Class I RPD is used (Carr *et al.*, 2011). However, the effect of the loading condition has not been investigated when an implant is retro fitted into a RPD.

Chapter Three

Method and Materials

Method

Model fabrication

A human mandible was obtained from the Department of Anatomy and Structural Biology at the University of Otago. A duplicate model was made using a polyurethane (Easycast[®]) covered with a 2mm layer of silicone (Deguform[®], DeguDent, Germany) (figure 1a & b).

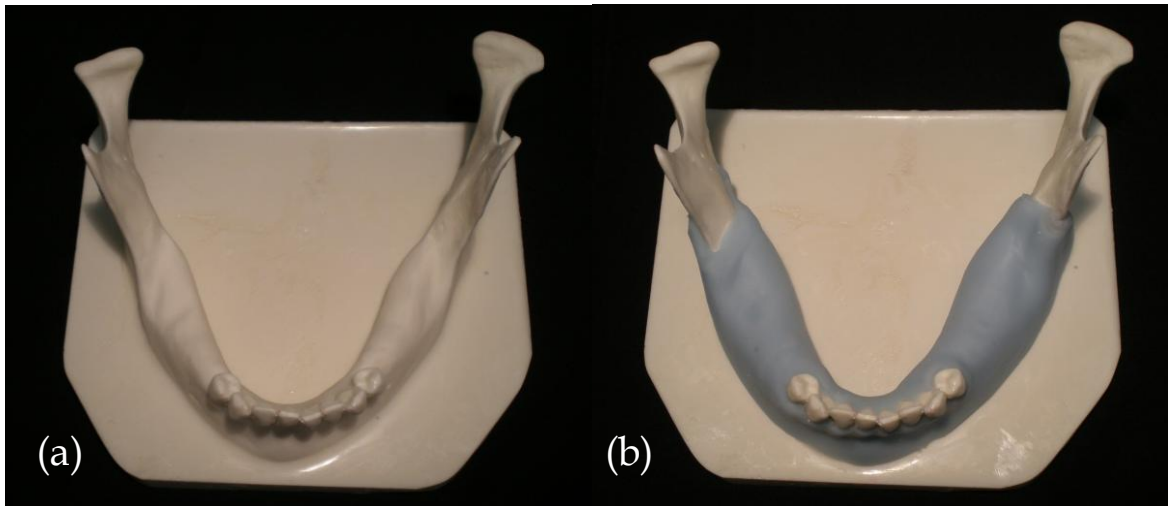


**Figure 1: (a) Fabricated model of polyurethane resin (Easycast[®])
(b) Soft tissue simulated with silicone (Deguform[®])**

The edentulous ridge areas of the mandibular model were covered with 2 mm of wax to simulate the maximum soft tissue thickness. A matrix was made with condensation silicone putty (Sil-Tech[®] Ivoclar Vivadent AG, Schaan/Liechtenstein). After removing the wax, Deguform[®] was injected into the matrix and a uniform silicone layer was produced.

An alginate impression was taken of the mandibular model using a custom tray. The impression was poured with type 4 stone (Fujirock® EP, GC Europe N.V., Leuven, Belgium) to make a master cast. A conventional Kennedy Class I RPD with a lingual bar (0.5 mm), mesial rest and I bar was designed. The path of insertion was determined, undercuts were blocked out and the distal extension area was given a 1 mm spacer. The cast was then duplicated with Deguform® and a refractory cast was poured (Wirovest®, BEGO, Bremer Goldschlägerei Wilh, Germany). The refractory cast was waxed up according to conventional Kennedy Class I RPD techniques. After investing, the framework was cast in a cobalt-chrome molybdenum alloy (Wironit® BEGO, Bremer Goldschlägerei Wilh, Germany). The framework was fitted and polished (figure 2).



Figure 2: Fabricated metal framework

Strain gauges

Strain gauges (Vishay Electronic GmbH, Germany) were placed on the fitting side of the framework. Two strain gauges were placed perpendicular to each other in the mesial areas of the bilateral distal extensions between the retention mesh and lingual bar. A further four gauges were placed radially around each implant site (figure 3).

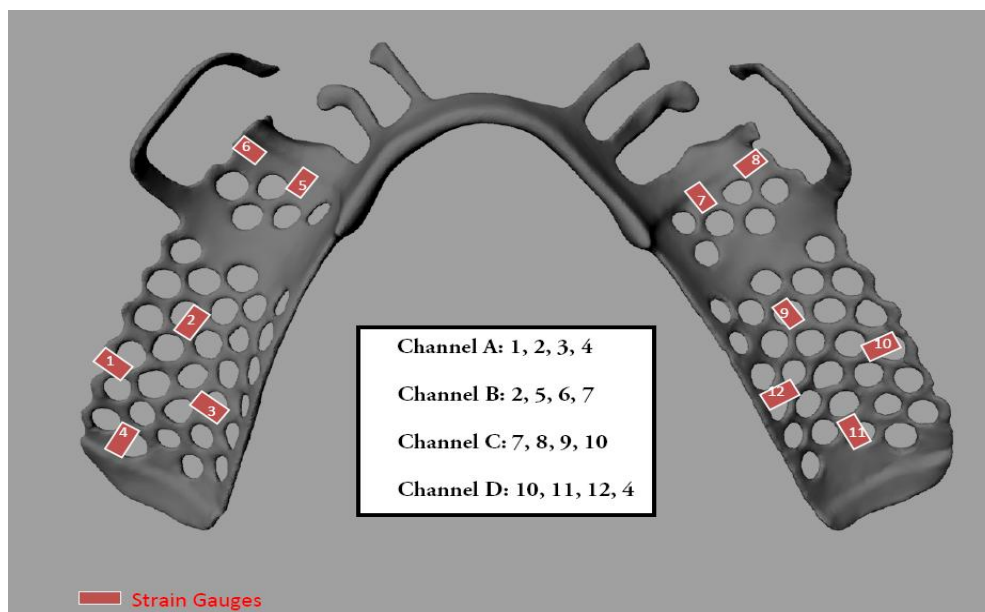


Figure 3: Numbered strain gauges and their placement

Because an RPD is a complex structure and measurement of general body displacement is almost impossible, so a novel research method utilizing strain gauges to measure strain on the surfaces near the boundary conditions was used. Biaxial and uniaxial strain fields are a determinant in choosing the type of strain

gauge used. In the case of a biaxial field, the question arises whether or not the direction of the principal strain is known. If the direction of the principal strain is unknown, three or four rosette strain gauges are required and if the direction of the strain is known, two rosette strain gauges are sufficient. In the case of a uniaxial strain field, a single gauge is enough to measure the strain (Dally and Riley, 1965). In this study, static loading was applied to the materials. This made the directions of the strains predictable and uniaxial. As only high strain areas were to be identified, the strategy was taken to place the strain gauges close to boundary conditions. In the area by the rests, gauges were placed to measure strain in the x and y directions. Around the implants, it was necessary to place the gauges radially to allow for the intended placement of the implant. The strain gauge orientation was critical and three different orientations were initially considered: radial, mesio-distal and mesio-distal bucco-lingual (figure 4).

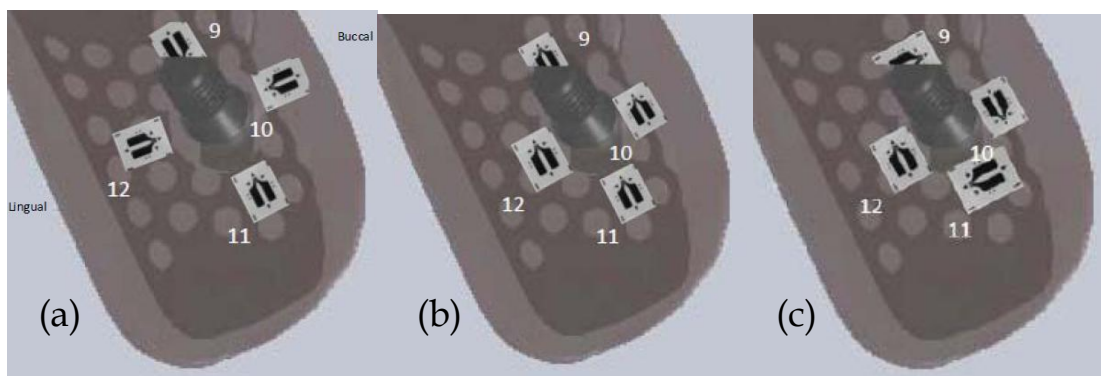


Figure 4: Placement positions of the strain gauges in: (a) Radial orientation; (b) Mesio-distal direction; (c) Mesio-distal bucco-lingual (not radial to implant)

Out of three scenarios, the radial orientation of strain gauges was decided on. This was because most of the strain would occur in the mesio-distal direction because of the deflection of the saddle and bucco-lingual direction due to tissue response to lateral displacement of the prosthesis.

Strain gauge length and width have an important role in the accuracy of a strain measurement. The smaller the length of the strain gauge, the more accurate the strain value at a given point (Dally and Riley, 1965). Therefore, small strain gauges with a length of 0.15mm length were used. The strain gauges were trimmed to the smallest size possible in order to accommodate them on the limited space the mesh framework had available. After the strain gauges were trimmed, isopropyl alcohol was used to clean the surface of framework. The strain gauges were then attached to the framework with cyanoacrylate adhesive, and wiring procedures were completed with 0.08 mm thickness copper based wires. The adhesion of the gauges can influence the resistance to stress relaxation and gauge resistance. To account for this, pressure is applied at temperature which helps minimize any residual stresses in the adhesive. Adequate bonding was tested by tapping the installed gauges with a soft rubber eraser and checking the strain readings (Dally and Riley, 1965).

Terminals (CPF-50C M-Line accessories, Measurement Group, INC., Raleigh, NC) were attached onto the model base and the strain gauge wires were attached to the appropriate channel. The models were left for 24 hours to make sure the strain gauges and terminals were secured, as heat introduced during the wire soldering

can affect bonding. After the strain gauges were numbered they were connected to the most convenient terminals. Four channels were used, with each terminal having four gauges attached. Figure 5 shows the terminals and channel layout. There was always one gauge in common with the following channel. This helped to verify data as the linked strain gauge should indicate the same micro-voltage in both channels.

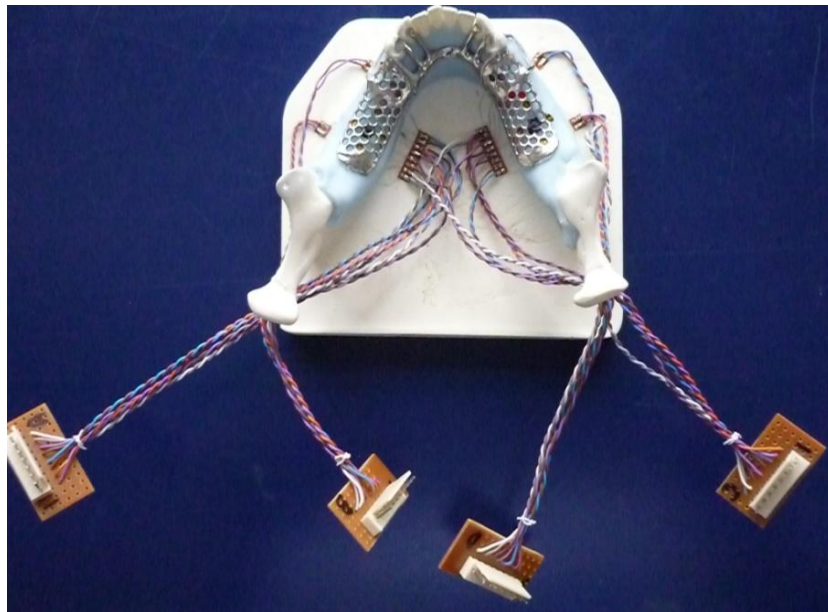


Figure 5: Strain gauges attached to the terminals and channel layout

After testing of the metal framework was complete, the strain gauges were disconnected from the terminals and the framework was transferred to the master cast so the teeth could be placed. The strain gauges were covered with a thin layer of clear spacer to separate the gauges from direct contact with chemicals and heat during polymerization. The partial denture was then processed with clear acrylic. Strain gauges were then placed on the acrylic surface in the same orientation as

the metal framework. The clear acrylic enabled the gauges to be directly aligned with the corresponding gauges placed on the metal framework (figure 6).

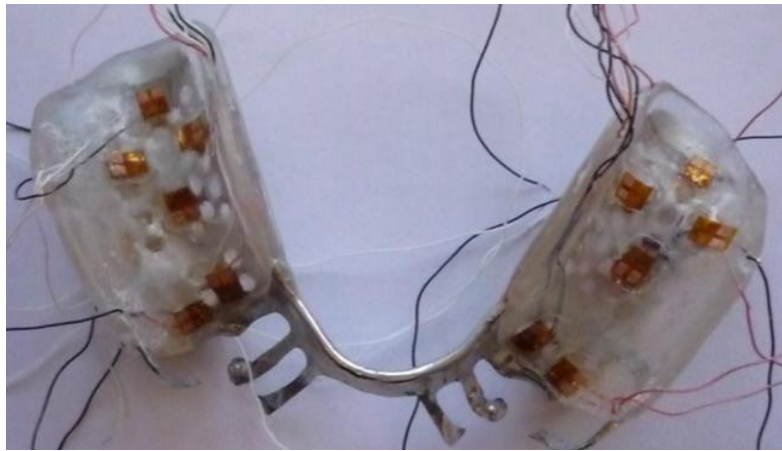


Figure 6: Placement of strain gauges on the acrylic surface

Strain measurement

Strain defined as change in the length divided by the initial length of a line segment parallel to one of three associated principal directions is known as normal strain (Dally and Riley, 1965). Consequently, slight changes in orientation of line segments parallel to each of the axes x , y and z can occur and this is known as shearing strain. In a two-dimensional state of strain, there are three cartesian strain components: ϵ_{xx} , ϵ_{yy} and ϵ_{xy} where ϵ_{xx} and ϵ_{yy} are normal strain and ϵ_{xy} is shear strain. Motion of the object can be translational/rotational or movement of points of a body relative to each other. Translational or rotational movement is known as rigid body motion and movement of the points of a body relative to each other is known as deformation (Dally and Riley, 1965).

Strain can be measured with several methods such as strain gauge, photo-elasticity, moiré fringe patterns, finite element analysis and holography. The strain

gauge method and finite element analysis are quantitative methods of strain measurement, while other methods are predominantly qualitative methods. A single measurement of displacement cannot accurately measure general body displacement and as a result, the conversion of displacement to strain does not reflect the general body strain. Therefore, it is recommended to utilize a strain gauge to measure surface strain (Dally and Riley, 1965).

Implant placement into model

The holes for the implants were prepared on the model using a milling unit. Drilling was performed parallel to the path of insertion of the partial denture. A 2.2 mm diameter pilot drill (number 044.211) (Straumann Group, SIX: STMN, Basel, Switzerland) was used initially, followed by a 2.8 mm diameter drill (number 044.216), and finally a 3.5 mm diameter drill (number 044.219) (figure 7).

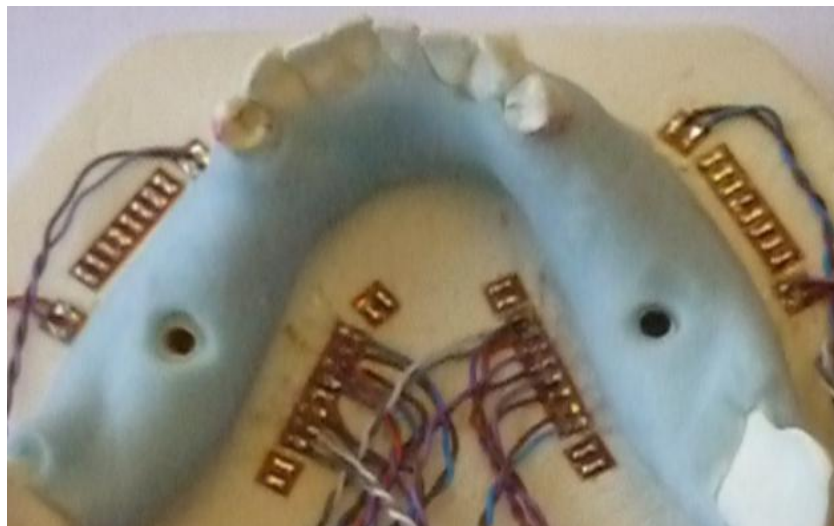


Figure 7: Prepared holes in the model for implant placement

Easycast® resin based material was poured into the holes and the implants were connected to the implant transfer screw and was screwed down and left for 72 hours to cure. Ball attachments were then placed on the implants and screwed down.

Holes were prepared inside the acrylic base of the partial denture to accommodate the retentive caps. The retentive caps (Straumann titanium matrix, reference number 048.450) were placed on the ball attachments and the partial denture was relined with self-cure acrylic to secure the retentive caps in place. After this, all the strain gauges were connected to the appropriate terminals (figure 8).

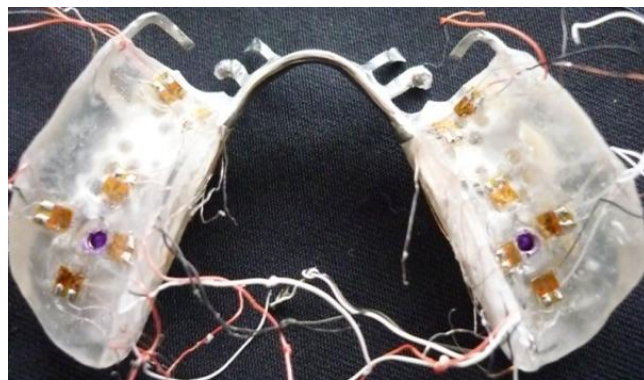


Figure 8: Completed RPD with retentive caps and strain gauges in place

Colour coded wires were used for strain gauges to aid identification (figure 9).

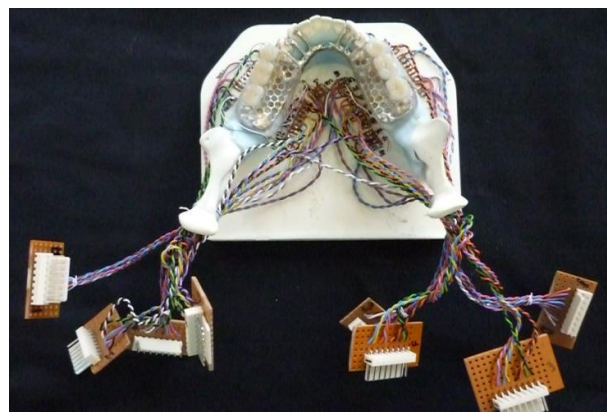


Figure 9: Colour coded wires attached to channels

Loading of the prosthesis

A compressive load of 120N was applied at a crosshead speed of 0.05mm/sec using a universal testing machine (Instron 3369, Norwood, MA, USA). It has a rigid frame controlled by Instron® Bluehill Lite software. Each loading condition was repeated eight times under the control of the software.

The output strain data were detected as μV and recorded with Chart 5 software and Power Lab system (AD Instruments, Sydney, Australia). Data were presented as a graph in the Chart 5 software and the highest strain point in each channel was manually recorded.

The teeth, or tooth bearing areas were loaded, bilaterally (figure 10) and unilaterally (figure 11). Each testing condition was loaded uniformly, in the premolar area and in the molar area.

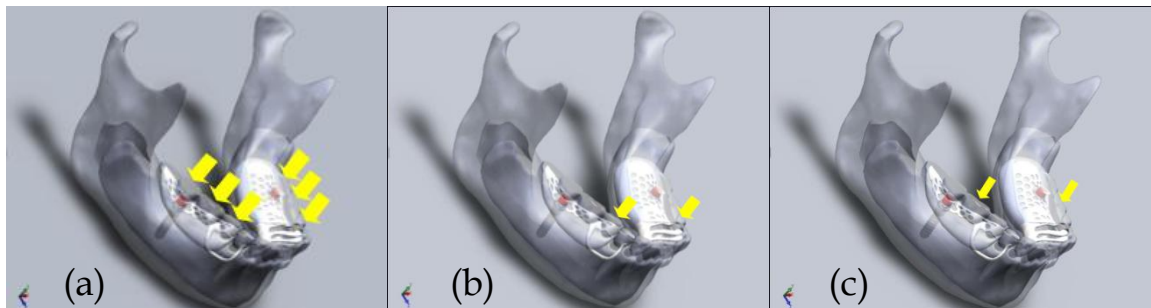


Figure 10: Bilateral loading; (a) Uniform (b) Premolar (c) Molar

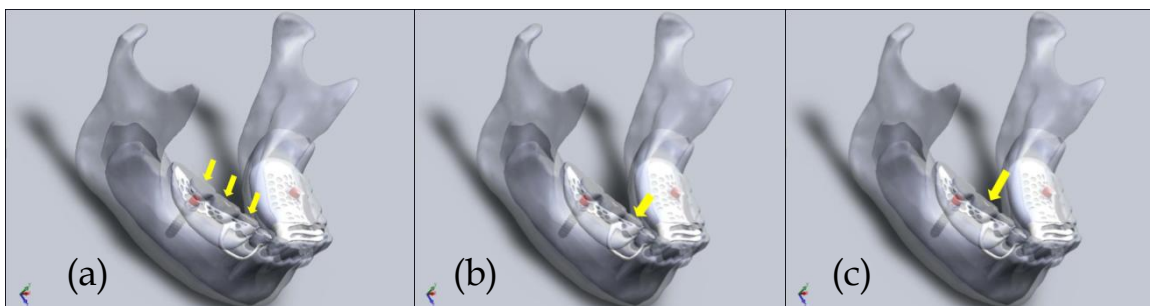


Figure 11: Unilateral loading; (a) Uniform (b) Premolar (c) Molar

Two steel bars with different widths were used for the bilateral loading condition. A wider bar that covered all the denture teeth was used for the uniform loading and a narrower bar was used to cover only the selected premolar and molar teeth. A thin silicone layer was placed between the bar and the teeth to distribute the forces evenly. The silicone was placed on top of the teeth and a small amount of load was applied with the loading machine to ensure that a level surface was achieved. The embedding of the bar into the silicone also minimized displacement of the steel bar during loading. A small V-shaped groove was created in the bar to locate the tip of the loading point accurately (figure 12).



Figure 12: Bilateral loading of premolar region in Instron universal testing machine

For the uniform unilateral condition a smaller bar was used which also had silicone between the teeth and the bar. Due to the small loading area, the unilateral loading of the premolar and molar areas could be done directly using a flat loading point attached to the Instron and with silicone between the load point and the teeth.

Converting the data to micro-strain values

Strain gauges convert relative mechanical displacement into an electrical signal, which is recorded as μV . The data then needs to be converted to μstrain (Watson, 2008). Electrical resistance change is the result of resistivity and dimensional changes of the thin metal wire. In order to measure small changes in resistance, strain gauges use a Wheatstone bridge arrangement with a voltage excitation. The voltage recorded needs to be converted to a resistance change value and then ultimately to a strain value. To find the resistance changes from voltage excitation in the Wheatstone bridge, the gauge factor needs to be calculated first. To calculate the gauge factor, the differential relationship between the area change and length change needs to be found. To calculate the differential relationship, the resistance needs to be calculated.

Resistance equation
$$R = \rho \frac{L}{A}$$

Differential equation
$$\frac{dR}{R} = \frac{d\rho}{\rho} + \frac{dL}{L} - \frac{dA}{A}$$

R=resistance (Ω), ρ =resistivity (Ωcm), L=length (cm), A=area of cross-section (cm^2)

Poisson's ratio is then calculated which then can be inserted into the differential equation which once combined gives the relative resistance change.

ν is Poisson's ratio
$$\frac{dA}{A} = -2\nu \frac{dL}{L}$$

Relative resistance change to change of length equation

$$\frac{dR}{R} = \frac{dp}{p} + \frac{dL}{L}(1 + 2\nu) \rightarrow \frac{dR/R}{dL/L} = \frac{dp}{p}(1 + 2\nu)$$

The relative resistance change to change of length equation shows the ratio of electrical resistance change of a conductor to the change in length, which is known as the gauge factor (GF).

Gauge factor equation
$$GF = \frac{dR/R}{dL/L}$$

An accurate measurement of the change of resistance is essential as strain rarely exceeds more than a few milli-strains or a few thousand micro-strains. In order to measure small changes in resistance, strain gauges are used in a bridge arrangement with a voltage excitation. A Wheatstone bridge is usually used to measure relative resistance change (Dally and Riley, 1965). The Wheatstone bridge consists of four resistors with output voltage difference at points B and D. Paths ABC and ADC (figure 13) divide the voltage. In this way the voltages for B and D can be calculated. This is calculated as

$$V_B = V_{in} \frac{R_2}{R_1 + R_2} \text{ and } V_D = V_{in} \frac{R_3}{R_3 + R_4} \text{ giving}$$

$$V_{out} = V_D - V_B = V_{in} \left[\left(\frac{R_3}{R_3 + R_4} \right) - \left(\frac{R_2}{R_1 + R_2} \right) \right] = \left[\frac{R_4 R_1 - R_2 R_3}{(R_3 + R_4)(R_1 + R_2)} \right]$$

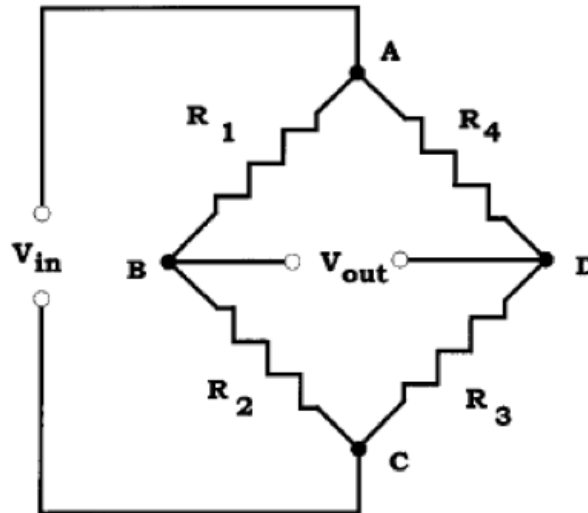


Figure 13: Wheatstone bridge arrangement. (R=resistors, V=voltage)

In a Wheatstone bridge R_1 , R_2 , R_3 or R_4 can record the strain and consequently a quarter, half, or the full bridge system can be used. We assume at least a quarter of the bridge is active with a changing resistance.

Output of the bridge is usually adjusted to zero before any strain application. Therefore, V_B will be equal to V_D and $R_1R_4 = R_2R_3$ and since the bridge is in a balanced condition $R_1=R_2=R_3=R_4=R$. When strain applies, the resistance value of R_1 will change slightly ($R+dR$) and the equations change too.

$$dV_{out} = V_{in} \left[\left(\frac{R}{R+R} \right) - \left(\frac{R}{(R+dR)+R} \right) \right] = V_{in} \left[\frac{dR}{4R+2dR} \right]$$

Since the resistance change is very small ($2dR \ll 4R$) the term $2dR$ can be eliminated and we calculate dV_{out} as follows:

$$dV_{out} = V_{in} \left[\frac{1}{4} \times \frac{dR}{R} \right]$$

Then, the relative resistance change equation can be derived from the gauge factor equation as follows:

$$GF = \frac{dR/R}{dL/L} \rightarrow \frac{dR}{R} = GF \frac{dL}{L}$$

By using the resistance change and the gauge factor, the strain can be calculated as follows:

$$dV_{out} = V_{in} \left[\frac{GF}{4} \times \frac{dL}{L} \right], \varepsilon = \frac{dL}{L}$$

$$dV_{out} = V_{in} \left[\frac{GF}{4} \times \varepsilon \right]$$

$$\varepsilon = \frac{4 \times dV_{out}}{V_{in} \times GF}$$

For this study all values obtained from the strain gauges were placed in the equation below to calculate micro-strain values. As the voltage excitation for the Power Lab system is 2.5 volts ($V_{in} = 2.5$) the equation was modified to:

$$\varepsilon = \frac{2.5 \times dV_{out}}{GF}$$

All strain gauges had a gauge factor of 2.07. Therefore, by placing the value of the output voltage in the strain equation, the value of strain can be calculated.

Materials

Implants

Standard plus regular neck (\varnothing 4.8 mm) Straumann dental implants were used. Straumann Standard implants with a diameter of 4.8 mm can be used for all oral endosteal implant indications in the maxilla and mandible, for functional and aesthetic rehabilitation of edentulous and partially edentulous patients with a ridge width of at least 6.8 mm (Straumann Product Catalogue). The implant site allows for the shoulder of the implant (crown margin) to be positioned 1-2 mm apical relative to the neighbouring cemento-enamel junction. The implants are made from unalloyed grade 4 titanium (Straumann Product Catalogue) (table 1).

Chemical composition					
O	Fe	C	N	H	Ti
0.45% max.	0.3% max.	0.1% max.	0.05% max.	0.015% max.	Reminder
Mechanical Properties					
	Strength	Elongation	Modulus of elasticity		
Forged/annealed	550 MPa min.	20% min.	110 GPa		
Cold-Worked	800 MPa typically	10% min.	110 GPa		

Table 1: Chemical and mechanical properties of Straumann dental implant (Straumann product catalogue 2006)

Model

The model was made with a polyurethane based material. Easycast[®] is a two-component rigid urethane casting compound with a Shore hardness scale of 65D. Easycast[®] can be sanded, drilled, and ground. Easycast[®] accepts a wide range of fillers and can reproduce details because of its low viscosity prior to curing. This material is commonly used for architectural models, model kits, collectibles,

masters and prototypes. Table 2 shows the physical and handling properties of Easycast®.

Physical Properties		
Hardness	Shore D	65±2
Specific Gravity, Cured	[g/cc]	1.03
Colour		White
Ultimate Tensile	[psi]	4730
Elongation	[%]	9.4
Heat Deflection	[°C]	75
Shrinkage, Linear	[in/in]	0.0041
Handling Properties		
Mix Ratio	By Weight	Part A: 100 pbw Part B: 90 pbw
Mix Ratio	By Volume	Part A: 100 pbv Part B: 100 pbv
Viscosity	cps@25°C	Mixed: 60
Work Time	100g mass@ 25°C	2-2.5 minutes
Gel Time	100g mass @25°C	3-4 minutes
Demould Time	@25°C	15+ Minutes
Cure Schedule	7 days ambient or 16 hours @ 70°C	

Table 2: Physical and handling properties of Easycast®.

Alloy

Wironit® cobalt-chrome molybdenum partial denture alloy (free of nickel and beryllium) was used to fabricate the partial denture frameworks. Table 3 shows the composition, mechanical and physical properties of the alloy.

Composition	Co	64.0
	Cr	28.6
	Mo	5.0
	Si	1.0
Type	ISO 22674	5
Density	g/cm ³	8.2
Vickers hardness	HV 10	350
Modulus of elasticity	GPa	211
Elongation limit	MPa	600
Tensile strength	MPa	880
Ductile yield	%	6.2
Melting interval	°C	1320-1350
Casting temperature	°C	1460

Table 3: Composition, mechanical and physical properties of Wironit®

Attachments

Two Straumann retentive resilient ball attachments (Straumann, number 048.439) were used with a height of 3.4 mm. Titanium retentive anchors (Straumann, number 048.450) with a height of 3.1 mm were used. A torque driver (Straumann, number 046.069) was used to torque down the ball abutments. Eighteen millimeter transfer pins (Straumann, number 048.109) were used to transfer the exact positions of the abutments to the master cast.

Strain gauges

Vishay Micro-Measurements SR-4 general purpose strain gauges (Vishay Electronic GmbH, Germany) were used for this study. Vishay Micro-Measurements manufacture strain gauges with a wide temperature stability range, which utilize high purity nickel-foil sensing grids. Pure nickel has the least resistance-versus-temperature change sensitivity of the three most commonly used materials (nickel, copper, Balco) and is normally selected for span-versus-temperature compensation strain gauge of transducers. The temperature coefficient of resistance is +0.59% per degrees Celsius over a temperature range of +10 to +65 degrees Celsius (Vishay Technical Note Manual) (table 4).


Figure	Type	Nominal Resitances (Ω)	Dimension (mm): Length	Approx. Gauge Factor (%) @ 24°C
	3057 CEA-06-015UW-120	120	0.15	2.07±2.0

Table 4: Vishay strain gauge properties (Vishay technical manual)

Silicone

Deguform[®] was used to duplicate the models; Deguform[®] is an addition curing, two component silicone. A ratio of 1:1 for the catalyst (white) and curing agent (blue) was used. Deguform[®] has a Shore A hardness of 14-16 and linear contraction of 0.08% (DeguDent product manual).

Acrylic

Vertex[™] Castapress Crystal Clear self-polymerizing pour denture base material was used to make the denture base. Technical specifications of this material are shown in table 5.

Pouring time (at 22 ° C)	up to 3 minutes
Dough time (at 22° C)	6 minutes
Curing time	30 minutes at 55°C and 2.5 bar
Mixing ratio by volume /parts by weight	1 ml / 0.95 g liquid (monomer) 1.5 g powder (polymer)
Impact-resistance	9.7 kJ/m ²
Flexural strength	75 MPa
Flexural modulus	2293 MPa
Water sorption	22.1 µg/mm ³
Solubility	0.7 µg/mm ³

Table 5: Vertex[™] Castapress technical specification (Vertex[™] Dental webpage) (<http://www.vertex-dental.com/castapressCrystalClear>)

Die stone

GC Fujirock[®] EP (GC Europe N.V., Leuven, Belgium) was used to fabricate the master cast. GC Fujirock[®] is a type 4 dental stone with a setting expansion of 0.08% and a compressive strength of 53 MPa. The recommended water/powder ratio is 20 ml/100 g.

Refractory material

Wirovest[®] (BEGO, Bremer Goldschlägerei Wilh, Germany) investment material was used to fabricate the refractory model. BegoSol[®] (BEGO, Bremer Goldschlägerei Wilh, Germany) with 40% liquid concentration was mixed with Wirovest[®] powder with a powder/liquid ratio of 100g/15ml.

Chapter Four

Results

Results are presented according to different loading conditions. All tests are divided into two main groups: bilateral and unilateral. Each group was subjected to three different loading conditions: uniform loading, premolar loading and molar loading and strains were recorded on the fitting side of the metal framework and acrylic base. Typical strain-time plots for strain gauges were recorded. Each test was done 4 times and the mean micro-strain values are presented in figures 15 to 26. The maximum mean micro-strain was identified in each figure. Figures are colour coded with blue representing tension micro-strain and red compressive micro-strain. The more intense red or blue refers to higher mean micro-strain value and less colour intensity refers to lower value. Below in figure 14 is an image showing the locations of the different gauges.

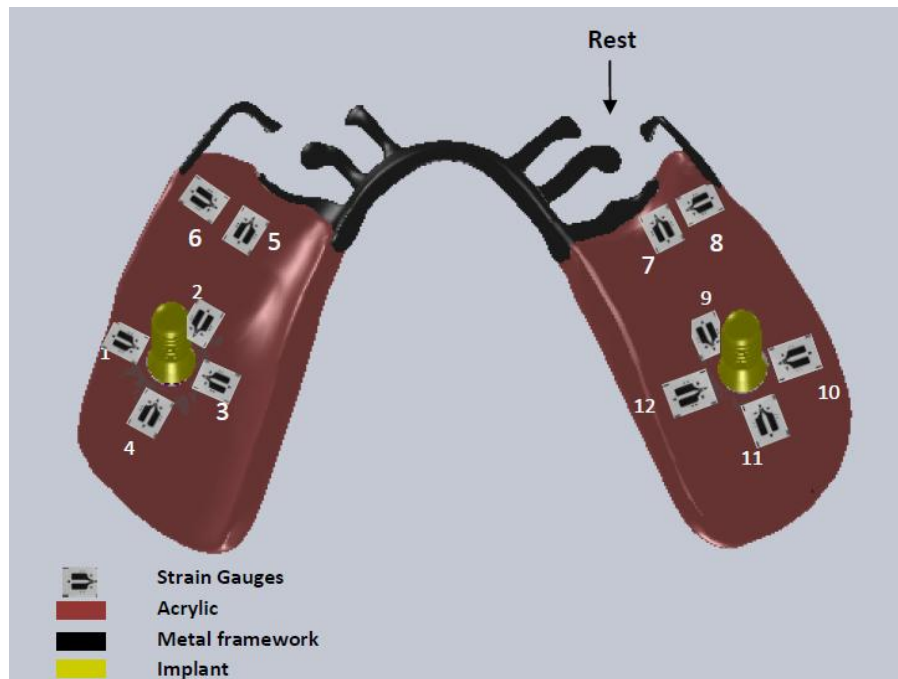


Figure 14: Strain gauge placement

Bilateral loading conditions

Micro-strain measurements at the acrylic base

Bilateral uniform loading

The strain gauges around the implants recorded the highest tensile strains. Gauges 10 and 12 recorded high tensile micro-strains. Gauge 10 had the largest tensile micro-strain value (figure 15). Blue outlines of increasing intensity were used on bar charts to highlight the strain gauges with larger tension strains and red outlines were used for larger compression strains.

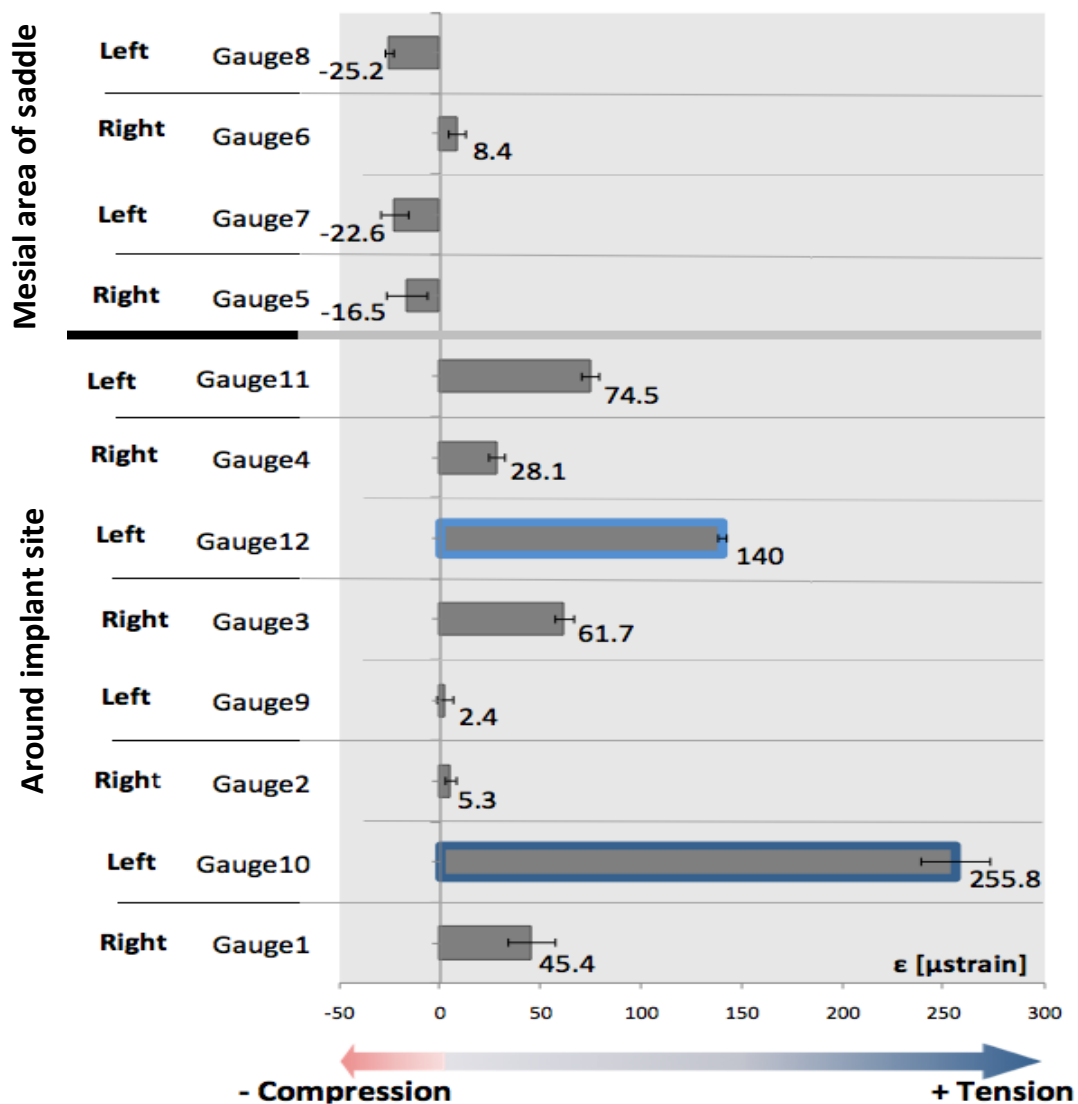


Figure 15: Maximum mean micro-strain measured on the acrylic base (bilateral uniform loading)

Bilateral premolar loading

In the bilateral premolar loading situation lower micro-strain values were recorded around the implants compared with those in the mesial area of the distal extension. All but one gauge showed tensile strain behaviour, with gauge 8 showing the largest value (figure 16).

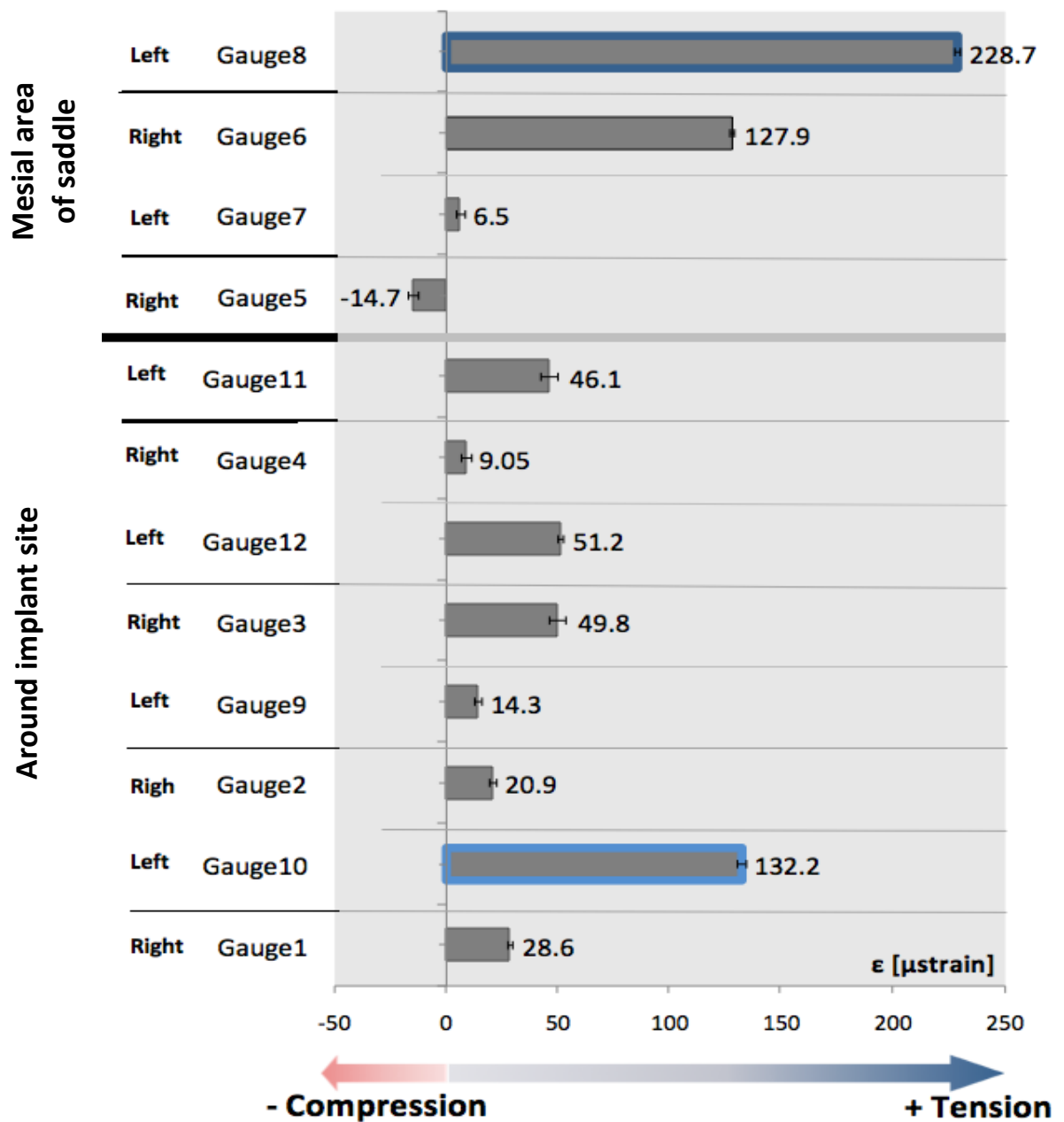


Figure 16: Maximum mean micro-strain measured on the acrylic base (bilateral premolar loading)

Bilateral molar loading

The strain pattern and direction produced by the bilateral molar loading exhibited high micro-strains value around the implant and mesial area of the distal extensions. The largest tensile micro-strain value was obtained from the gauge 10 on the buccal side of the implant (figure 17).

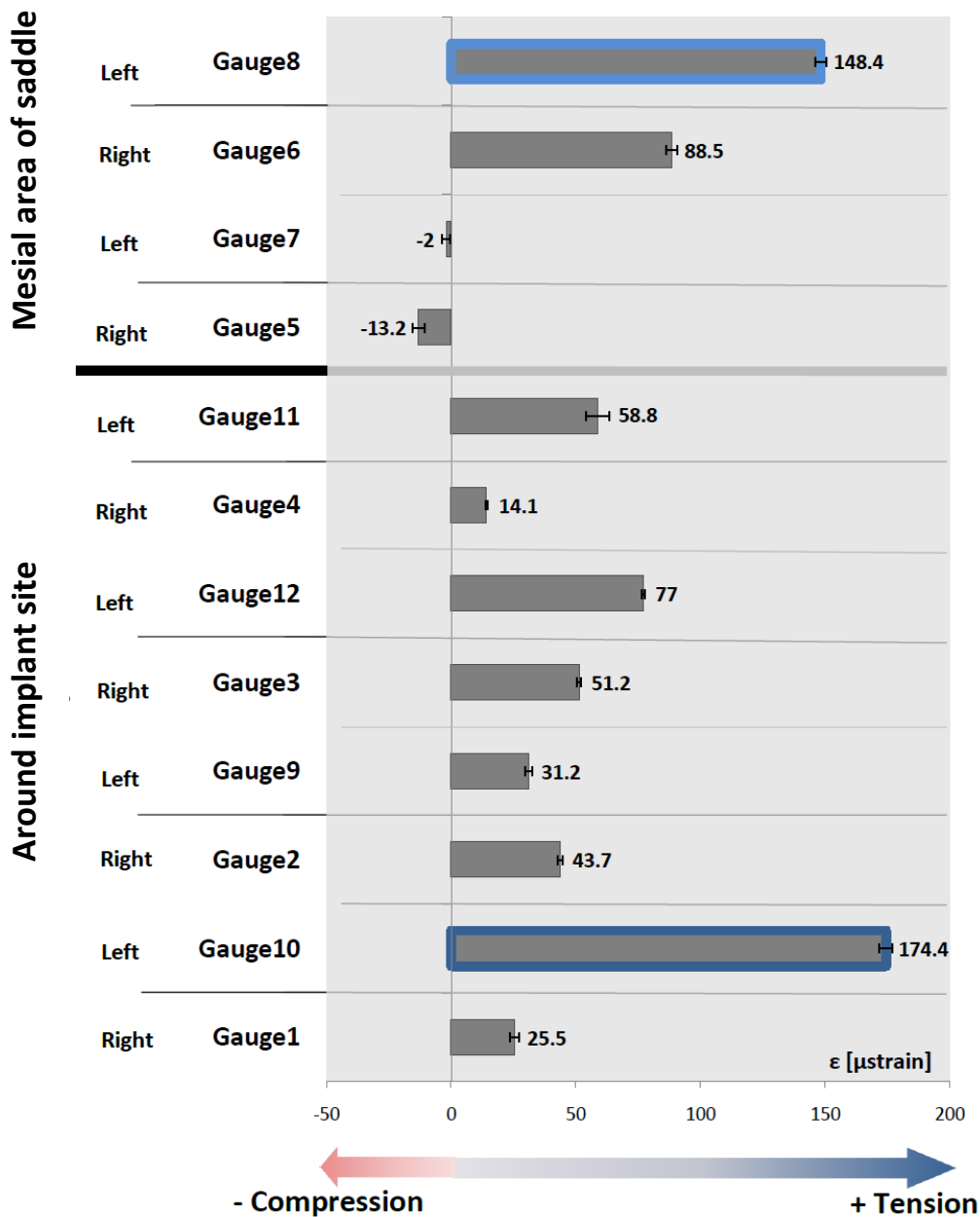


Figure 17: Maximum mean micro-strain measured on the acrylic base (bilateral molar loading)

Micro-strain measurements at the metal framework

Bilateral uniform loading

Gauge 6 showed the largest tensile micro-strain of 109.5, the corresponding gauge on the opposite side (gauge 8) also recorded a high tensile micro-strain of 59.5. Smaller values were measured by the gauges in the implant areas (gauges 1, 2, 3, 4, 9, 10 and 11) as shown in figure 18.

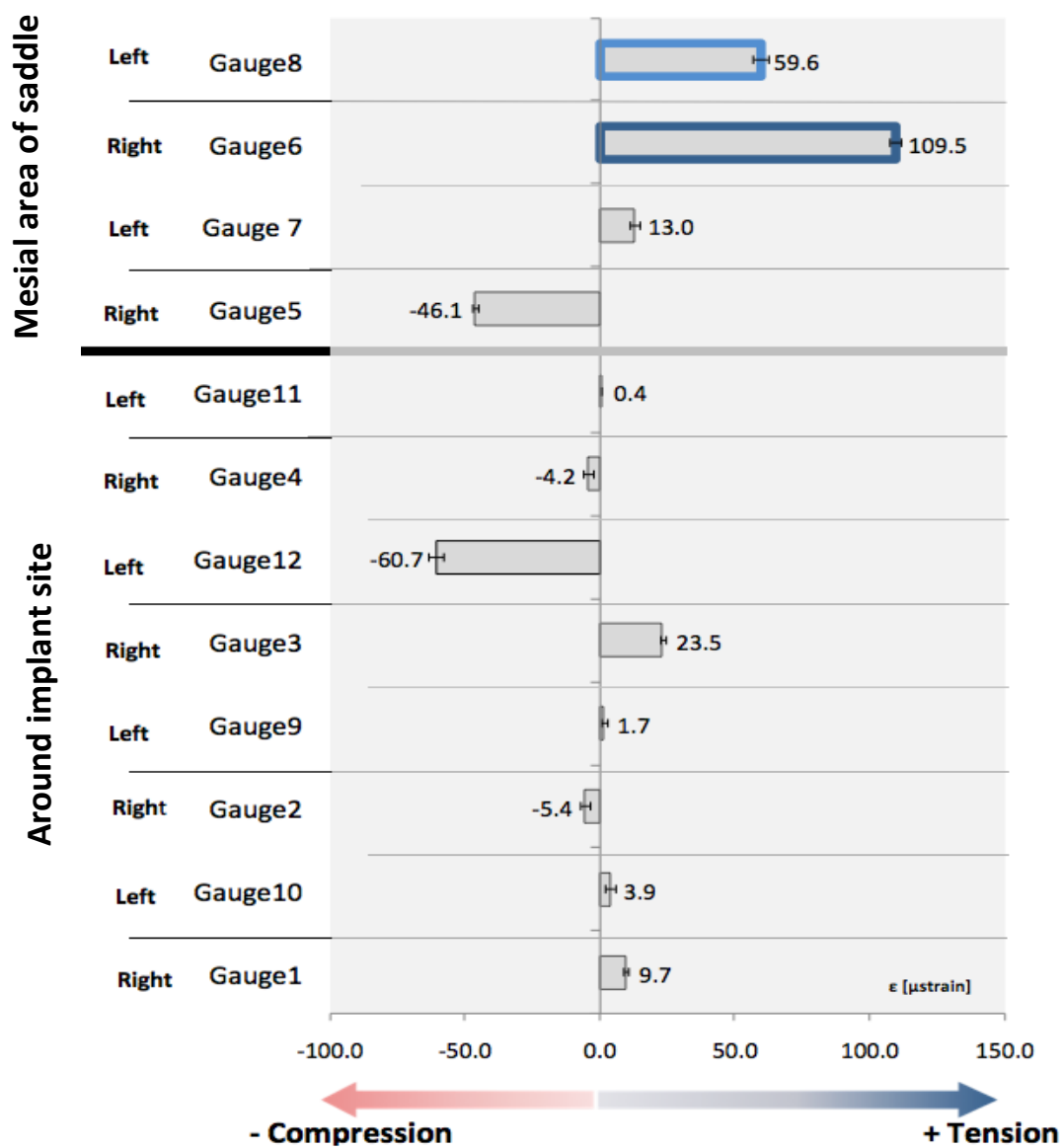


Figure 18: Maximum mean micro-strain measured on the metal framework (bilateral uniform loading)

Bilateral premolar loading

Similar to uniform loading, gauges 6 and 8 showed tensile strain behaviour, with gauge 6 showing the largest value (figure 19). Bilateral premolar loading produced lower micro-strain values around the implants compared with those at the mesial area of the distal extension.

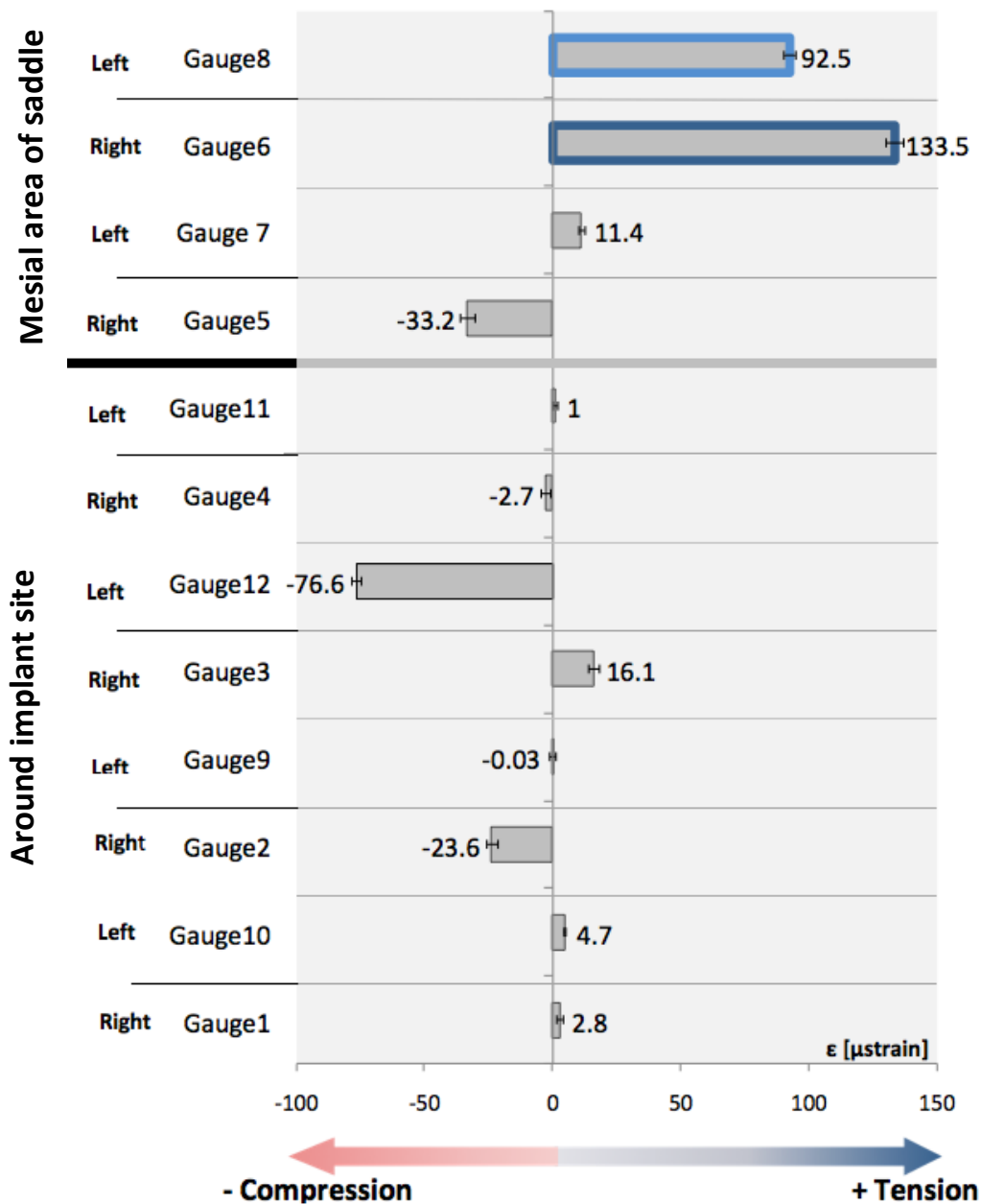


Figure 19: Maximum mean micro-strain measured on the metal framework (bilateral premolar loading)

Bilateral molar loading

The strain produced by bilateral molar loading showed high values around the implant and mesial areas of the distal extension. The largest tensile micro-strain value was obtained from gauge 6 in the mesial area of the distal extension (figure 20).

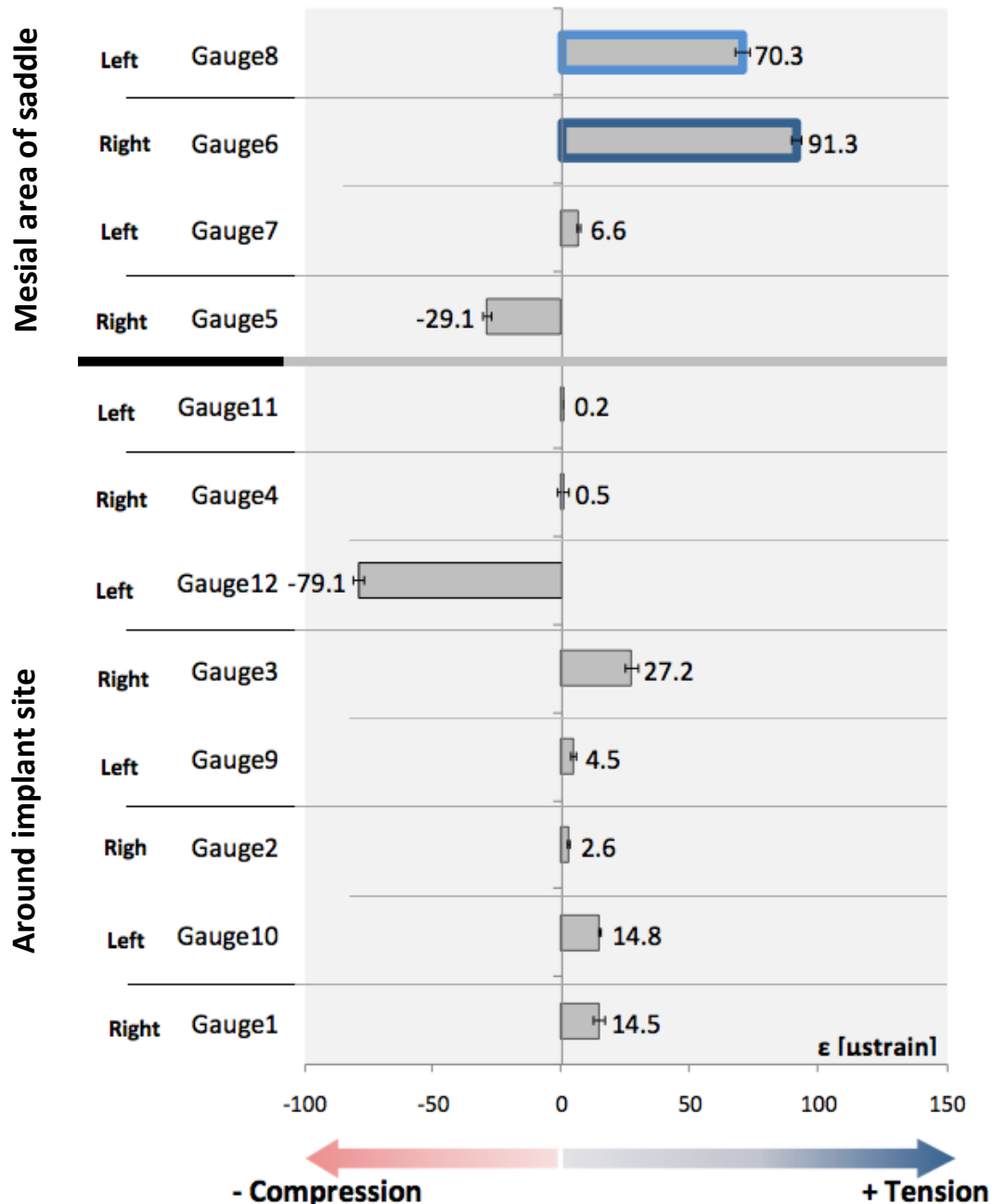


Figure 20: Maximum mean micro-strain measured on metal framework (bilateral molar loading)

Unilateral loading conditions

Micro-strain measurements at the acrylic base

Unilateral uniform loading

Lower strain values were generated by the uniform unilateral loading condition compared with bilateral loading. A tensile pattern of strain was observed around the implants, with the highest value recorded on the lingual side (figure 21). Gauge 6 recorded tensile micro-strain in the bucco-lingual direction.

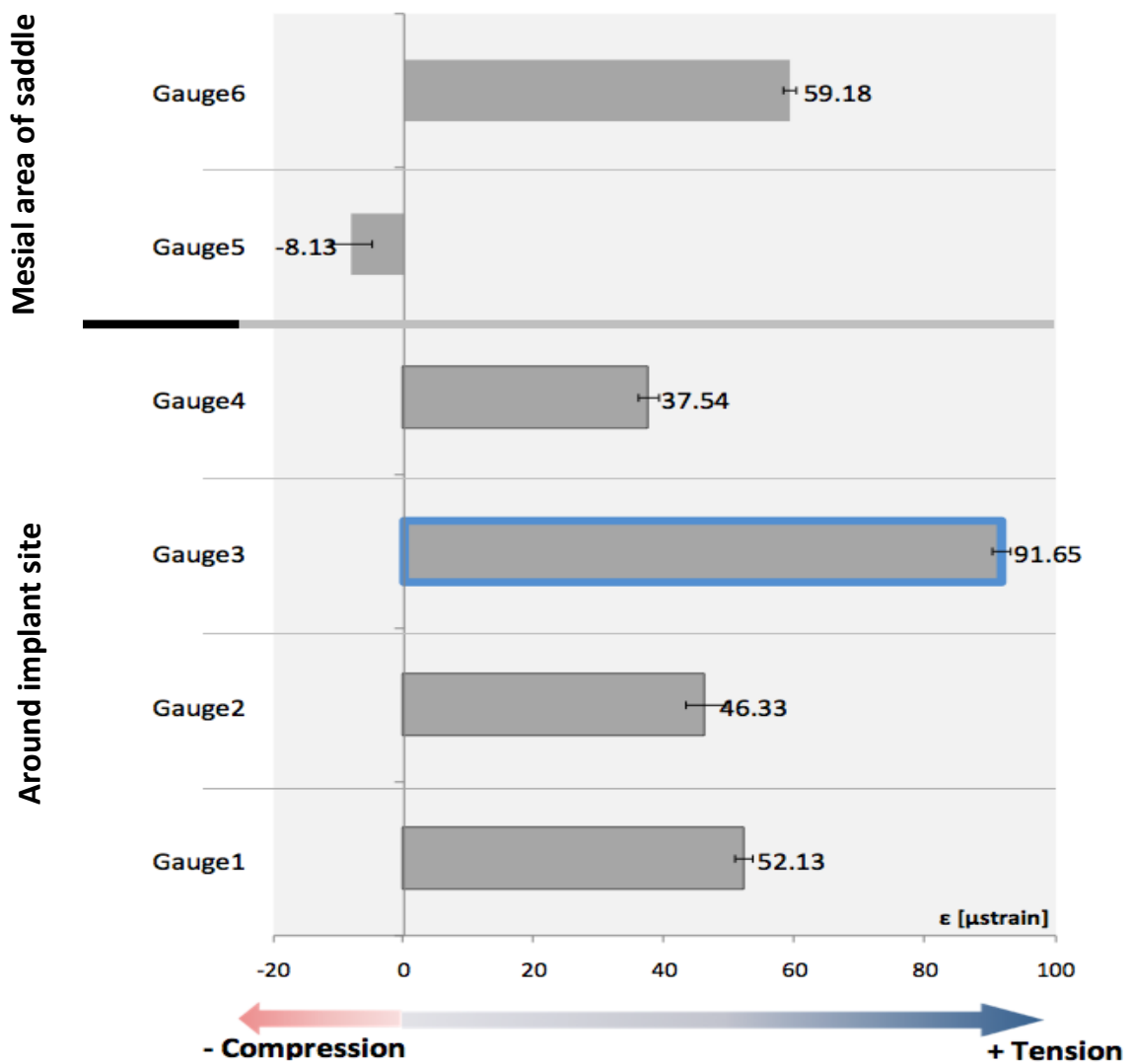


Figure 21: Maximum mean micro-strain measured on the acrylic base (unilateral uniform loading)

Unilateral premolar loading

Similar to the bilateral premolar loading condition, the strain gauges in the mesial area of the distal extension showed the highest deformation under unilateral premolar loading. The micro-strain values around the implants were the lowest among all the tested unilateral loading conditions. Both gauges number 4 and 2 showed small amounts of strain. This appears to be related to the forces directed away from the long axis of the ridge (figure 22).

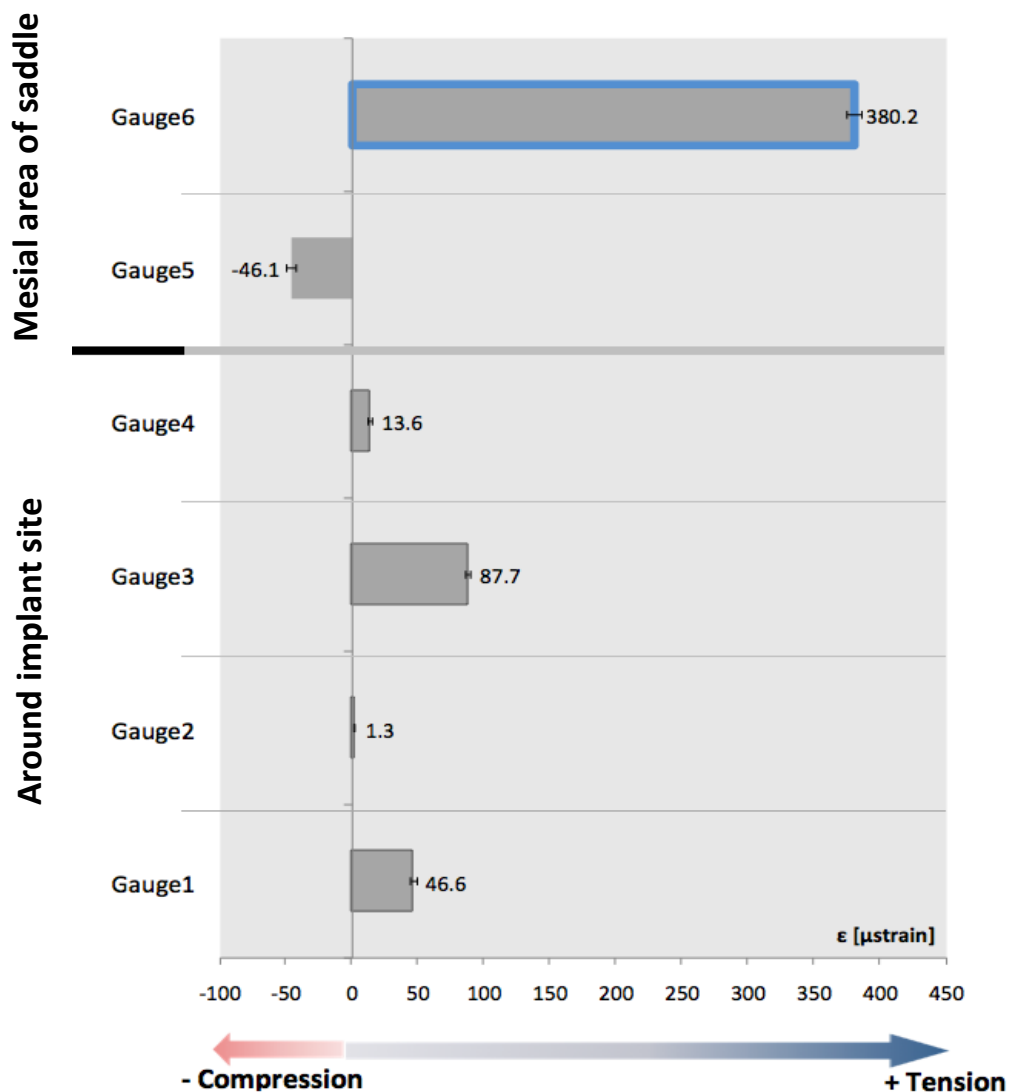


Figure 22: Maximum mean micro-strain measured on the acrylic base (unilateral premolar loading)

Unilateral molar loading

Under the molar loading condition, the largest micro-strain value was concentrated around the mesial area of the distal extension. This is similar to the unilateral premolar condition. However, the strain was more evenly distributed around the implant area (figure 23).

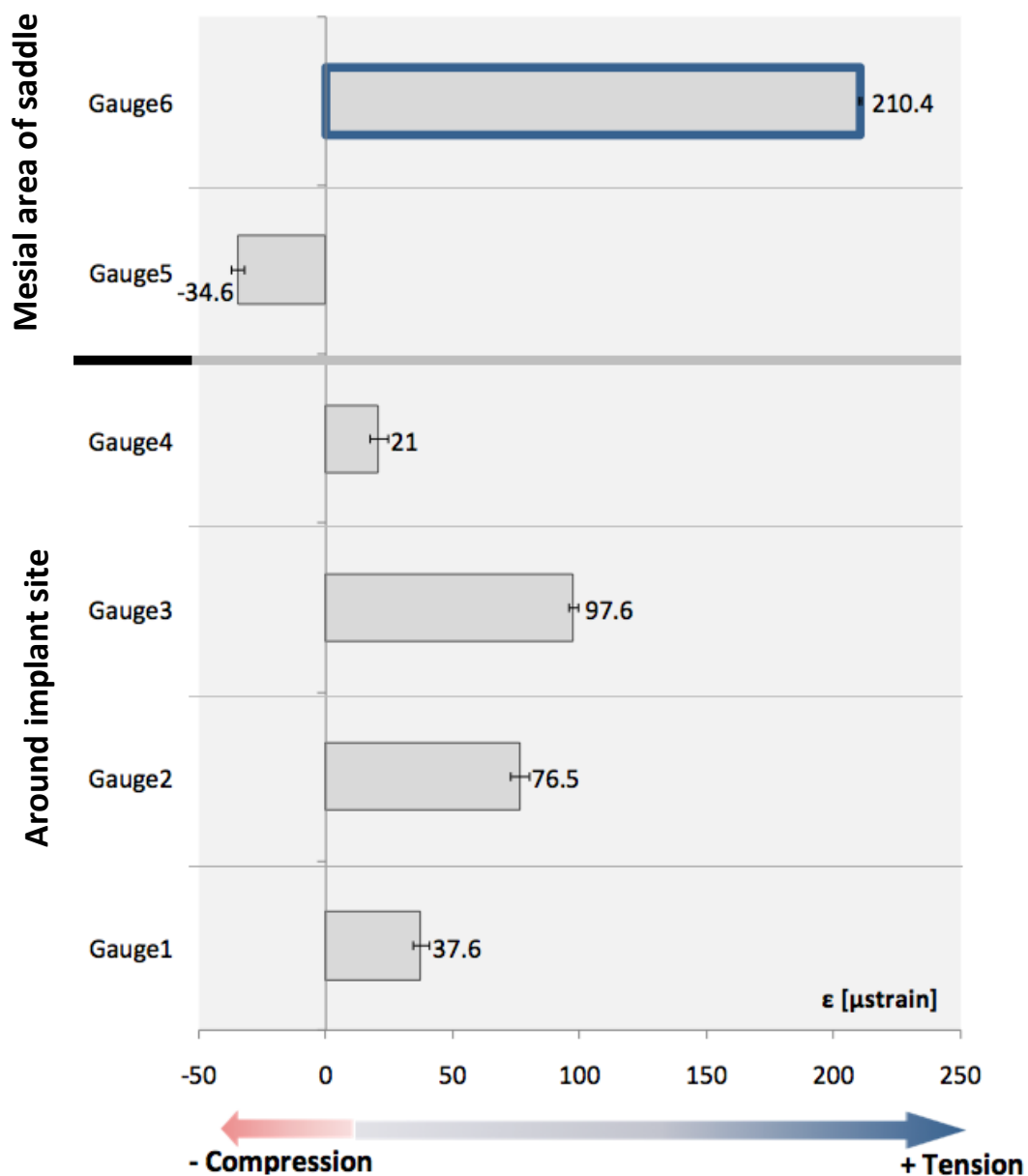


Figure 23: Maximum mean micro-strain measured on the acrylic base (unilateral molar loading)

Micro-strain measurements at the metal framework

Unilateral uniform loading

Lower strain values were generated by the uniform unilateral loading condition than the bilateral one on the metal surface. Compressive micro-strain was recorded around the mesial area of the distal extension with the highest value recorded on the buccal side (figure 24).

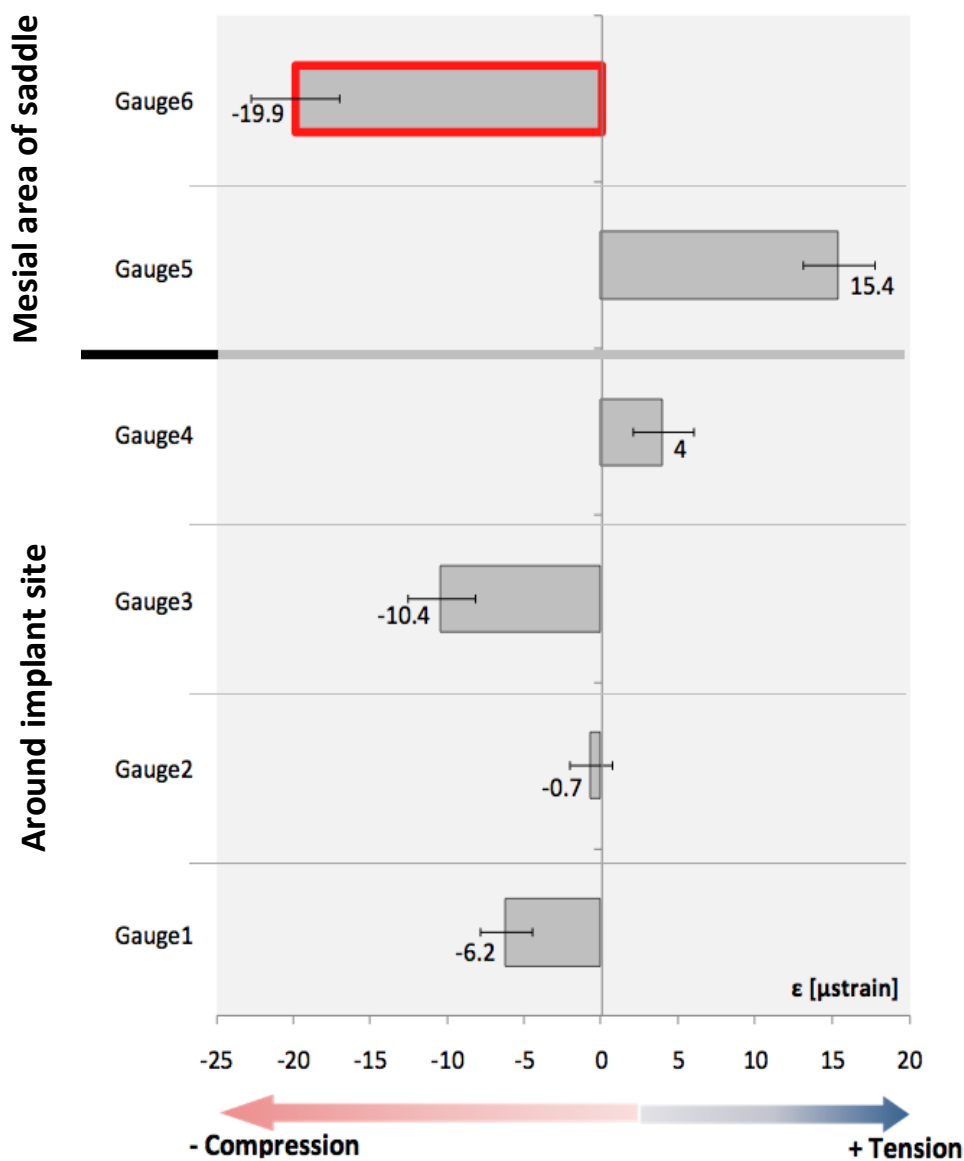


Figure 24: Maximum mean micro-strain measured on the metal framework (unilateral uniform loading)

Unilateral premolar loading

The unilateral loading condition recorded high compressive micro-strain around the mesial area of the distal extension, this is in contrast to bilateral premolar loading, where high tension micro-strain was recorded in the same area (figure 25).

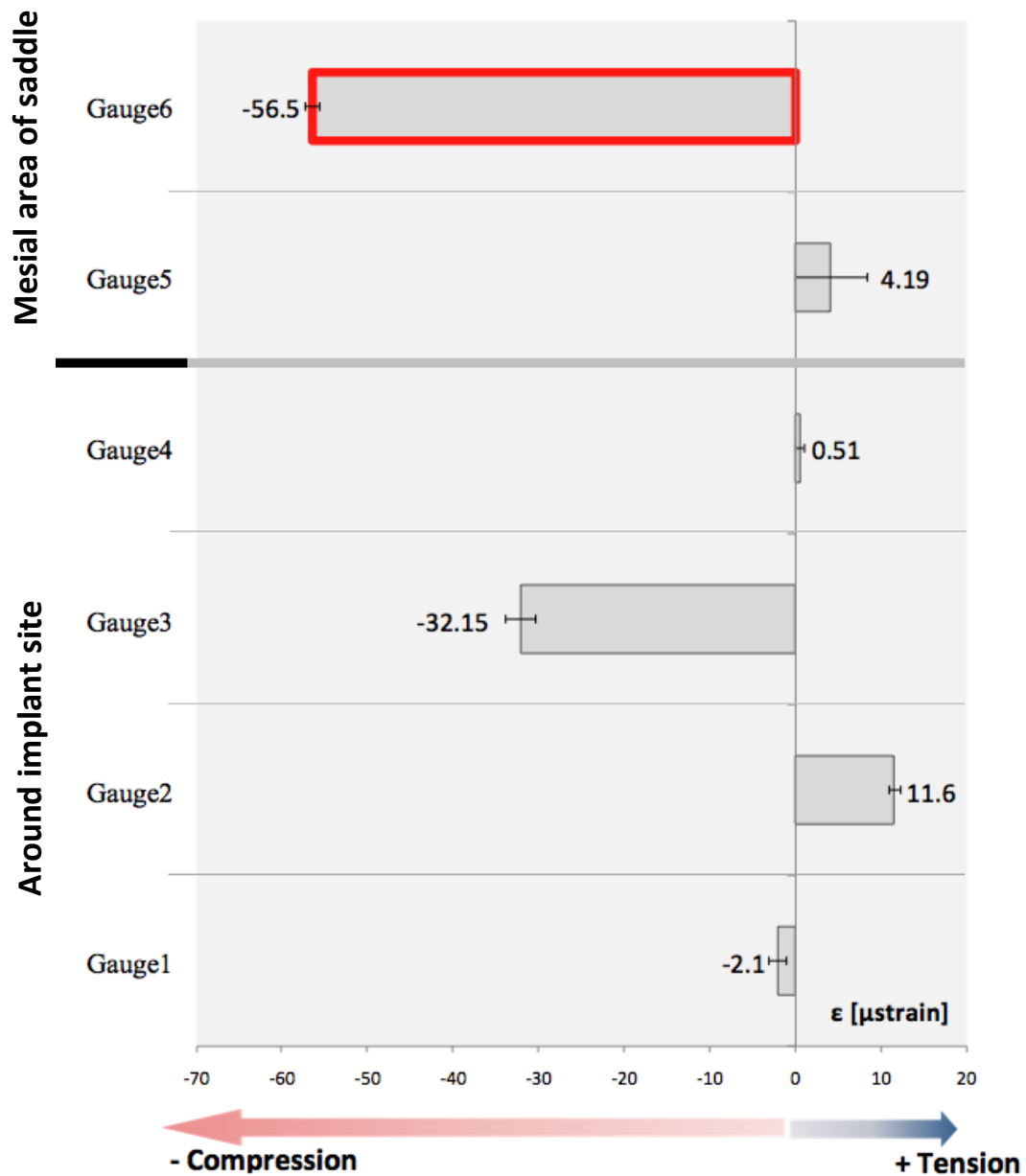


Figure 25: Maximum mean micro-strain measured on the metal framework (unilateral premolar loading)

Unilateral molar loading

Under the molar loading condition, the largest compressive micro-strain value was concentrated around the mesial area of the distal extension. This is similar to the unilateral uniform loading condition. However, the strains were less evenly distributed around the implant areas (figure 26).

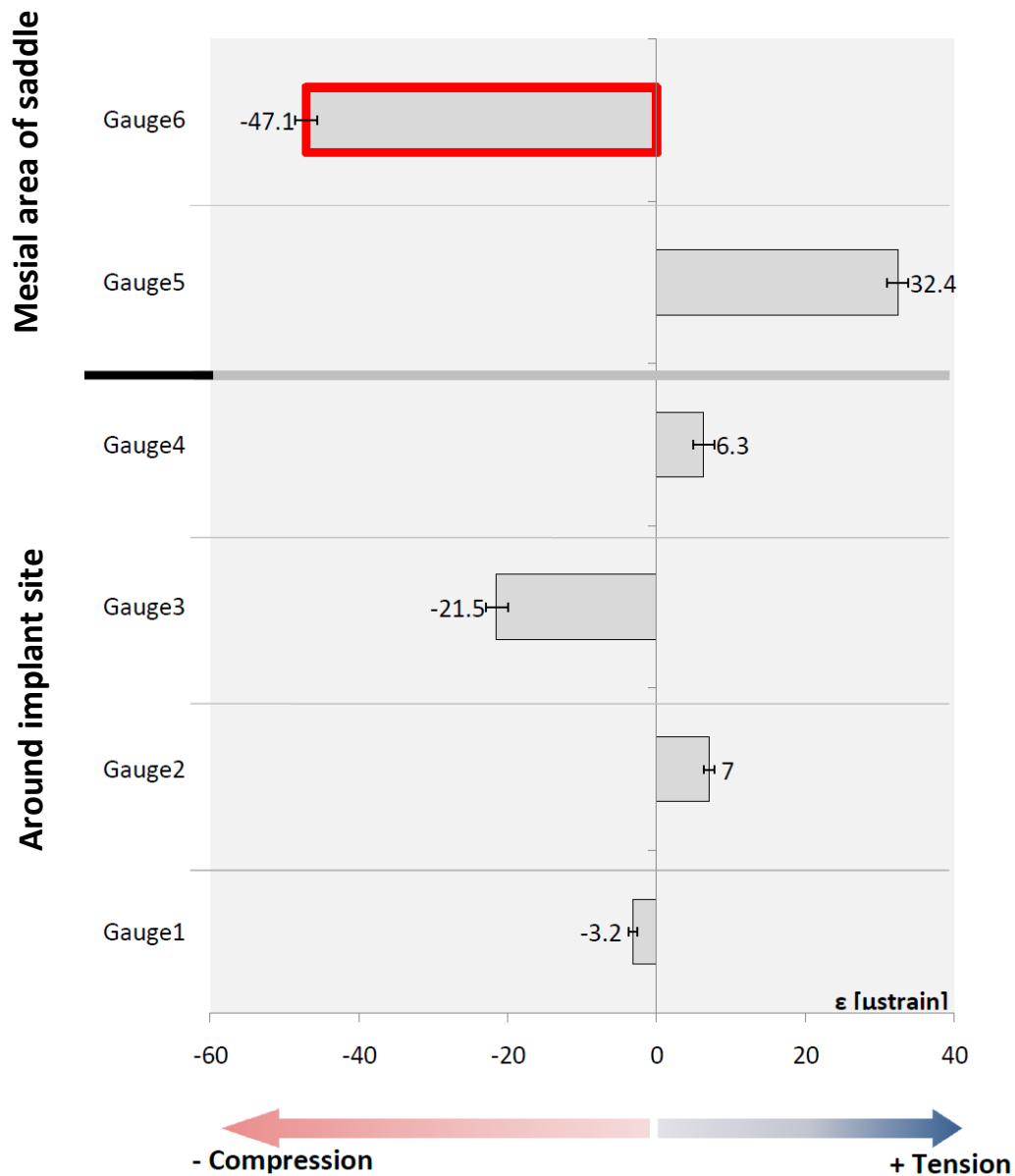


Figure 26: Maximum mean micro-strain measured on the metal framework (unilateral molar loading)

The differences in micro-strain values under different loading conditions

The differences in micro-strain values were analyzed in terms of the different loading regimes (uniform, premolar and molar loading) for both bilateral and unilateral loading conditions. Results of the largest mean micro-strain values are presented according to the site and direction of strain.

Because both implant and mesial areas of the distal extensions showed high micro-strain values under different loading conditions, it was important to identify whether the differences were statistically significant. Statistical analysis was performed with SPSS 18.0 (SPSS, Inc., Chicago, IL, USA) to compare maximum micro-strain values in all three loading conditions. ANOVA was used to compare maximum mean micro-strain values identified in each loading condition (table 6).

A comparison of the maximum mean micro-strain values between the three different loading regimes showed a highly significant increase in the recorded mean micro-strain value ($p < 0.001$) around the mesial area of the distal extension in the bucco-lingual direction as the loading point moved forward. In contrast, a significant decrease of the mean micro-strain values ($p < 0.001$) was observed in the bucco-lingual direction around the implant area as the loading point moved forward (table 6).

Load	Area	Site	Uniform		Molar		Premolar		df	P-value
			Max. Mean (N=4)	SD	Max. Mean (N=4)	SD	Max. Mean (N=4)	SD		
Bilateral	Rest	BL (gauge 8)	-25.2	2.09	148.4	2.31	228.7	1.37	2	<0.001*
	Implant	BL (gauge 10)	255.8	15.19	174.4	2.72	132.2	2.01		<0.001*

SD: Standard Deviation, *: Significant at $P \leq 0.05$

Table 6: Statistical comparison of maximum micro-strain values of three loading conditions

A correlation analysis in figure 28 shows the reverse correlation when moving the load forward with an increase in the maximum micro-strain value ($R = - 0.985$). During the bilateral loading conditions, molar loading showed more even distribution of micro-strain value around both the mesial of the distal extension and implant areas on the acrylic surface.

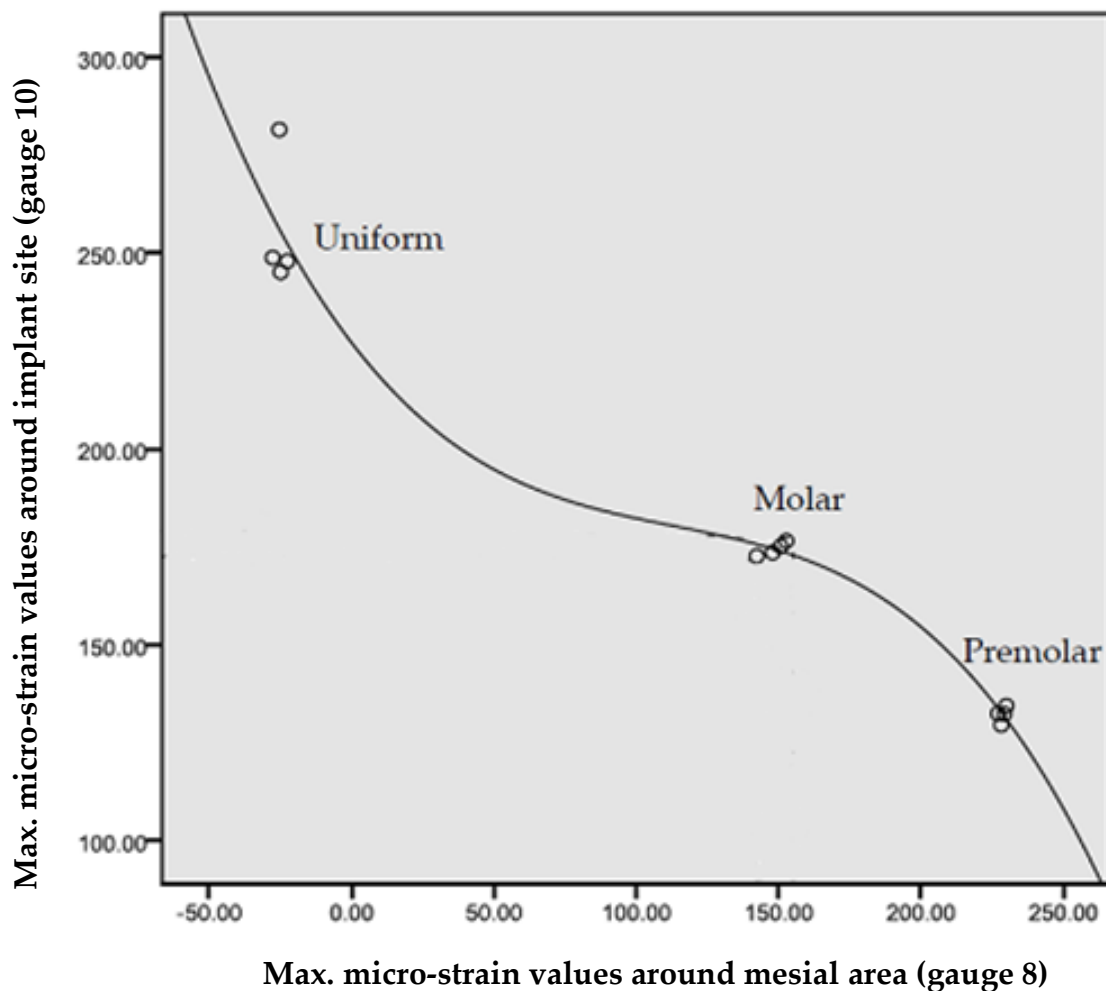


Figure 28: An inverse correlation between maximum micro-strain in bucco-lingual direction in mesial area of the distal extension versus around the implant as the loading point moves forward

Micro-strain behaviour of metal framework (bilateral loading conditions)

The bilateral loading showed the highest micro-strain value around the mesial area of the distal extension on the metal surface. The highest micro-strain value remained in the mesial area of the distal extension as the loading point moved forward. As the loading point moved forward, the micro-strain values increased around the mesial area of the distal extensions. The highest micro-strain value exhibited was in the bucco-lingual direction around the mesial area of the distal extension (figure 29).

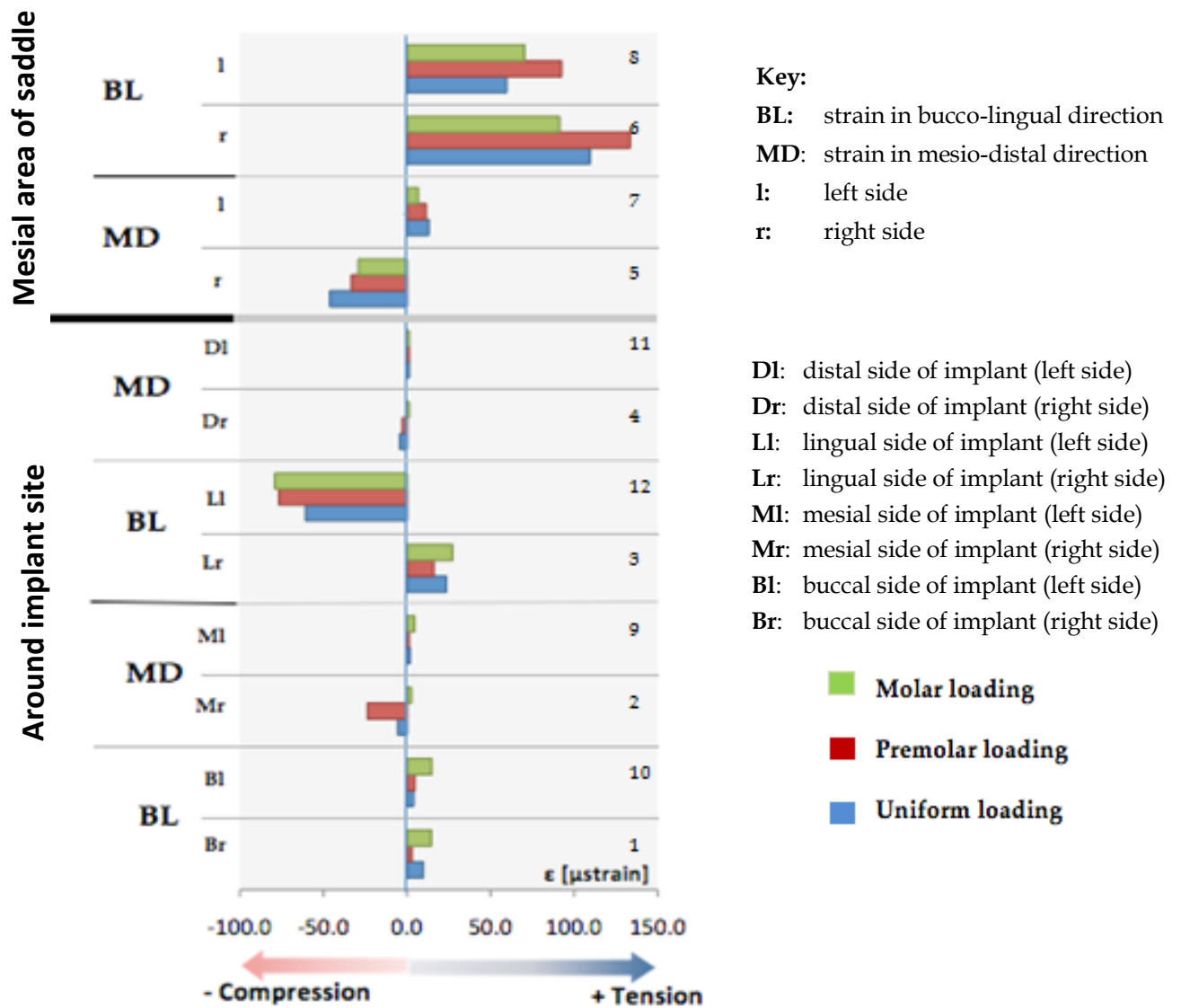


Figure 29: Micro-strain values for metal framework (bilateral loading conditions)

Statistical analysis of the highest micro-strain values of all three loading conditions showed that there were significant differences ($p < 0.001$) in the mesial area of the distal extension in the bucco-lingual direction (table 7).

Load	Area	Site	Uniform		Molar		Premolar		df	P-value
			Max. Mean (N=4)	SD	Max. Mean (N=4)	SD	Max. Mean (N=4)	SD		
Bilateral	Rest	BL (gauge 6)	109.5	2.09	91.3	1.96	133.5	3.43	2	<0.001*

SD: Standard Deviation, *: Significant at $P \leq 0.05$

Table 7: Statistical analysis of gauge 6 maximum mean micro-strain values for all three bilateral loading conditions

The maximum micro-strain values in the mesial area of the distal extension (gauge 6) are shown in figure 30 to illustrate consistency of data and enable comparisons with similar areas on the acrylic surface. Among the three loading conditions, molar loading showed the lowest micro-strain values (figure 30) which were a better match than corresponding maximum micro-strain recorded on the acrylic surface during uniform and premolar loading micro-strain (figure 28).

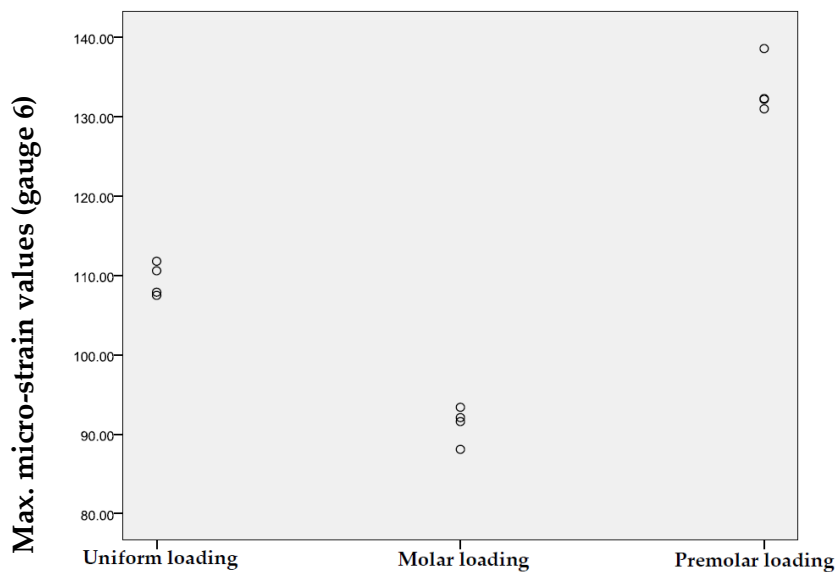


Figure 30: Maximum mean micro-strain values of metal surface for all three bilateral loading conditions (gauge 6)

Micro-strain behaviour of acrylic base (unilateral loading conditions)

Unlike bilateral loading, the recorded micro-strain values generated by the unilateral loading, showed more consistency between uniform, premolar and molar loadings. In the three loading conditions, the highest recorded values of tension micro-strain were observed around the mesial area of the distal extension in the bucco-lingual direction (figure 31).

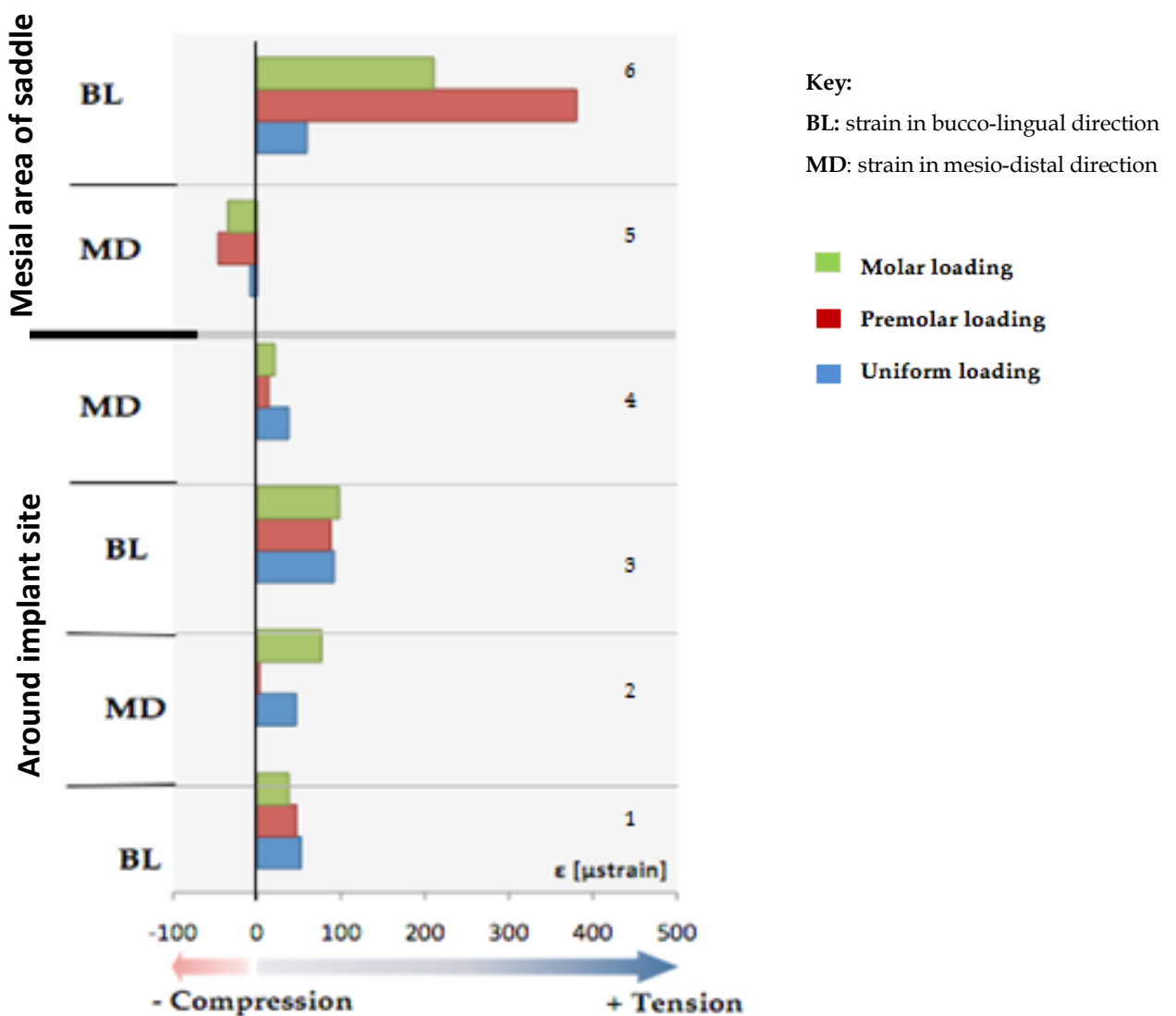


Figure 31: Micro-strain values for acrylic base (unilateral loading conditions)

Maximum mean micro-strain values were recorded in the mesial area of the distal extension in the bucco-lingual direction during molar and premolar loading, whereas in uniform loading, maximum micro-strain values were recorded around the implant in the bucco-lingual direction. There were significant differences ($p<0.001$) between the maximum micro-strain value of the three loading conditions (table 8).

Load	Area	Site	Uniform		Molar		Premolar		df	P-value
			Max. Mean (N=4)	SD	Max. Mean (N=4)	SD	Max. Mean (N=4)	SD		
Unilateral	Rest	BL (gauge 6)	59.18	0.99	210.4	0.53	380.2	5.62	2	<0.001*
	Implant	BL (gauge 3)	91.65	1.4	97.6	1.82	87.7	1.85		<0.001*

SD: Standard Deviation, *: Significant at $P \leq 0.05$

Table 8: Statistical analysis of maximum mean micro-strain of all three loading conditions

A correlation analysis was carried out between the maximum micro-strain of two areas around the implant and mesial areas of the distal extension as the loading point moved forward. This indicated the maximum micro-strain moved to the mesial area of the distal extension and continued to increase in the same area. The micro-strain was more evenly distributed in both areas in uniform loading and showed a lower micro-strain value compared with the other two loading conditions (figure 32).

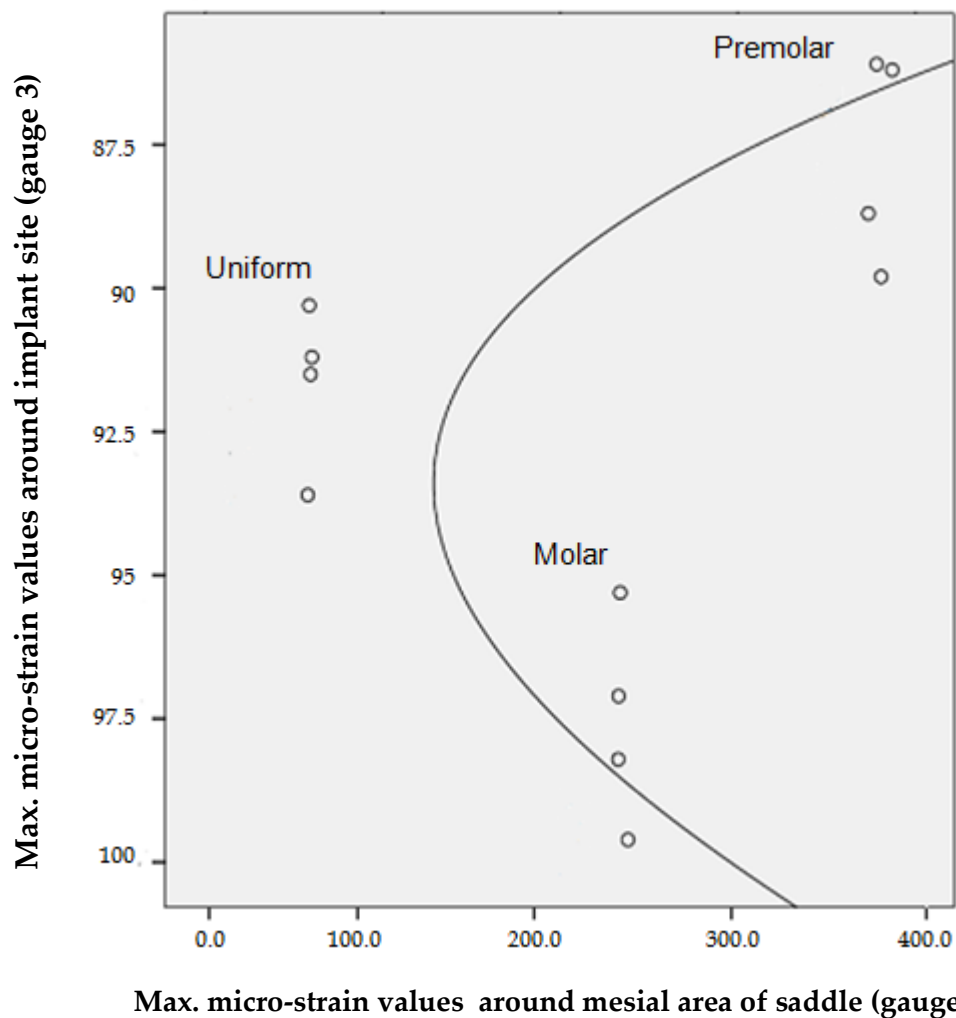


Figure 32: Direct correlation between movement of the loading point forward and location of maximum micro-strain

Micro-strain behaviour of metal framework (unilateral loading conditions)

Similar to bilateral loading, the recorded micro-strain values generated by the unilateral loading were highest around the mesial area of the distal extension. However, in terms of compression and tension the pattern was different (figure 33).

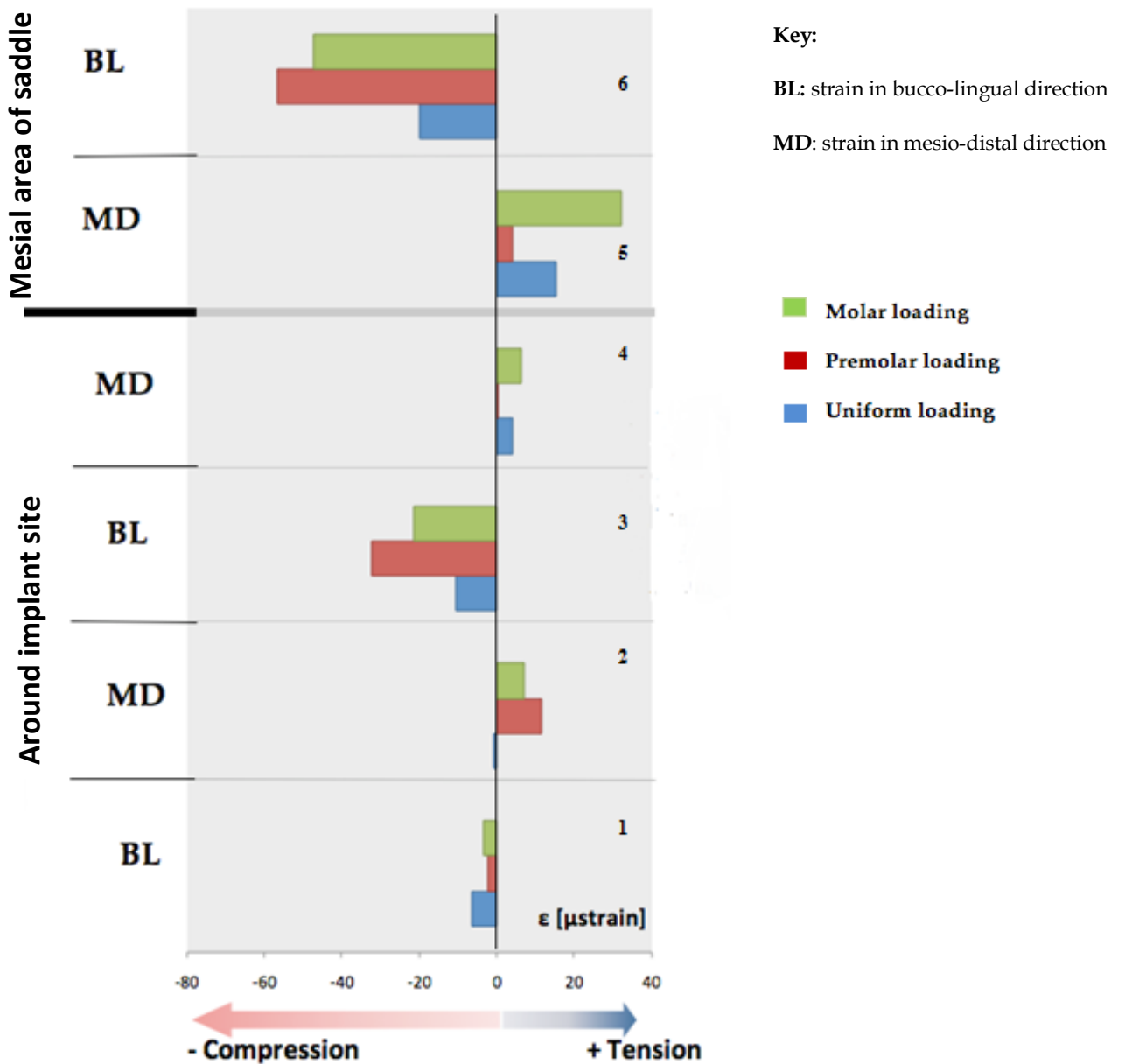


Figure 33: Micro-strain values for metal framework (unilateral loading conditions)

In the three loading conditions, the highest micro-strain values were recorded around the mesial area of the distal extension. There were a significant differences ($p<0.001$) between the maximum micro-strain values of all three loading conditions, and as the loading point moved forward there was a significant increase in the compression micro-strain (table 9).

Load	Area	Site	Uniform		Molar		Premolar		df	P-value
			Max.Mean (N=4)	SD	Max.Mean (N=4)	SD	Max.Mean (N=4)	SD		
Unilateral	Rest	BL (gauge 6)	-19.9	2.87	-47.1	1.51	-56.5	1.76	2	<0.001*

SD: Standard Deviation, *: Significant at $P \leq 0.05$

Table 9: Significant differences in mean maximum micro-strain exhibited between all three loading conditions

Uniform loading resulted in less micro-strain in the area around the implant and mesial area of the distal extension, with more evenly distributed micro-strain in both areas (figure 34). Uniform loading created more favourable micro-strain distribution in both framework and acrylic base.

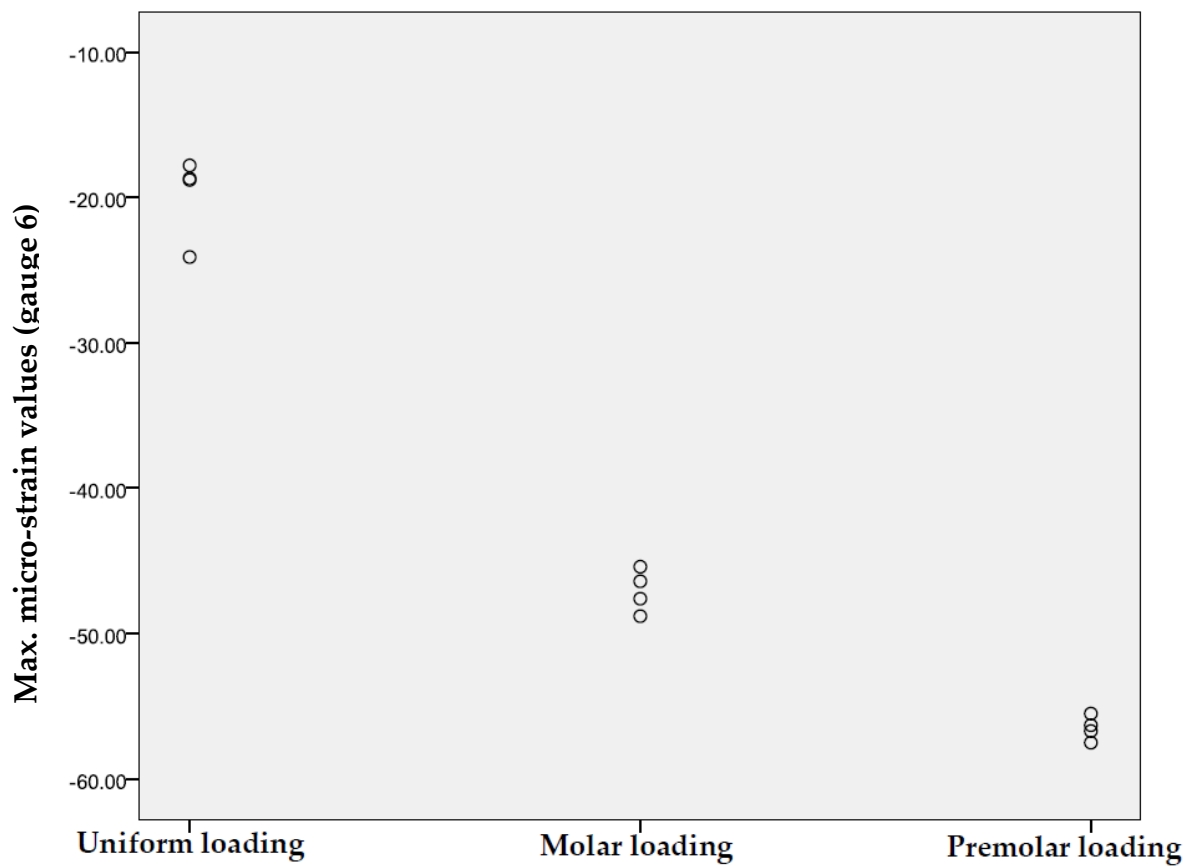


Figure 34: Direct correlation for the value and location of the maximum micro-strain upon moving the loading point forward

Micro-strain behaviour of metal framework and acrylic base (bilateral loading conditions)

For all bilateral loading conditions, maximum micro-strain values, for the framework and acrylic base were compared. This was done to identify the most favourable loading condition. Unscrambler X V10.1 software (The Unscrambler X, Camo, Norway) was used to draw a 3D scatter plot graph. The molar loading condition showed less micro-strain and the best matching micro-strain behaviour between both surfaces (figure 35).

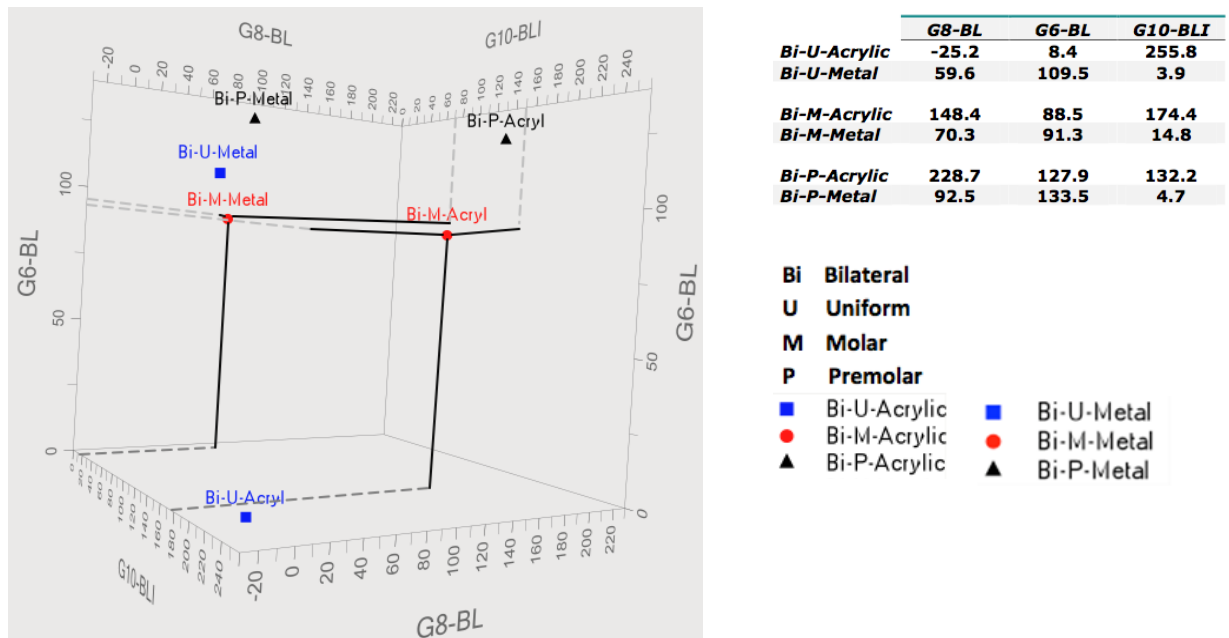


Figure 35: Comparison of micro-strain values in both metal framework and acrylic base (bilateral loading conditions)

Micro-strain behaviour of metal framework and acrylic base (unilateral loading conditions)

The uniform unilateral loading showed lesser micro-strain value in both framework and acrylic structure with more evenly distributed micro-strain value than premolar and molar loadings. However, mismatch of strain type (tension in acrylic surface and compression in framework surface) was evident in all unilateral loading condition (figure 36).

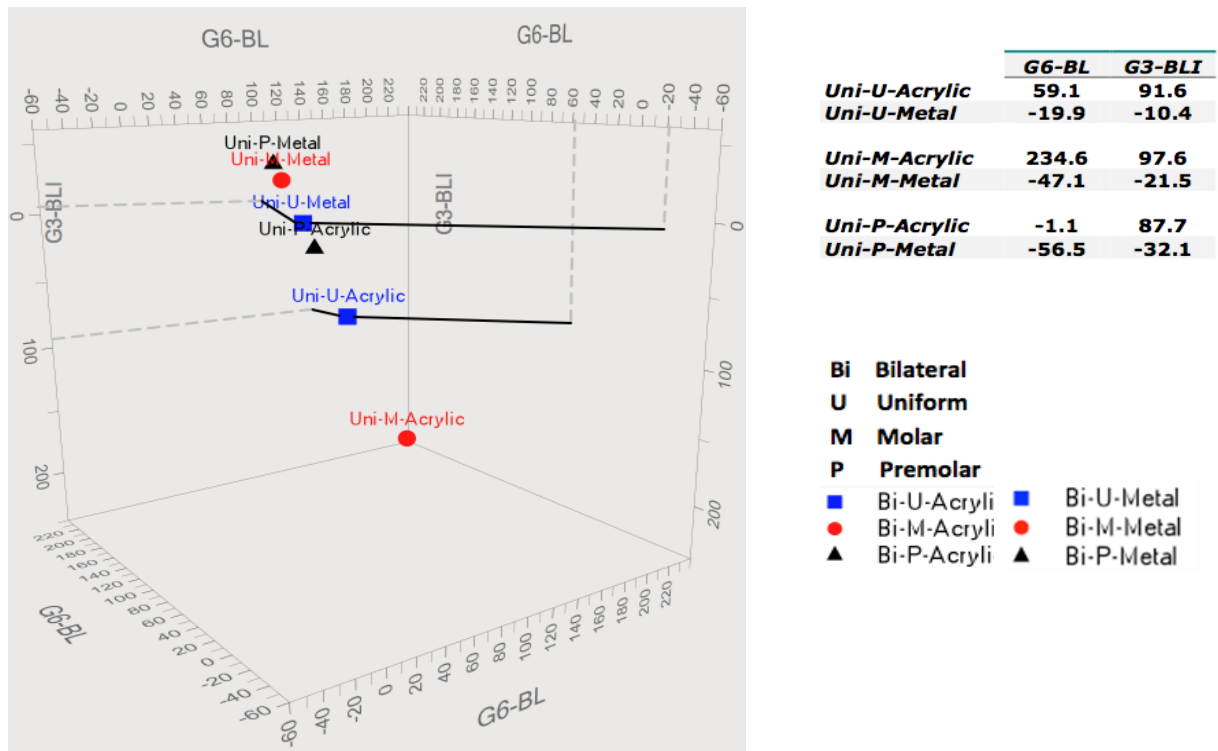


Figure 36: Comparison of micro-strain values in both metal framework and acrylic base (unilateral loading conditions)

Chapter Five

Discussion

Fracture of acrylic denture bases has been reported as a complication of the mandibular bilateral distal extension IARPD where oral implants are incorporated into an existing RPD opposing a maxillary complete denture (Payne *et al.*, 2006). Although the implant-tooth borne RPD and the conventional designs are subjected to similar masticatory movements, the occlusal forces are greater and more distally located in the former design (Ohkubo *et al.*, 2008).

A bilateral balanced occlusion engages contacts on the non-working side to prevent the prosthesis from being dislodged during function (Jambhekar *et al.*, 2010). Although the placement of implants in the posterior area of a distal extension will limit the prosthesis dislodgment, the general balanced occlusion concept may still be appropriate for a mandibular IARPD when the opposing maxillary arch is fully edentulous or the maxillary opposing arch is a Kennedy Class I/II (Wismeijer *et al.*, 1995).

This study used different loading conditions, unilateral and bilateral, with three different loading areas; premolar, molar and uniform. These loading conditions were used because the prosthesis can be subjected to similar situations during function. However mastication is more complex and it was not the aim of this study to simulate masticatory function. It would not have been possible to simulate the masticatory situation due to the complexity of loading, and the many

different loading combinations that would have been required. This investigation aimed to identify the influence of the premolar, molar and uniform loading conditions to give an understanding of the general strain developed in the IARPD structure.

This study has certain limitations: (1) the strain gauges used measured only the surface micro-strain at one point and in one direction; (2) the micro-strain patterns developed in IARPDs are complex; (3) the implant osseointegration and the physiological mobility of the abutment teeth was not considered; (4) The implant fixture on one side was placed more towards the buccal and this could have influenced the magnitude of micro-strain generated on that side. However, it had no effect on the direction of micro-strain as both sides showed a similar direction of micro-strain.

The IARPD has raised concerns with regard to stresses on bone, implant components and restorative materials (Cibirka *et al.*, 1992). This research was conducted to better understand the influence of the loading conditions of mandibular distal extension IARPD by directly measuring the micro-strain at the metal framework level and the acrylic base level. Micro-strain was measured in two main areas, around the implant and in the mesial area of the distal extension. It was evident that the highest micro-strain values in the acrylic base followed the loading point as it moved forward. In contrast, the metal framework behaved differently as the highest micro-strain values remained in the mesial area of the distal extension, regardless of the loading condition. Figures 21 to 23 in the

previous chapter show that the micro-strain values on the acrylic base increased by up to six times in the unilateral loading groups as the loading point moved forward. In this chapter the bilateral loading condition will be discussed first, followed by unilateral loading.

Bilateral loading of metal and acrylic

For the uniform bilateral loading condition, the highest micro-strain value was identified in the labial area around the left implant on the acrylic surface in the bucco-lingual direction. Figure 37 is an illustration of a cross-section of the implant areas of the prosthesis.

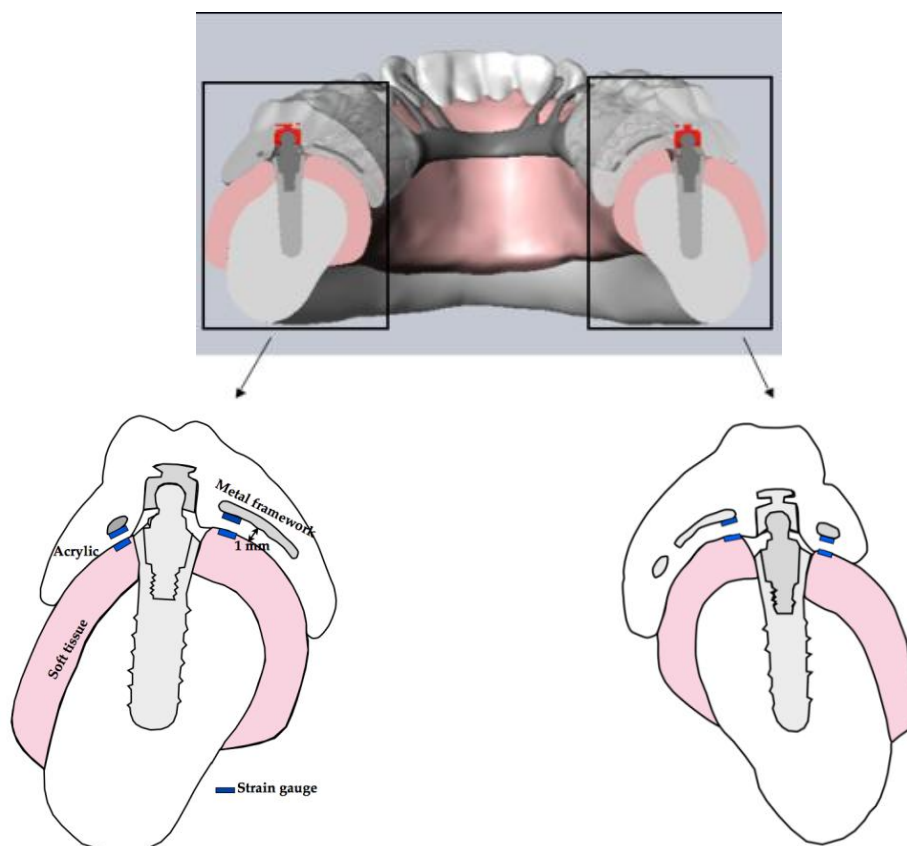


Figure 37: Cross-section illustration of the areas around the implants in coronal plane, showing the locations of the micro-strain gauges on the acrylic and metal structures.

The lingual side of the left implant showed the next highest micro-strain value in a similar direction. The areas and directions of micro-strain on the acrylic surface around the implant during the bilateral uniform loading are shown in figure 38. Blue represents tension micro-strain and the intensity of the blue is representative of a higher micro-strain value.

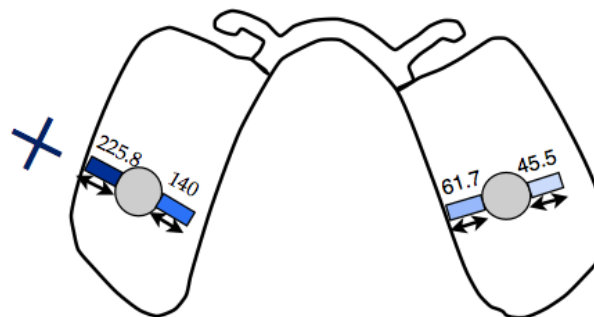


Figure 38: Highest micro-strain value acrylic base recorded on labial side of left implant during bilateral uniform loading

Although areas around both implants showed tension micro-strain in the bucco-lingual direction, on the right side of the prosthesis the higher micro-strain value was recorded on the lingual side of the implant. The position of the implant might have contributed to the change in the micro-strain. However, the area of maximum micro-strain remains in the bucco-lingual direction on both sides of the prosthesis, regardless of the position of the implant.

Placing the implant more buccally or more lingually resulted in the placement of the micro-strain gauges slightly further down the ridge incline on one side. Thus, one side of the denture came in contact with the soft tissue earlier than the other side. This is more evident from the graphical output for each of the micro-strain

gauges (figure 39 & 40). The micro-strain-time graphs show a change in the slope of the loading curve at different time points. In the case of gauge 1, contact occurred after 12 seconds, whereas for gauge 10 this took place after 19 seconds. This change of slope at initial commencement of loading occurs because of the contact between the acrylic denture and the underlying soft supporting tissue which takes place at different times.

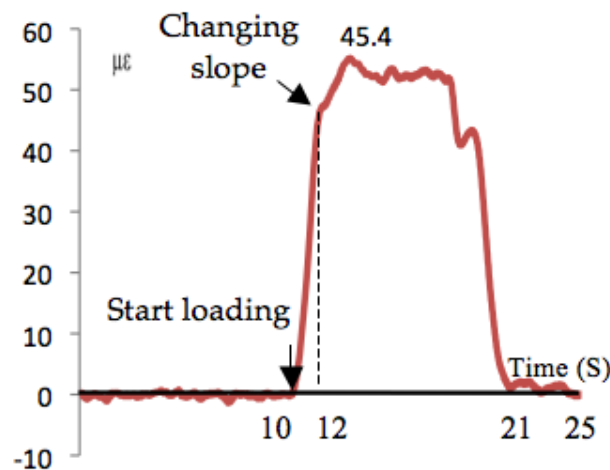


Figure 39: Micro-strain-time plot of gauge 1 on buccal side of right implant during bilateral uniform loading

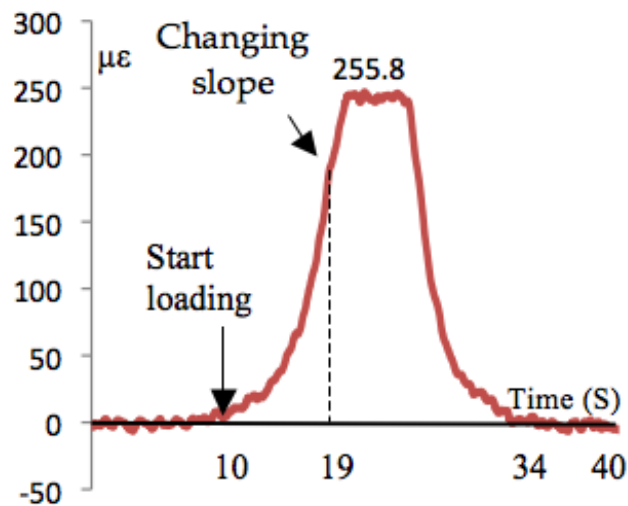


Figure 40: Micro-strain-time plot of gauge 10 on buccal side of left implant during bilateral uniform loading

The micro-strain-time plot for gauge 1 shown in figure 41 provides further information about the micro-strain behaviour during loading, and unloading, as well as the maximum micro-strain value developed.

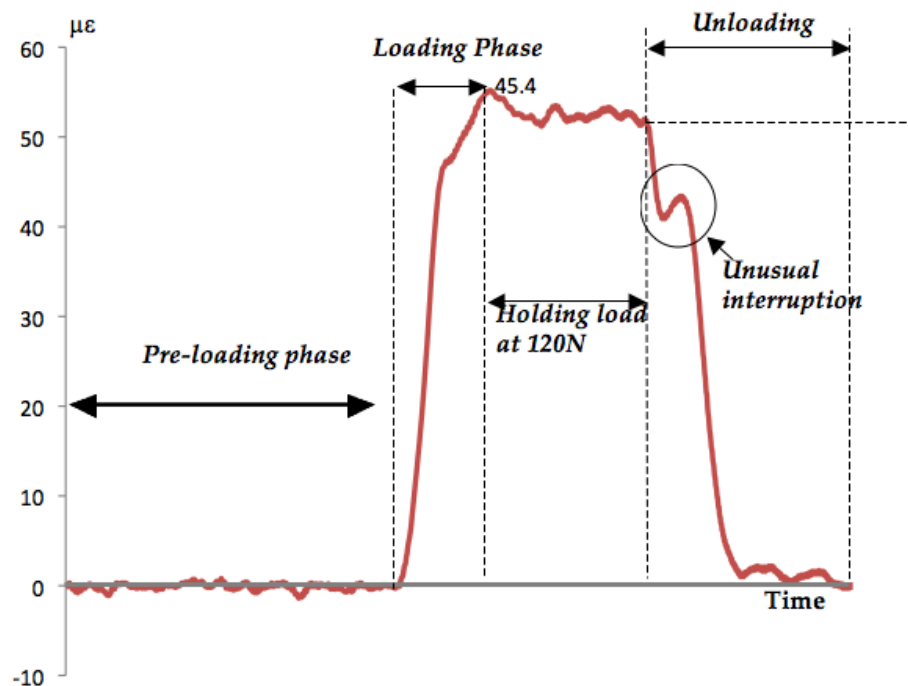


Figure 41: Micro-strain-time plot of gauge 1 illustrating pre-loading, loading and unloading micro-strain behaviour during a bilateral uniform loading cycle

The micro-strain is in the bucco-lingual direction around the implant during the bilateral loading condition. During the loading phase, the micro-strain-time curve changed its slope just prior to reaching a maximum value during the loading phase. The contacting of the supporting tissue during the loading phase limited the flexure of the denture and thereby reduced the gradient of micro-strain with further increase in load. A possible explanation is that as the load continued to increase, the prosthesis was in contact with the silicone, and further increase in load deflected both the acrylic and also the underlying soft tissue resulting in a lower rate of micro-strain increase.

During the unloading phase there was an unusual interruption of micro-strain identified in the plot graph. A gradual decline of micro-strain values was observed during the initial unloading stage due to the recovery of the structure as the load was released. However, an interruption was noted during the unloading stage. This is consistent with an apparent partial reload during the unloading process. As indicated above, the acrylic made contact with tissue, so during unloading, initially the acrylic will recover, and the adhesion of the tissue will add additional force (the slight rise) before it releases and the flexure of the acrylic is reduced.

In the distal area adjacent to the implant, low micro-strain developed during bilateral uniform loading, but this area is subjected to higher micro-strain compared with the mesial area of the distal extension (figure 42).

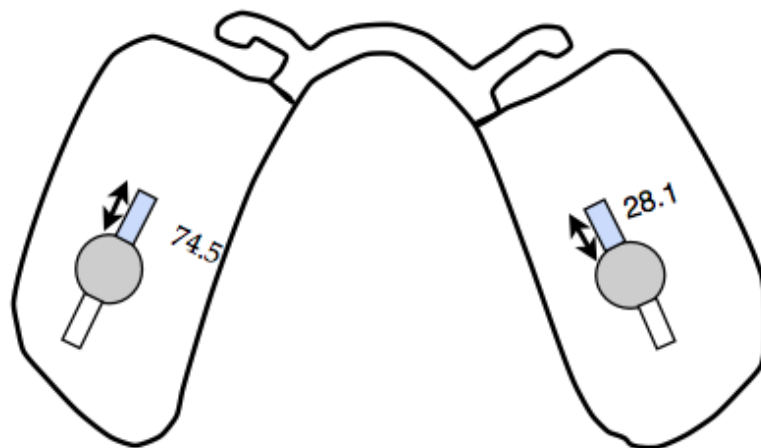


Figure 42: Micro-strain value on acrylic base around the implant in mesio-distal direction (bilateral uniform loading)

Also, when bilateral loading is uniformly applied to the prosthetic posterior teeth, the material above the implants acts as a load barrier, and as the loading force increases, this area is subjected to higher micro-strain compared with the mesial area of the distal extension (figure 43). Since the material above the implant acts as the primary load support, the distal region to the implant does not develop micro-strain.

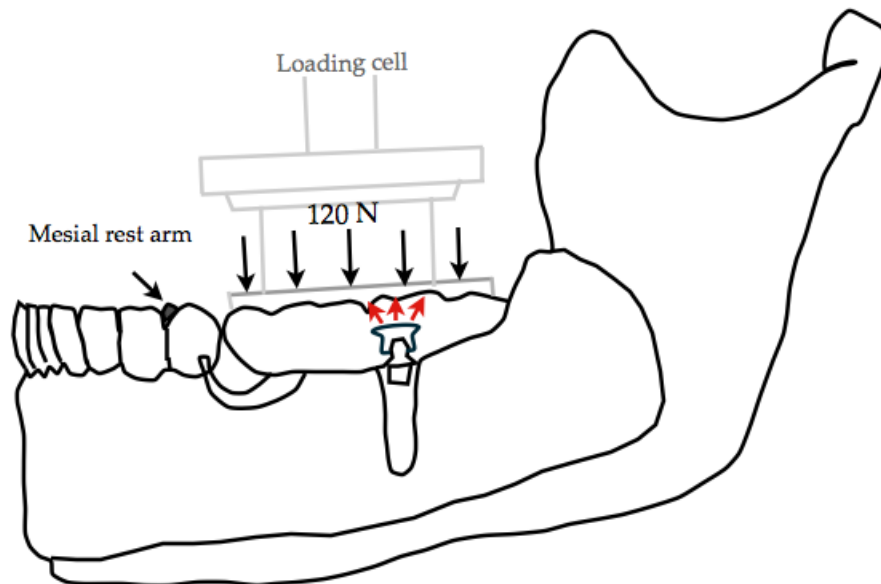


Figure 43: Implant acting as the primary load support point during bilateral uniform loading

A simplified schematic illustration of the prosthesis structure is shown in figure 44 to better appreciate the effect of the loading conditions. Rest arms are depicted as springs, because they can elastically deflect during loading without breaking or becoming permanently deformed. Vertical displacement is restrained by the two virtually rigid implants and therefore, the areas around the implants will be subjected to the most micro-strain. This finding was only evident for bilateral uniform loading. Micro-strain did occur in the distal area adjacent to the implant when the bilateral loading was applied to the molar and premolar regions (figure 16 & 17).

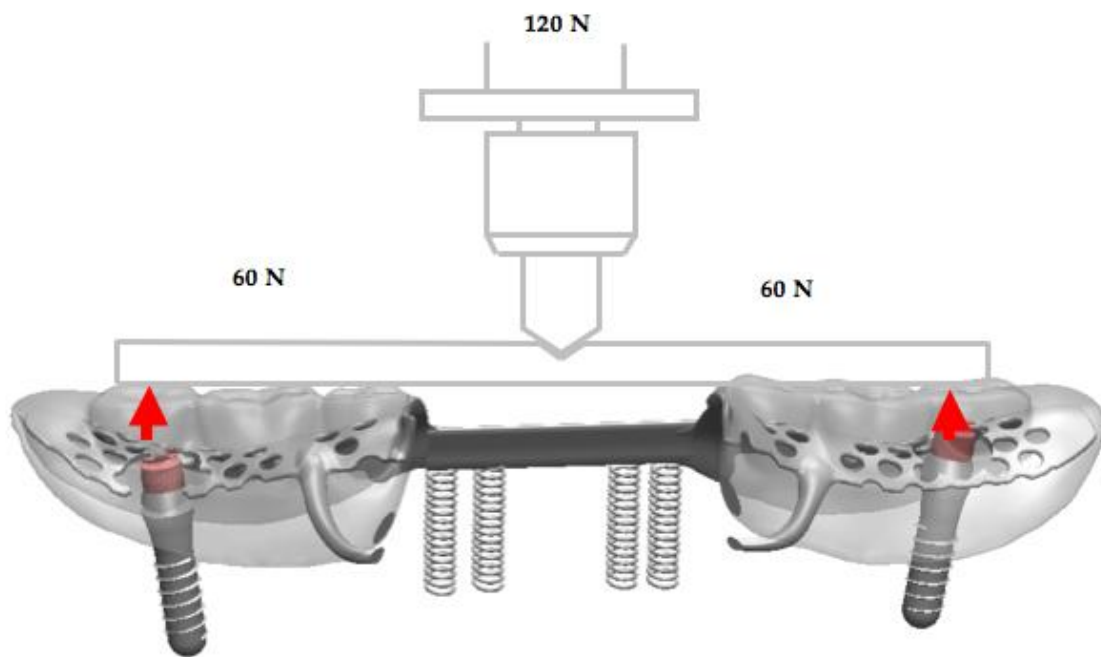


Figure 44: A simplified schematic image of IARPD subjected to bilateral uniform loading

As the loading point is moved forward, it can be seen that the implants are not the only structure supporting the load. The RPD is now acting as a beam with forces applied medially relative to the implants. The micro-strain is more evenly distributed between the two supporting structures (figure 45). Therefore, more uniform micro-strain development throughout the denture can be expected rather than local micro-strain development about the implant.

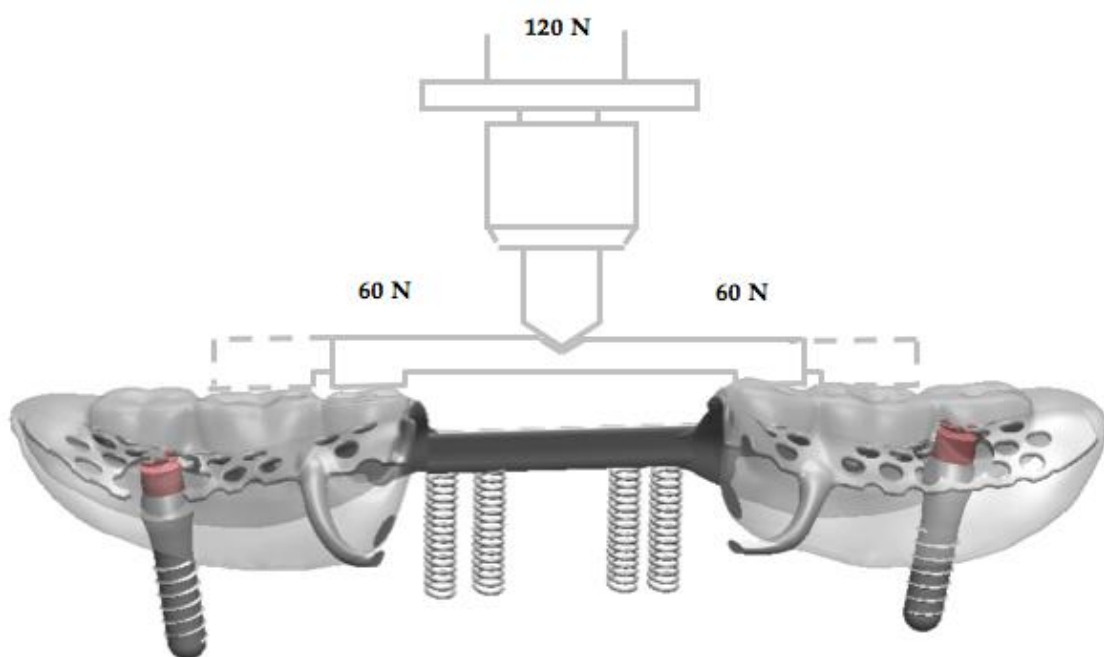


Figure 45: Simplified schematic illustrating the molar (broken) and premolar (solid) loading conditions showing the loading forces are now medially placed relative to the rigid implant support locations

As the load is moved toward the premolar area it is logical to expect the micro-strain values to increase in the mesial area of the distal extension. In addition, by moving the loading area closer to a supporting structure, there will be a reduced bending moment developed and a corresponding reduced amount of deflection in the beam. The additional increase in micro-strain could be due to the distance

between the location of the load and the supporting structure and the associated curvature which creates a greater off-axis lever arm. This lever arm may create lateral movement, resulting in deflection during the premolar loading in the bucco-lingual direction (figure 46). Micro-strain values could also be influenced because of the locations of the micro-strain gauges directly under the premolar loading areas.

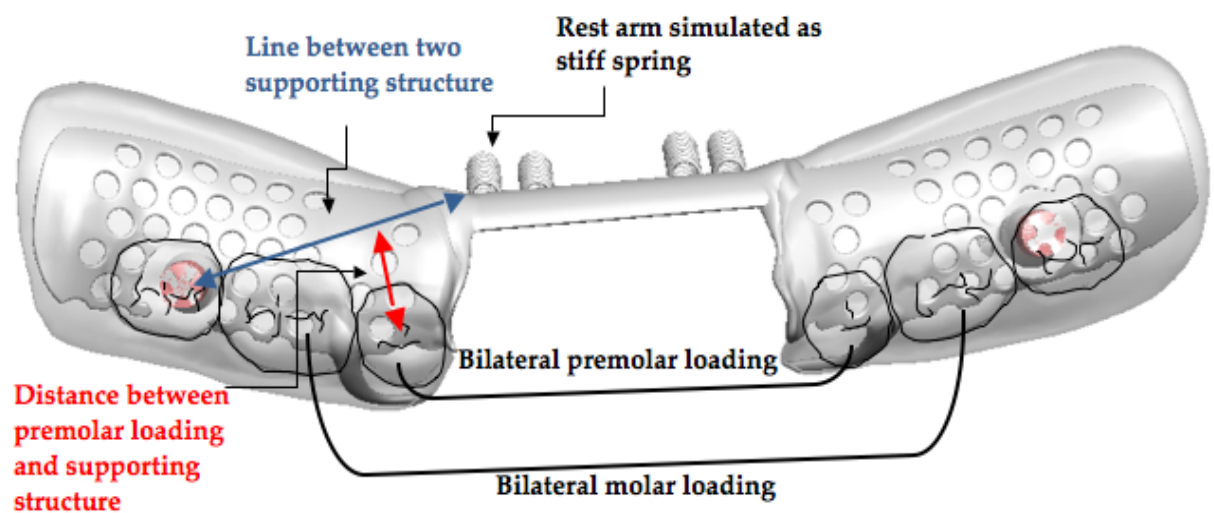


Figure 46: Schematic illustration indicating that premolar loading generates greater off-axis lever arm distance from the line between supporting structures

The direction of the micro-strain in the prosthesis forms in the buccal lingual direction, which does fit with the beam deflection situation suggested above. If we assume that the prosthesis is a typical beam because both the implant, and to a lesser extent the rest, restrain the prosthesis from vertical movement, this should result in most of the micro-strain expected to develop due to a bending of the structure in the mesio-distal direction.

The reason the typical beam behaviour is not seen is because the acrylic surface is in contact, especially adjacent to the premolar area, with soft tissue resulting in micro-strain development due to the additional resistance the tissue presents. The larger the tissue displacement during loading, the greater the flexural resistance, and consequently, the higher micro-strains developed about the premolar area of the acrylic. Figure 47 shows the shape of the cross-sectional area of the prosthesis in the mesial area of the distal extension.

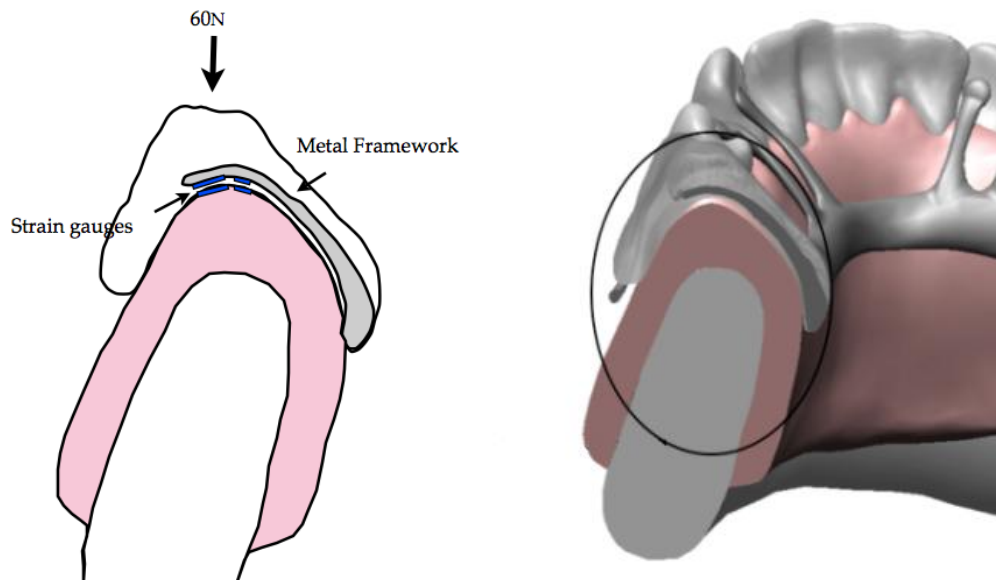


Figure 47: Cross-sectional image of area around the mesial area of the distal extension in coronal plane with bilateral premolar loading

All high micro-strain values were recorded in the bucco-lingual direction. Bucco-lingual micro-strain requires a lateral movement of the prosthesis. Since the load is applied on the acrylic teeth along both sides of the prosthesis, it is expected that most of the micro-strain develops in the same direction (i.e. mesio-distal direction). However, the line between the implant and rest (resistance arm) is not

in alignment with the loading area (effort arm). Misalignment between the resistance arm and effort arm could possibly be the cause of lateral movement. Bilateral loading minimizes lateral displacement through the rest arms, whereas moving the loading point forward increases the length of effort arm and as a result, generates greater mechanical advantage (figure 48). As a consequence, less force is required to displace the prosthesis. Since the loading force is unchanged in all loading conditions, therefore, the most forward loading condition will cause the greatest displacement. More displacement will result in larger tissue response and consequently, greater micro-strain on the acrylic surface. This series of events leads to having higher micro-strain values in the bucco-lingual direction, which move in a more anterior direction as the load moves forward.

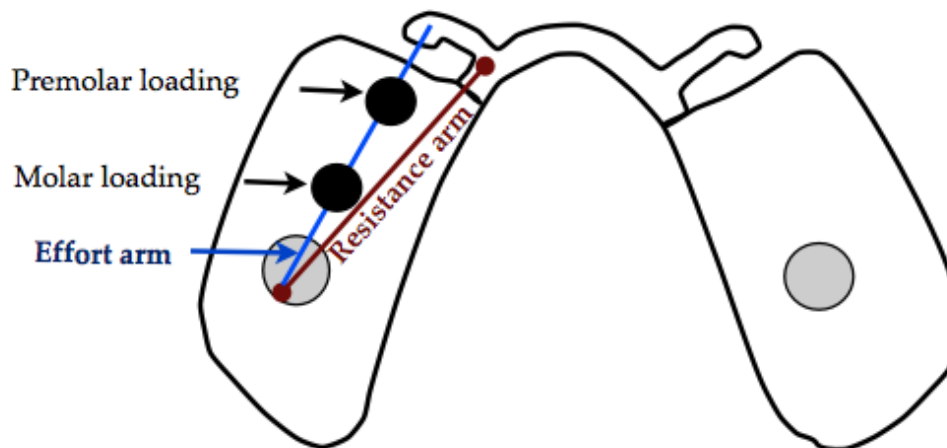


Figure 48: Moving the loading point forward will increase the ratio of the effort arm to resistance arm

For bilateral premolar loading, on the other hand, as the load was moved forward the micro-strain also increased anteriorly, while the micro-strain values around the implant decreased to almost half of their values under similar loading

conditions. Thus, a considerable amount of micro-strain still developed around the area of the implants in the bucco-lingual direction, despite the forward movement of the loading condition (figure 49).

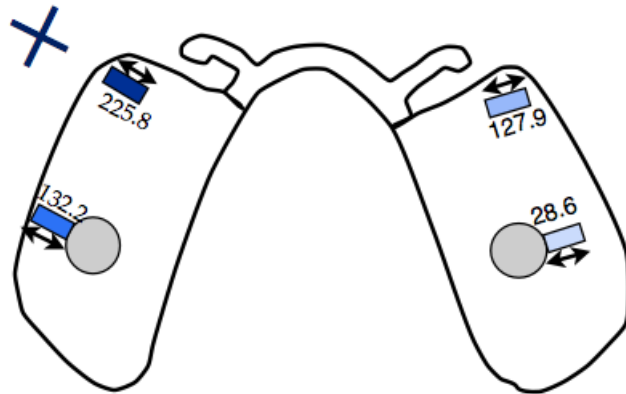


Figure 49: Highest micro-strain values were recorded in mesial area of the distal extension on the acrylic base under bilateral premolar loading

The micro-strain measured on the metal surface showed a somewhat different behaviour when bilaterally loaded. Under all of the three loading conditions investigated, the highest micro-strain values were evident around the mesial area of the distal extension in the bucco-lingual direction (figure 50).

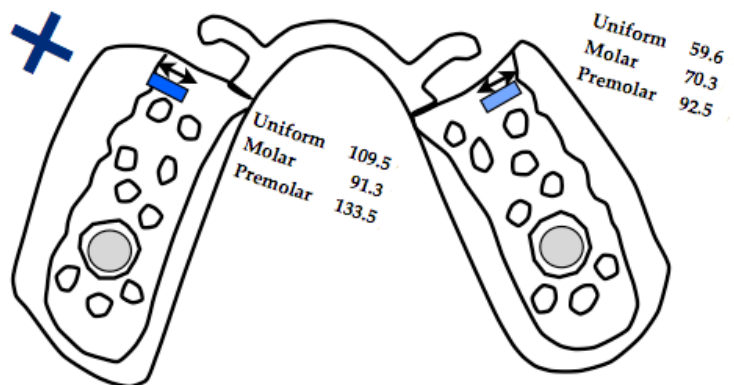


Figure 50: Highest micro-strain values were recorded in the mesial area of the distal extension in the metal framework for all three bilateral loading conditions

Moving the loading area forward did not influence the micro-strain in the metal surface around the implant. This is understandable as the metal structure did not have direct contact with the implant but did have support from contact via the rests placed on the abutment teeth. Hence, the rest arms supported the metal structure and upon loading, the areas close to the rest arm were subjected to a high level of micro-strain.

The micro-strain values recorded in the molar loading condition were more evenly distributed between the metal and acrylic surfaces with the tensile micro-strain values being similar for both (figure 51 a & b).

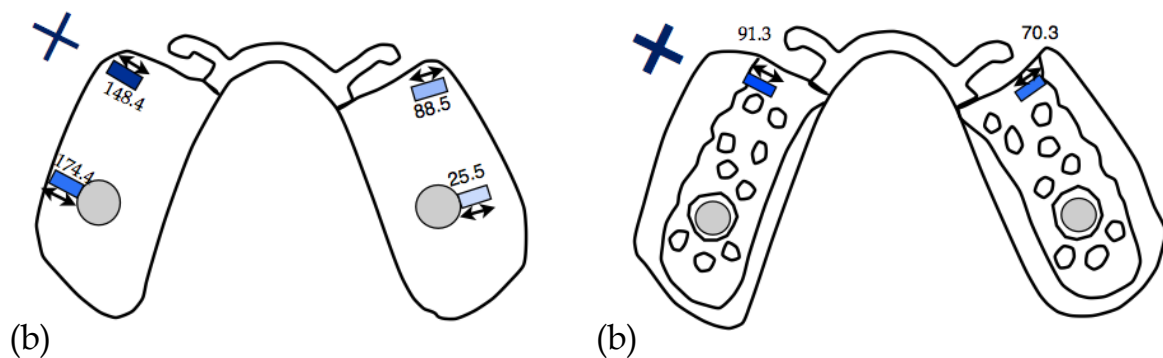


Figure 51: Bilateral molar loading; (a) Micro-strain values around the implants and mesial areas of the distal extensions on acrylic base (b) Micro-strain values around the mesial areas of the distal extension on the metal framework

The metal and acrylic surfaces are in very close contact and thus act as if they are bonded together. Acrylic is thus reinforced by the metal structure, which is placed 1 mm above the lower face of the acrylic, when the acrylic beam is subjected to a positive bending moment. As acrylic is weak in tension and has low elastic modulus, most of the flexural tensile forces are preferably carried by the metal structure, while the upper part of the acrylic beam will be exposed to the compressive load. Therefore, the neutral axis of the saddle will be influenced by

the greater rigidity of the metal structure. If the distal extension area is considered as a beam, then during bending the maximum micro-strain will occur on the external surface and a lower micro-strain will occur at the neutral axis. The position of the metal towards the inner surface helps to reduce the flexure of the structure and lowers the tensile micro-strains developed on the inner surface of the acrylic.

Unilateral loading of the metal and acrylic

Despite the fact that the same amount of load was applied during unilateral loading conditions (120N), much lower micro-strain values were recorded on the metal surface compared with the bilateral loading conditions. This suggests that the metal framework was less involved in terms of supporting the prosthesis during the unilateral loading conditions. When loading occurs on one side of the prosthesis, the material above the implant acts as the primary load support, but the lack of support from the other side subjects both areas about the implant and mesial of the distal extension to strain (figure 52).

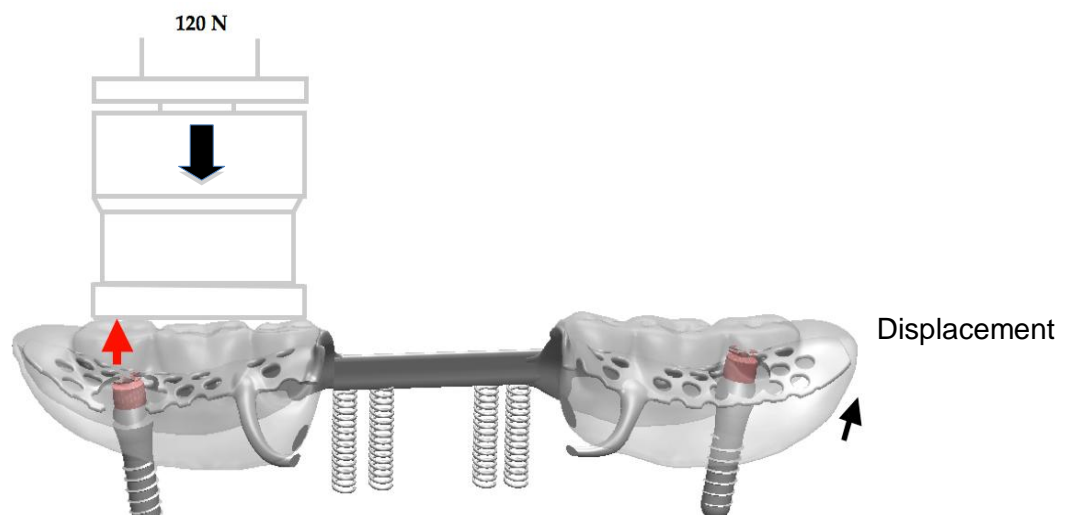


Figure 52: A simplified schematic image of IARPD subjected to unilateral uniform loading

Under uniform unilateral loading the acrylic showed the highest micro-strain value around the implant in the bucco-lingual direction. The direction of the micro-strain is due to the fulcrum movement of the prosthesis, which also results in the load intensification. Separate to this there is also a significant increase in the micro-strain value on the mesial area of the distal extension as the loading point is moved forward (unilateral molar and premolar loading). The micro-strain value on the mesial area of the distal extension increased more than six times as the loading point moved forward (figure 53 a, b & c).

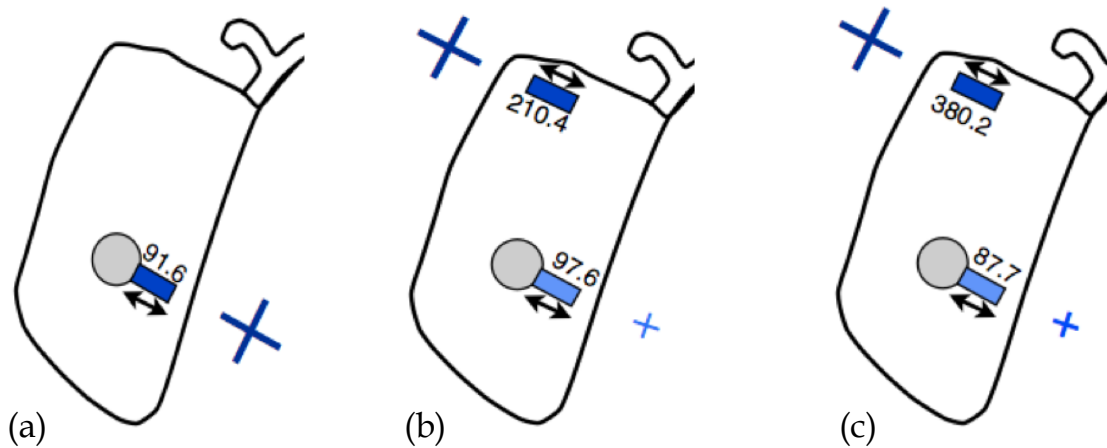


Figure 53: Highest micro-strain value in acrylic base; (a) Unilateral uniform loading (b) Unilateral molar loading (c) Unilateral premolar loading

The significant jump in micro-strain is due to the change in the loading area. Uniform loading was applied over a greater area, whereas the molar and premolar loadings were supported by a smaller loading area. In addition, the premolar loading was directly above the micro-strain gauges. Under uniform loading, the forces act over the greater area, whereas under molar and premolar loading, the

forces act over smaller areas and for the premolar loading condition the load is directly above the micro-strain gauges. This is very similar to the bilateral loading with the only difference being that the implant and the rest on one side act as the primary support structures (figure 54).

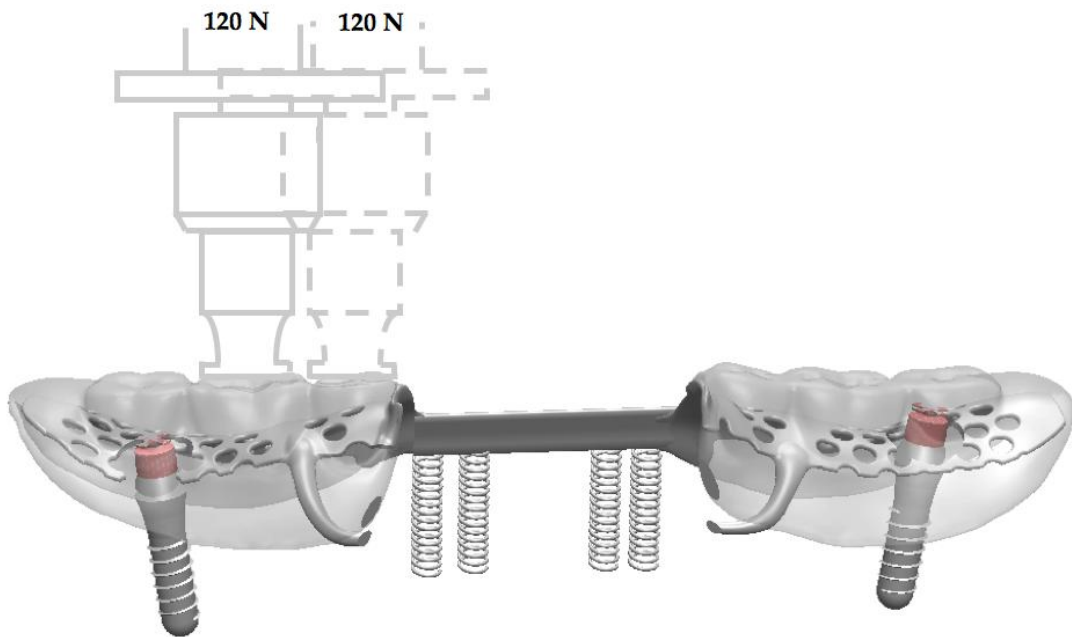


Figure 54: Simplified schematic illustrating the molar and premolar loading condition showing the loading forces are now medially positioned relative to the rigid implant support.

The micro-strain in the metal surface exhibited a different behaviour during unilateral premolar loading. As the loading point moved forward, the location of the highest micro-strain remained in the mesial area of the distal extension, similar to bilateral loading but with a different micro-strain outcome. This may be related to the lateral movement of the prosthesis causing more micro-strains on the implant as the rest is displaced away from the tooth. This lateral movement may

have contributed to the type of micro-strain that was recorded on the metal surface, which was compression rather than tension (figure 55 a, b & c).

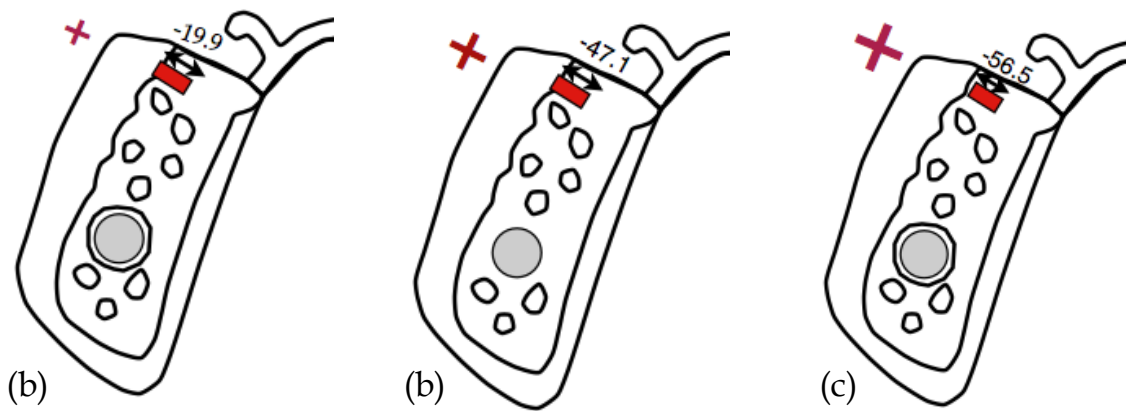


Figure 55: Highest micro-strain value area on metal framework; (a) Unilateral uniform loading (b) Unilateral molar loading (c) Unilateral premolar loading

A combination of lateral movement and vertical displacement may possibly be responsible for the different micro-strain behaviour on the metal structure during unilateral loading compared with bilateral loading. The nature of bilateral loading gives the prosthesis more vertical stability despite lateral movement, whereas unilateral loading can induce vertical and lateral displacement at the same time. Figure 56 illustrates such a different effect of unilateral versus bilateral loading. The distance between the location of the load and supporting structure and the curvature associated with the dental arch may create lateral movement. This indicates that premolar loading generates a greater off-axis lever arm distance from the line between supporting structures for both bilateral and unilateral loading. However, simultaneous loading of both sides in the case of bilateral loading gives more stability and consequently generates more micro-strain to the area about the rest arm, whereas during unilateral loading the load response can displace the whole prosthesis laterally as well as vertically. Since ball attachments

provide retention and lateral resiliency, loading one side displaces the whole prosthesis, especially the rear portion of the prosthesis on the non-loaded side. Therefore, the rest arm on the loaded side will no longer act as a vertical support but rather act as a fulcrum point during displacement and allow twisting or torsion of the metal structure. Since the attachment remains the major structure that provides retention and in addition resists displacement, it is expected most micro-strain will be developed around the implant during the twisting effect. However, the metal structure is not in contact with the implant and twisting of the very rigid lingual bar will have an influence, resulting in a compressive micro-strain being developed on the metal surface. In contrast twisting will increase the tissue response against the acrylic and result in much greater tension on the external surface of the acrylic, as mentioned previously. Therefore, as the load moves forward, the effect of twisting becomes greater and results in greater compressive micro-strains occurring around the mesial area of the distal extension.

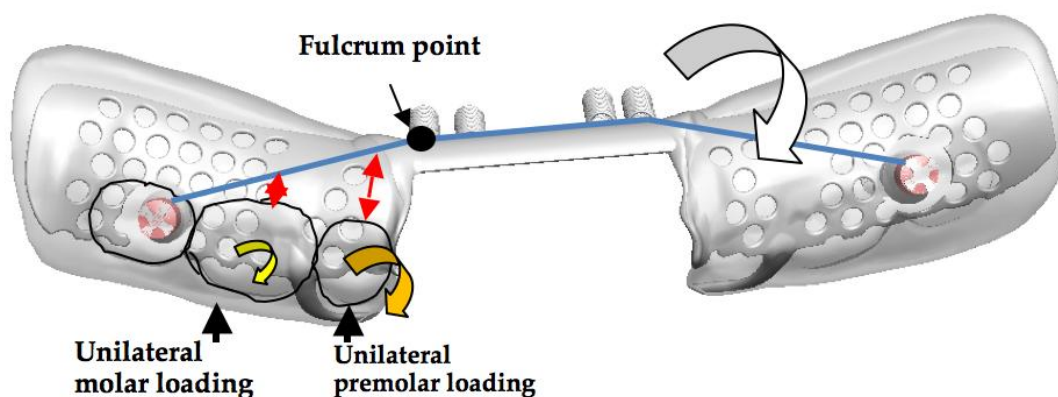


Figure 56: Effect of unilateral loading conditions on metal framework

The unilateral molar loading produced tensile micro-strain on the acrylic surface, and compressive micro-strain on the metal surface. In addition, the micro-strain values on the acrylic surface were approximately four times larger than those recorded on the metal surface (figure 57 a & b).

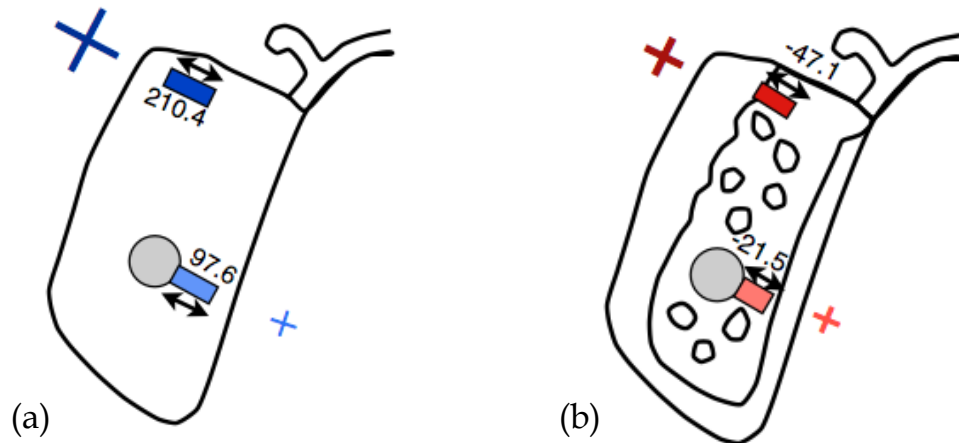


Figure 57: Micro-strain values of unilateral molar loadings on; (a) acrylic and (b) metal framework

Interpretation of the result of unilateral loading can be summarized as follows: the compression micro-strain of the metal surface is due to flexure in the bucco-lingual direction during loading, while the acrylic goes into tension as it deflects away from the soft tissue on the buccal side. The smaller micro-strain values in the metal structure may indicate less involvement of the metal framework, which could be attributed to the dislocation of the rest away from the abutment tooth during the unilateral loading. Also, the ball attachments may have contributed to the lateral displacement of the prosthesis due to the resilient nature of the attachments.

The fact that the metal framework had no contact with the implant could also explain the different response of the materials to load. This may play a part in the lateral displacement of the prosthesis during unilateral loading.

A combination of all three planes of rotation; sagittal, coronal and horizontal in tooth-tissue supported a distal extension RPD cause dynamic movement of RPD (Carr *et al.*, 2011). The IARPD showed a small micro-strain generated in the mesio-distal direction that indicates small movement of IARPD in the sagittal plane. However, high micro-strain values were generated in the bucco-lingual directions that indicate that rotation in the coronal plane still exists. Combinations of rotation in the frontal (rotation around a longitudinal axis) and horizontal (rotation around a vertical axis near the centre of the arch) planes are identified in unilateral loading conditions.

Chapter Six

Summary

The IARPD showed small micro-strain generation in the mesio-distal direction. However, high micro-strain values were generated in the bucco-lingual direction, highlighting rotation in the coronal plane (longitudinal axis).

Bilateral loading showed more favourable micro-strain on the IARPD structure. As acrylic is weak in tension and has a low elastic modulus, most of the flexural tensile forces are preferably carried by the metal structure, while the upper part of the acrylic beam will be exposed to the compressive load. Therefore, the neutral axis of the saddle is influenced by the greater rigidity of the metal structure. During loading, the metal framework helps reduce the flexure of the structure and lowers the tensile micro-strain developed on the inner surface of the acrylic. Bilateral loading also provides more stability and consequently generates more micro-strain on the rest arms.

During unilateral loading of an IARPD the curvature of the dental arch created displacement laterally as well as vertically. When the premolar region is loaded an off-axis lever arm is created. Therefore, the rest arm on the same side as the loading became a fulcrum point during displacement and caused twisting/torsion of the metal structure. As the load moved toward the mesial of the distal extension, the effect of twisting became greater. Since the implant attachment provides retention and additional resistance to displacement, most of the micro-strain was transferred to the areas surrounding the mesial of distal extension. The

twisting also increased the tissue response against the acrylic and resulted in greater tension on the external surface of the acrylic. The metal structure is not in contact with the implant and twisting of the rigid lingual bar resulted in compressive micro-strain being developed on the metal surface.

In both unilateral and bilateral loading conditions, as the loading point moved forward the maximum micro-strain value moved forward in the acrylic base, whereas maximum micro-strain values remained in mesial area of the distal extension on the metal framework regardless of the loading condition.

Conclusions

Lateral movement/displacement was evident during bilateral and unilateral loading of the IARPD and this resulted in high micro-strains values in the bucco-lingual direction and small micro-strain in the mesio-distal direction.

When looking at the maximum micro-strain values of the IARPD molar bilateral loading produced the lowest value on both metal framework and acrylic base, with a less destructive micro-strain dynamic developed between the metal framework and acrylic base (both acrylic base and metal framework in tension).

When looking at the maximum micro-strain values of the IARPD uniform unilateral loading produced the lowest value on both metal framework and acrylic base. However, a destructive micro-strain dynamic developed between the framework and acrylic base (acrylic base in tension and metal framework in compression).

Recommendations

- 1) When considering that an implant may be incorporated into a RPD at a later stage, consideration should be given to the rigidity of the appliance.
- 2) The micro-strain patterns indicated in this research draws attention to the need for further studies to properly determine the ideal design of a RPD that is converted to a IARPD

References

Bakke M, Holm B, Gottfredsen K (2002). Masticatory function and patient satisfaction with implant-supported mandibular overdentures: a prospective 5-year study. *International Journal of Prosthodontics* 15(6):575-581.

Bergman B, Hugoson A, Olsson CO (1982). Caries, periodontal and prosthetic findings in patients with removable partial dentures: a ten-year longitudinal study. *Journal of Prosthetic Dentistry* 48(5):506-514.

Brudvik JS (1999). Advanced removable partial dentures. Chicago: Quintessence Pub. Co.

Campbell RL (1960). A comparative study of the resorption of the alveolar ridges in denture-wearers and non-denture-wearers. *Journal of American Dental Association* 60(Feb):143-153.

Carlsson GE (1998). Clinical morbidity and sequelae of treatment with complete dentures. *Journal of Prosthetic Dentistry* 79(1):17-23.

Carr AB, Brown DT, McGivney GP (2011). McCracken's removable prosthodontics. 12th ed. St. Louis: Elsevier Mosby.

Chikunov I, Doan P, Vahidi F (2008). Implant-retained partial overdenture with resilient attachments. *Journal of Prosthodontics* 17(2):141-148.

Cho HW (2002). Load transfer by distal extension RPD with implant assisted support. *Journal of Dental Research* 81 (Special Issue A):A-156.

Cibirka R, Razzoog M, Lang B, Stohler C (1992). Determining the force absorption quotient for restorative materials used in implant occlusal surfaces. *Journal of Prosthetic Dentistry* 67(3):361- 364.

Crum RJ, Rooney JR (1978). Alveolar bone loss in overdentures: A 5 year study. *Journal of Prosthetic Dentistry* 40(6):610-613.

Cunha LD, Pellizzer EP, Verri FR, Pereira JA (2008). Evaluation of the influence of location of osseointegrated implants associated with mandibular removable partial dentures. *Implant Dentistry* 17(3):278-287.

Dally JW, Riley WF (1965). *Experimental stress analysis* New York: McGraw-Hill, Inc.

Douglass CW, Watson AJ (2002). Future needs for fixed and removable partial dentures in the United States. *Journal of Prosthetic Dentistry* 87(1):9-14.

Eliason CM (1983). RPA clasp design for distal-extension removable partial dentures. *Journal of Prosthetic Dentistry* 49(1):25-27.

Ettinger RL, Taylor TD, Scandrett FR (1984). Treatment needs of overdenture patients in a longitudinal study: five-year results. *Journal of Prosthetic Dentistry* 52(4):532-537.

Ettinger RL (1988). Tooth loss in an overdenture population. *Journal of Prosthetic Dentistry* 60(4):459-462.

Fields H, Jr., Campfield RW, Jr. (1974). Removable partial prosthesis partially supported by an endosseous blade implant. *Journal of Prosthetic Dentistry* 31(3):273-278.

Geurs NC, Vassilopoulos PJ, Reddy MS (2010). Soft tissue considerations in implant site development. *Oral and Maxillofacial Surgery Clinics of North America* 22(3):387-405.

Goodman JJ (1963). Balance of force in precision free-end restorations. *Journal of Prosthetic Dentistry* 13 (2):302-308.

Grossmann Y, Nissan J, Levin L (2009). Clinical effectiveness of implant-supported removable partial dentures - a review of the literature and retrospective case evaluation. *Journal of Oral and Maxillofacial Surgery* 67(9):1941-1946.

Halterman S, Rivers J, Keith J, Nelson D (1999). Implant support for removable partial overdentures: A case report. *Implant Dentistry* 8(1):74-78.

Hindels GW (2001). Load distribution in extension saddle partial dentures. *Journal of Prosthetic Dentistry* 85(4):324-329.

Igarashi Y, Ogata A, Kuroiwa A, Wang CH (1999). Stress distribution and abutment tooth mobility of distal-extension removable partial dentures with different retainers: an in vivo study. *Journal of Oral Rehabilitation* 26(2):111-116.

Imai Y, Sato T, Mori S, Okamoto M (2002). A histomorphometric analysis on bone dynamics in denture supporting tissue under continuous pressure. *Journal of Oral Rehabilitation* 29(1):72-79.

Itoh H, Sasaki T, Nakahara H, Katsube T, Satoh M, Matyas J *et al.* (2007). Load transmission by distal extension RPD with implant assisted support. *Journal of Dental Research* 86 (Special Issue A):1476

Jambhekar S, Kheur M, Kothavade M, Dugal R (2010). Occlusion and occlusal consideration in implantology. *Indian Journal of Dental Advancements* 2(1):125-130.

Jepson NJ, Thomason JM, Steele JG (1995). The influence of denture design on patient acceptance of partial dentures. *British Dental Journal* 178(8):296-300.

Jozefowicz W (1970). The influence of wearing dentures on residual ridges: A comparative study. *Journal of Prosthetic Dentistry* 24(2):137-144.

Kapur KK (1991). Veterans Administration Cooperative Dental Implant Study-comparisons between fixed partial dentures supported by blade-vent implants and removable partial dentures. Part IV: Comparisons of patient satisfaction between two treatment modalities. *Journal of Prosthetic Dentistry* 66(4):517-530.

Kelly E (2003). Changes caused by a mandibular removable partial denture opposing a maxillary complete denture. *Journal of Prosthetic Dentistry* 90(3):213-219.

Keltjens HM, Kayser AF, Hertel R, Battistuzzi PG (1993). Distal extension removable partial dentures supported by implants and residual teeth: considerations and case reports. *International Journal of Oral & Maxillofacial Implants* 8(2):208-213.

Krol AJ (1973). Clasp design for extension-base removable partial dentures. *Journal of Prosthetic Dentistry* 29(4):408-415.

Lacerda TESP, Lagana DC, Gonzalez-Lima R, Zanetti AL (2005). Contribution to the planning of implant-supported RPD in the distal region. *Revista de Pós-Graduado* 12(3):293-300.

Lum LB (1991). A biomechanical rationale for the use of short implants. *Journal of Oral Implantology* 17(2):126-131.

Manderson RD, Wills DJ, Picton DCA Biomechanics of denture-supporting tissues. Proceedings of the Second International Prosthodontic Congress, 1979, St. Louis: The C. V. Mosby Co.

Mijiritsky E, Ormianer Z, Klinger A, Mardinger O (2005). Use of dental implants to improve unfavorable removable partial denture design. *Compendium of Continuing Education in Dentistry* 26(10):744-746.

Mijiritsky E (2007). Implants in conjunction with removable partial dentures: a literature review. *Implant Dentistry* 16(2):146-154.

Mijiritsky E, Ben Ur Z, Shershevsky A, Brosh T (2007). Mechanical behavior of major connectors part 2: influence of denture teeth height and loading direction. *Refuat Hapeh Vehashinayim* 24(2):27-31, 70.

Mitrani R, Brudvik JS, Phillips KM (2003). Posterior implants for distal extension removable prostheses: a retrospective study. *International Journal of Periodontics and Restorative Dentistry* 23(4):353-359.

Miyaura K, Morita M, Matsuka Y, Yamashita A, Watanabe T (2000). Rehabilitation of biting abilities in patients with different types of dental prostheses. *Journal of Oral Rehabilitation* 27(12):1073-1076.

Mizuuchi W, Yatabe M, Sato M, Nishiyama A, Ohyama T (2002). The effects of loading locations and direct retainers on the movements of the abutment tooth and denture base of removable partial dentures. *Journal of Medical and Dental Sciences* 49(1):11-18.

Monteith BD (1984). Management of loading forces on mandibular distal-extension prostheses. Part I: Evaluation of concepts for design. *Journal of Prosthetic Dentistry* 52(5):673-681.

Mori S, Sato T, Hara T, Nakashima K, Minagi S (1997). Effect of continuous pressure on histopathological changes in denture-supporting tissues. *Journal of Oral Rehabilitation* 24(1):37-46.

Ohara K, Sato T, Imai Y, Hara T (2001). Histomorphometric analysis on bone dynamics in denture supporting tissue under masticatory pressure in rat. *Journal of Oral Rehabilitation* 28(7):695-701.

Ohkubo C, Kurihara D, Shimpo H, Suzuki Y, Kokubo Y, Hosoi T (2007). Effect of implant support on distal extension removable partial dentures: in vitro assessment. *Journal of Oral Rehabilitation* 34(1):52-56.

Ohkubo C, Kobayashi M, Suzuki Y, Hosoi T (2008). Effect of implant support on distal-extension removable partial dentures: in vivo assessment. *International Journal of Oral & Maxillofacial Implants* 23(6):1095-1101.

Orr S, Linden GJ, Newman HN (1992). The effect of partial denture connectors on gingival health. *Journal of Clinical Periodontology* 19(8):589-594.

Palmqvist S, Carlsson GE, Owall B (2003). The combination syndrome: A literature review. *Journal of Prosthetic Dentistry* 90(3):270-275.

Payne A, Solomons YF (2000). The prosthodontic maintenance requirements of mandibular mucosa-and implant-supported overdentures: A review of the literature. *International Journal of Prosthodontics* 13(3):238-243.

Payne A, Kuzmanovic DV, De Silva KR, van Staden IP (2006). Mandibular removable partial dentures supported by implants: One-year prosthodontic outcomes. *Journal of Dental Research* 85 (Special Issue B):Poster 2570.

Pellizzer EP, Luersen MA, Rocha EP (2003). Finite element analysis of masticatory force in distal-extension removable partial denture associated with a implant. *Journal of Dental Research* 82 (Special Issue B):B-254.

Pellizzer EP, Lucas LVM, Rocha EP, Verri FR, Pereira JR, Braz DB (2004). Influence of bite force in RPD associated with osseointegrated implant. *Journal of Dental Research* 83 (Suppl 1):124-128.

Pellizzer EP, Verri FR, Falcon-Antenucci RM, Goiato MC, Gennari Filho H (2010). Evaluation of different retention systems on a distal extension removable partial denture associated with an osseointegrated implant. *Journal of Craniofacial Surgery* 21(3):727-734.

Pond LH, Barghi N, Barnwell GM (1986). Occlusion and chewing side preference. *Journal of Prosthetic Dentistry* 55(4):498-500.

Renner RP, Boucher LJ (1987). Removable partial dentures. Chicago: Quintessence Pub. Co.

Renner RP (1990). Removable partial overdentures. *Dental Clinics of North America* 34(4):593-606.

Rissin L, Feldman RS, Kapur KK, Chauncey HH (1985). Six-year report of the periodontal health of fixed and removable partial denture abutment teeth. *Journal of Prosthetic Dentistry* 54(4):461-467.

Rocha EP, Luersen MA, Pellizzer EP (2003). Distal extension removable partial denture associated with an osseointegrated implant. Study by the finite element method. *Journal of Dental Research* 82 (Special Issue B):B-254.

Salvador MCG, Valle AL, Ribeiro MCM, Pereira JR (2007). Assessment of the prevalence index on designs of combination syndrome in patients treated at Bauru School of Dentistry, University of Sao Paulo. *Journal of Applied Oral Science* 15(1):9-13.

Santos CMDF, Pellizzer EP, Rocha EP (2006). Influence of osseointegrated implant angulation associated with mandibular RPD. *Journal of Dental Research* 85 (Special Issue B):0017.

Shahmiri RA, Atieh MA (2010). Mandibular Kennedy Class I implant-tooth-borne removable partial denture: a systematic review. *Journal of Oral Rehabilitation* 37(3):225-234.

Shahmiri RA, Atieh MA (2011). Attachments in implant-assisted removable partial dentures: A design dilemma. *International Poster Journal of Dental Oral Medicine* 13(1):Poster 515.

Stern N, Brayer L (1975). Collapse of the occlusion-aetiology, symptomatology and treatment. *Journal of Oral Rehabilitation* 2(1):1-19.

Tolstunov L (2007). Combination syndrome: classification and case report. *Journal of Oral Implantology* 33(3):139-151.

Vahidi F (1978). Vertical displacement of distal-extension ridges by different impression techniques. *Journal of Prosthetic Dentistry* 40(4):374-377.

van Kampen FM, van der Bilt A, Cune MS, Bosman F (2002). The influence of various attachment types in mandibular implant-retained overdentures on maximum bite force and EMG. *Journal of Dental Research* 81(3):170-173.

Verri FR, Pellizzer EP, Rocha EP, Pereira JA (2007). Influence of length and diameter of implants associated with distal extension removable partial dentures. *Implant Dentistry* 16(3):270-280.

Watson BW (2008). Bonded electrical resistance strain gages. In: Springer handbook of experimental solid mechanics. New York: Springer Science.

Watt DM, MacGregor AR (1984). Designing partial dentures. Bristol: Wright.

Wetherell JD, Smales RJ (1980). Partial denture failures: a long-term clinical survey. *Journal of Dentistry* 8(4):333-340.

Wismeijer D, van Waas MAJ, Kalk W (1995). Factors to consider in selecting an occlusal concept for patients with implants in the edentulous mandible. *Journal of Prosthetic Dentistry* 74(4):380-384.

Witter DJ, De Haan AF, Kayser AF, Van Rossum GM (1994). A 6-year follow-up study of oral function in shortened dental arches. Part II: Craniomandibular dysfunction and oral comfort. *Journal of Oral Rehabilitation* 21(4):353-366.

Zarb GA (1978). Prosthodontic treatment for partially edentulous patients St. Louis: Mosby.

Review Article

Mandibular Kennedy Class I implant-tooth-borne removable partial denture: a systematic review

R. A. SHAHMIRI & M. A. ATIEH *Sir John Walsh Research Institute, Faculty of Dentistry, University of Otago, Dunedin, New Zealand*

SUMMARY The purpose of this systematic review is to evaluate the use of implant-tooth-borne removable partial dentures in prosthetic rehabilitation of Kennedy Class I partially edentulous arches. A comprehensive search was performed in MEDLINE, EMBASE, Cochrane Oral Health Group's Trials Register, Cochrane Central Register of Controlled Trials, UK National Research Register, Australian New Zealand Clinical Trials Registry (ANZCTR), conference proceedings and abstracts up to 25 August 2009. Searching the reference list of the selected articles and hand searching of several journals were also performed. A total of nine studies were included. Of these, two were randomized, three were retrospective and four were case reports. All but two had a low reporting quality (level IV on a four-level hierarchy of evidence). Nevertheless, the improve-

ment in function, aesthetics and stability has been demonstrated in all studies with minimal prosthetic care. Within the limitations of this study, implant-assisted/supported removable partial denture may provide a simple, economical and less invasive treatment modality. The predictability of such approach in the management of bilateral distal-extension situation is, however, still questionable. A higher quality of published studies namely with a focus on long-term randomized clinical trials are needed.

KEYWORDS: implant-assisted removable partial denture, implant-supported removable partial denture, Kennedy Class I, patient satisfaction, prosthetic maintenance, systematic review

Accepted for publication 21 November 2009

Introduction

In the last decade, industrialized countries have shown a significant improvement in oral health and dental care. Data collected from studies conducted by several health organizations including the US National Health, Nutrition Examination Survey (NHANES), UK Adults Dental Health Survey, Fourth German Oral Health Study (DMS IV), and Australia's National Oral Health Plan revealed a considerable reduction in the percentage of edentulous adults (1–4). The demand for treatment with different partial denture prostheses will therefore increase, as more individuals will have more teeth when they get older (5, 6).

There are several treatment options for rehabilitation of partial edentulism including the use of conventional

or implant-retained fixed prostheses. However, such prosthetic options cannot always be possible because of compromised general and oral health (i.e. loss of supporting tissues, medical reasons and extensive surgical protocol) as well as the affordability of patients (6). Several authors considered a well-constructed removable partial denture (RPD) as cost-effective and acceptable alternative treatment option for rehabilitation of partially dentate patients (7–11).

Based on the location of edentulous spaces, Kennedy classification (12) has been proposed to enhance the planning of the RPD design as well as the communication between dental practitioners and technicians. However, Kennedy did not take into consideration the quality of the remaining ridges and axial position of teeth as well as the condition of the opposing dental

arch. Distal-extension RPDs (Kennedy Class I and II) were associated with several problems related to its limited stability, retention, aesthetics and masticatory efficiency (13–16). In addition, a high percentage of failure was reported because of caries and periodontal disease, needed regular replacement, did not improve eating, had poor retention and poor stability and did not achieve patient satisfaction and oral comfort (15, 17).

Another common problem is combination syndrome, which is found in patients wearing mandibular bilateral distal-extension RPD opposing a maxillary complete denture. This condition, first described by Kelly in 1972 (18), is characterized by overgrowth of the maxillary tuberosities, papillary hyperplasia in the hard palate, resorption of the anterior part of the maxilla, extrusion of the mandibular anterior teeth, resorption under the RPD bases and marked tipping of the occlusal plane (18, 19). The relationship between combination syndrome and distal-extension RPD is still controversial. While Shen and Gongloff (20) recognized such relationship and showed that 24% of the patients wearing a maxillary complete denture opposing a distal-extension RPD developed those signs, others questioned the evidence that such a relationship exists and expressed that combination syndrome lacked adequate reasons to be considered a true medical syndrome (21, 22).

It has been suggested that the proper placement of one or more implants in conjunction with RPD may overcome some of the common problems with conventional RPD (CRPD). Implants incorporated into RPD provided support through the use of healing caps, hence the term *implant-supported*. The term *implant-assisted* described the use of resilient attachment to improve retention. Implant-supported/assisted RPDs offered equality in force distribution and enhanced the aesthetics by avoiding the buccal retentive clasps. Placing two distal implant abutments has been recommended to transform Kennedy Class I to a Kennedy Class III situation to improve the RPD design (13). The aim of the current review is to systematically evaluate existing evidence to identify whether implant-supported RPD (ISRPD) or implant-assisted RPD (IARPD) provided a better performance compared to other treatment modalities.

Materials and methods

This systematic review was developed according to the PRISMA (preferred reporting items for systematic

reviews and meta-analyses) statement (23). The review question was formulated using the PICO (participant, intervention, comparison and outcome) approach (24):

- (1) Participant: partially edentulous patients.
- (2) Intervention: mandibular bilateral distal-extension ISRPD or IARPD.
- (3) Comparison: CRPD or other forms of prosthetic treatment.
- (4) Outcome: clinical performance and patient satisfaction.

Search methodology

Electronic searching was performed in the following databases

- (1) MEDLINE (1969 to 25 August 2009)
- (2) EMBASE (1980 to 25 August 2009)
- (3) The Cochrane Oral Health Group's Trials Register (to 25 August 2009)
- (4) The Cochrane Central Register of Controlled Trials (CENTRAL)
- (5) UK National Research Register
- (6) Australian New Zealand Clinical Trials Registry (ANZCTR)
- (7) ISI Proceedings for relevant conference abstracts

The following search terms were used alone or in combination: 'dental implant', 'oral implant', 'implant-supported', 'implant-retained', 'implant-assisted', 'bilateral distal extension', 'removable partial denture', 'mastication', 'patient satisfaction' and 'partially edentulous patients'. Hand searching of the years from 1998 to 2009 involved the following relevant journals: *Clinical Implant Dentistry & Related Research*, *Clinical Oral Implants Research*, *Implant Dentistry*, *International Journal of Oral & Maxillofacial Implants*, *International Journal of Periodontics & Restorative Dentistry*, *International Journal of Prosthodontics*, *Journal of Oral Implantology*, *Journal of Oral Rehabilitation* and *Journal of Prosthetic Dentistry*. Bibliographies of selected articles were further searched for potentially relevant articles.

Selection criteria

The literature review and data extraction were performed by the two authors (R.S., M.A.), with any disagreements resolved through discussion. Studies were eligible for inclusion in the review if they met the following criteria:

- (1) English-language publication.

- (2) All types of *in vivo* studies, ranging from randomized controlled trials to case reports.
- (3) The intervention included rehabilitation of partially edentulous patients with a bilateral distal-extension ISRPD or IARPD, in which implants are not splinted to the remaining teeth.
- (4) Only mandibular situations were included.

In addition, no restriction on the length of the follow-up period was applied. A data extraction form was developed to collect general information (title, year of publication, location of the study, site and number of implants used, implant system, implant length and diameter, outcome variable, prosthetic complications and follow-up period). In addition, the National Health and Medical Research Council (NHMRC) hierarchy of evidence was used to evaluate the quality of the selected studies (Table 1) (25). In case of possible duplication, only the most recent publication was included.

Results

The electronic search identified 404 titles (Fig. 1). Based on the review of the titles and abstracts, 15 articles were selected for more evaluation. Further, seven articles were excluded from the review, of which two studies reported on maxillary IARPD (26, 27), two described a unilateral distal-extension condition (28, 29), two assessed implant-retained fixed partial dentures (30,

31) and one had duplicate data (32). Masking was not attempted during the assessment as it was suggested that masked assessment did not affect the overall results of systematic reviews (33). A total of nine studies (34–42) were included in the review (Table 2). Among these, one article was retrieved from conference abstracts (42). The hand search did not provide any additional studies.

Description of studies

Among the included nine studies, three were retrospective studies (35, 39, 40), one was part of multi-centre, randomized clinical trial (42), one was a randomized crossover pilot study (41). The remaining four studies were case reports (34, 36–38). All the included studies were poorly rated in terms of quality of its evidence as only two studies (41, 42) had a moderate level of evidence. However, ISRPD/IARPD may be considered as a promising treatment approach as the selected studies described its advantages as follows:

- (1) Enhanced stability and retention (36, 38, 41).
- (2) Improved aesthetic results (34, 35).
- (3) Facilitate oral hygiene maintenance (34).
- (4) Reduced bone resorption under the denture base (36, 37, 40).
- (5) Easily converted to CRPD in case of implant failure (34).
- (6) Modify unfavourable arch configurations (35, 38).
- (7) Improved patient satisfaction (37, 40, 41).
- (8) Prosthetic maintenance is less required than a CRPD (34).
- (9) Reduced extension of the RPD base (40).
- (10) Reduced cost compared to implant-supported fixed prosthesis (34, 37).
- (11) Reduced likelihood of combination syndrome (37).

The data included a total of 183 implants placed in 94 subjects with follow-up period between 3 weeks and 120 months. All the selected studies placed the implant in the most distal position in the molar region to modify the Kennedy Class I in the mandible to a more favourable Kennedy Class III arch configuration. Nevertheless, a more anterior position of the implant, adjacent to the existing abutment has been suggested (35). Moreover, improved patient satisfaction and masticatory efficiency were also reported in all the studies.

Fields and Campfield (34) were the first to report the use of an implant in conjunction with CRPD in the

Table 1. Hierarchy of evidence (25)

Level of evidence	Study design
I	A systematic review of randomized controlled trials
II	A randomized controlled trial
III-1	A pseudorandomized controlled trial (i.e. alternate allocation or some other method)
III-2	A comparative study with concurrent controls: Non-randomized, experimental trial Cohort study Case-control study Interrupted time series with a control group Systematic reviews of such comparative studies
III-3	A comparative study without concurrent controls: Historical control study Two or more single arm study Interrupted time series without a parallel control group
IV	Case series

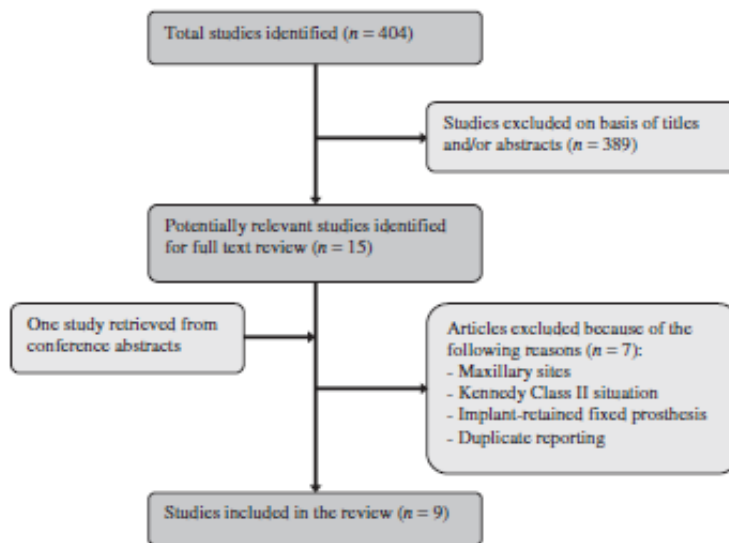


Fig. 1. Search strategy.

treatment of the bilateral distal extension of mandible. The authors used endosseous blade implant on one side, while the other side of the partially edentulous mandible had the usual denture base coverage and was used as a control. To lower the rotational point of prostheses, the height of the post was reduced to half, and a lingual plate was used as a major connector. On the control side, a stress-relieving hinge was adopted. The hinge could prevent unnecessary stress on the remaining teeth or implant, while allowing a distal extension to move during the function. Despite a relatively short 7-month follow-up period, it was reported that no bone loss was detected around the implant and the tissue around the implants remained healthy.

Grossmann *et al.* (35) reported a retrospective study of 35 patients treated with both unilateral and bilateral distal-extension ISRPDs/IARPDs. The most common arch configuration was mandibular Kennedy Class II (10 patients) followed by mandibular Kennedy Class I (eight patients). A total of 67 implants were placed to provide support using healing caps or retention using resilient attachments. An overall survival rate of 97.1% was achieved during a mean follow-up period of 35.4 months.

Halterman *et al.* (36) described an ISRPD, in which the RPD was made of nickel–chromium alloy with 18-gauge wrought wire clasps. The healing caps on fixtures were used to support the RPD. The authors failed to

report the length of the follow-up period but showed that combining the implant and natural teeth in supporting RPD is more likely to reduce the posterior occlusion collapse compared to CRPD.

Keltjens *et al.* (37) reported two cases of mandibular implant-tooth-borne RPDs opposing full denture prostheses. The first case was an ISRPD, where a 3.3 mm × 10.5 mm implant was used, and the metal framework had a cup-shaped cavity resting on a rounded implant head. In the second case (IARPD), a 3 mm × 10 mm implant was used and magnets placed over the implants to provide additional retention. The authors stated that the risk of combination syndrome was reduced by preventing the resorption in the anterior maxilla.

Kuzmanovic *et al.* (38) reported a case of mandibular distal-extension IARPD in which a chromium–cobalt RPD was fabricated using a modified intracoronal attachment method of the channel shoulder pin system in metal ceramic crowns on mandibular canines. Ball attachments with gold matrices on the mandibular RPD were used to provide retention and support of the IARPD. Minor prosthetic maintenance in the form of simple activation of the gold matrices was reported after 2-year follow-up.

Mijiritsky *et al.* (39) followed up 15 partially edentulous patients wearing IARPDs for a period of 2–7 years. Both Kennedy Class I and II were included. Ball attachments and bar designs were used in conjunction

Table 2. Summary of included studies

Study design	Fields & Campfield (34)	Grossmann <i>et al.</i> (35)	Halberman <i>et al.</i> (36)	Kelijens <i>et al.</i> (37)	Kuzmanović <i>et al.</i> (38)	Mijiritsky <i>et al.</i> (39)	Mitrani <i>et al.</i> (40)	Ohkuba <i>et al.</i> (41)	Payne <i>et al.</i> (42)
Country	United States	Israel	United States	The Netherlands	New Zealand	Israel	United States	Japan	New Zealand
Year of Publication	1974	2009	1999	1993	2004	2005	2003	2008	2006
No. of participants/ no. of implants	1/1	35/67	1/2	2/4	1/2	15/33	10/16	5/10	24/48
Implant system	Endosseous blade implant	Zimmer Dental 3i Implant Innovations ^g MIS Implants Technologies ^h	Sulzer Calcheke ^e	IMZ implant ^f Dyna implant ^{**}	ITI implants ^{††}	Not clear	Brånemark ^{††} ITI implants ^{††}	Brånemark TU MK III ^{††}	ITI implants ^{††}
Implant length (mm)	Not clear	Not clear	13	10.0, 10.5	12	≥10	Not clear	8.5–11.5	10.0, 10.5
Implant diameter (mm)	Not clear	Not clear	3.25	3.0, 3.3	4.1	≥3.7	Not clear	3.75	3.0, 3.3
Implant abutment (attachment)	Implant post	Healing caps Locator attachment [§] O-ring attachment (Zimmer Dental) [*]	5-mm healing caps	Case 1: Implant provided support: Implant rounded head Case 2: Dyna magnets	Patrices on implants attached to gold matrices of the RPD	Ball attachments and bar connections	Group 1: modified healing abutment Group 2: Resilient attachment [OSO, Attachments International; Zaag, Preat; Hader Bar and Clip Attachments International; or extraoral resilient attachment (ERA), Sterngold]	Healing abutment simulate an ISRPD situation and healing caps simulate a CRPD situation	Control group: CRPD Test group: ISRPD with healing caps (Stage I) and IARPD with patrices (Stage II)

Table 2. (Continued).

	Fields & Campfield (34)	Grossmann <i>et al.</i> (35)	Halterman <i>et al.</i> (36)	Kelijens <i>et al.</i> (37)	Kuzmanovic <i>et al.</i> (38)	Mijiritsky <i>et al.</i> (39)	Mitrani <i>et al.</i> (40)	Ohlba <i>et al.</i> (41)	Payne <i>et al.</i> (42)
Outcomes evaluated	Patient satisfaction Marginal bone loss	Patient satisfaction Masticatory efficiency	Not reported	Patient satisfaction	Prosthetic maintenance	Prosthetic maintenance patient satisfaction	Patient satisfaction Soft and hard tissue response	Patient satisfaction Masticatory efficiency	Prosthetic maintenance Marginal bone loss
Complications (maintenance)	Adjustment of acrylic base 30 days after insertion	Two failed implants	Not reported	Repeated relining	Activation of the gold matrices	Only one case of rest rupture	Fitting Screw loosening Framework fracture Hyperplastic tissue	Not reported	Loose healing cap (Stage I) Matrix activation Adjustment of wrought wire clasp Fracture of acrylic denture base
Level of evidence	IV	IV	IV	IV	IV	IV	IV	III-1	III-1
Follow-up period (months)	7	9-120 months	Not reported	24	24	24-84	12-48	<1 (measurements taken at 3 weeks)	12 months
Implant survival rate (%)	100	97-1	100	100	100	100	93-75	100	100

RPD, removable partial denture; CRPD, conventional removable partial denture; ERPD, implant-supported removable partial denture; IARPD, implant-assisted removable partial denture.
 *Carlsbad, CA, USA.
 †Palm Beach, Gardens, FL.
 ‡Shlomi, Israel.
 §Locator, Zest, Escondido, CA.
 ¶Friedrichsfeld AG, Heideberg, Germany.
 **Dyna Dental Engineering, Bergen op Zoom, The Netherlands.
 ††Straumann AG, Waldenburg, Switzerland.
 ‡‡Nobel Biocare, Göteborg, Sweden.

with 3-7-mm or more diameter implants. The authors evaluated the prosthetic maintenance and patient satisfaction. Inconsiderable complication of only one rest rupture was reported during the follow-up period. Patients showed both improved chewing ability and satisfaction.

Mitrani *et al.* (40) carried out a retrospective study of 10 patients with Kennedy class I and II partially edentulous situations. Two groups of patients were evaluated. In the first group, implants were solely used as vertical stops with single contact points created using dome-shaped healing abutments. In the second group, a resilient attachment was used as a retentive element. More complications were reported in the first group such as pitting of the surface of the healing abutment, screw loosening and framework fracture. The authors, nevertheless, concluded that ISRPD/IARPD improved patient satisfaction, maintained the stability of the peri-implant soft and hard tissues within normal limits.

Ohkubo *et al.* (41) reported a pilot, randomized study in which five partially edentulous patients (Kennedy Class I) were evaluated for masticatory movements, occlusal forces and patient comfort following placement of ISRPD. The healing abutments were placed to provide support to the RPD, and then the healing caps were used instead of healing abutments to simulate a CRPD situation. The study showed no significant differences between both designs in terms of masticatory movements, whereas the occlusal force and contact area were greater and more distally located in the ISRPD. In addition, patients showed significant improvement when implants were used for support.

Payne *et al.* (42) reported the results of one treatment center, which was part of a multicenter randomized clinical trial that evaluated the prosthetic maintenance of ISRPD/IARPD. Twenty-four patients were randomly allocated to control (CRPD opposing maxillary complete denture) or test (implant-tooth-borne RPD opposing maxillary complete denture). The patients had healing caps in stage I (ISRPD) and then patrices in stage II (IARPD). The prosthetic maintenance was evaluated after 12 months and included loosening of healing caps in 84% of the patients in the test group (Stage I). Matrix activation or deactivation, adjustment of wrought wire clasp and fracture of denture base were observed in 58.3% of the test group (Stage II).

Discussion

This systematic review followed the recent guidelines of PRISMA in searching for the best available evidence for using implants in assisting/supporting RPD in Kennedy Class I mandibular arches. The prosthetic rehabilitation of mandibular bilateral distal extension partially edentulous patients by the use of ISRPD/IARPD was largely described in the form of clinical case reports (34, 36–38). In addition, three retrospective studies (35, 39, 40) and two randomized trials (41, 42) were identified. However, the majority of the selected studies were poorly reported and failed to mention details such as follow-up period, implant size and length. The level of evidence of the available literature was generally low as two studies (41, 42) were classified as NHMRC level III-1 and seven studies as NHMRC level IV (34–40). Moreover, a quantitative systematic review or meta-analysis was not conducted because of lack of sufficient number of randomized or non-randomized controlled trials in the literature.

Implants have been incorporated in the RPD design to provide support by using healing caps or retention by carrying retentive means (i.e. attachments). The former was associated with complications such as pitting of the surface or screw loosening, which can be overcome by polishing the abutment head and relining as well as the use of antirotational features to avoid abutment loosening. Attachments can be generally categorized into two types: studs or bars. The type of resilient attachment usually used in IARPD is extracoronar resilient attachment (ERA), o-ring system or a similar attachment system (13). Locator abutments have also been recommended (43) because of their availability in different heights in addition to their resiliency and retention. Locator abutment can also be easily repaired and replaced which enhance their durability (44). Cho (45) studied the load transfer characteristics of IARPD and showed that the use of resilient attachment with distal implants reduced the stress concentration around implants and abutment tooth. In contrast, Itoh *et al.* (46) used a photoelastic model of mandibular bilateral distal-extension implant-tooth-borne RPD and found that both healing abutments and ball attachments provided support to the RPD with no difference in stress concentration. However, there is currently no available evidence to suggest one design over the other in terms of retention and support.

With regard to implant location, distally placed implants were used to transform Kennedy Class I in the mandible to a more favourable arch configuration, namely Kennedy Class III. Finite element analysis (FEA) has, however, showed more tendency to displacement when implants were placed in a second molar position, and suggested a more central position in the arch (i.e. first molar region) (47). On the other hand, Ohkubo *et al.* (48) showed that implant placement in the second molar region reduced the distal placement and bone resorption. Likewise, Grossmann *et al.* (35) recommended a second molar location for the implant to enhance support and stability, but also suggested placing the implant adjacent to the distal abutment in case of inadequate posterior alveolar ridge, possible future use for fixed implant-supported prosthesis or to improve aesthetics by avoiding the use of a retentive clasp. Further studies are still needed to evaluate the most effective position of the implant.

The optimal length and diameter of the implants associated with RPD have not been determined yet. In a biomechanical study, Verri *et al.* (49) created six models and used FEA to examine the dimensions of implants incorporated in the design of RPD. The authors showed that increasing both the length and diameter of implants were likely to reduce the tension values. Yet, it is expected that the implants used to support a RPD can be shorter with smaller diameter than implants supporting a fixed prostheses particularly in sharp mandibular residual ridges.

Several review articles have been published on the use of the ISRPD/IARPD and discussed its clinical procedure, fabrication, indications, advantages and limitations (35, 43, 50). Grossmann *et al.* (35) and Mijiritsky (50) provided a summary of the current literature regarding the use of implants in conjunction of both maxillary and mandibular RPD. The former also presented an evaluation of retrospective case series along with the review. Chikunov *et al.* (43) described the clinical procedures and fabrication of IARPD. Resilient attachments were selected through the use of locator abutments, and the implants were placed anterior to the mental foramina (in the premolar site). The authors reported the indications and contraindications as well as the advantages of using such prosthetic design. The current systematic review is different from previous studies in two aspects: first, only studies that reported on mandibular bilateral distal extension partially edentulous situations were included. Second, all

types of studies including case reports were summarized in this review.

The numerous difficulties associated with the CRPD are well established, particularly the inability to achieve both a satisfactory patient and oral comfort as defined by the absence of chewing difficulties and compromised aesthetics (51). Nevertheless, CRPD will remain an economically adequate and non-invasive treatment option, particularly in non-industrialized countries, where the patient's economic status has a profound effect on the prosthodontic choice (17). On the other hand, an implant-supported fixed prosthesis is an adequate alternative and a well-documented treatment modality for the distal-extension edentulous situation (52, 53). However, it is beyond the financial capabilities of some patients (54). The concept of shortened dental arch (SDA) is another treatment option that needs to be considered in treatment planning of partially edentulous patients. The SDA approach provides an affordable treatment modality that may provide an acceptable oral function and improves both oral hygiene and patient satisfaction. When compared with CRPD, SDA showed a long-term oral comfort and functionality (55). Nevertheless, the number of teeth needed to satisfy patients' functional demands should be individually evaluated. In addition, more research is needed before SDA concept is widely accepted and practised in the prosthodontic community (56, 57).

Although the use of an ISRPD/IARPD lacks research-based evidence, it can be considered, within the limitation of the current review, a possible treatment option to improve stability, aesthetics and preserve the remaining soft and hard tissues. In addition, ISRPD/IARPD maintains the integrity of the vertical dimension of occlusion, thus reducing the risk of combination syndrome and moves the center of the occlusal force distally. Providing a distal occlusal support has been suggested to minimize the onset of temporomandibular joint (TMJ) syndrome and reduce the denture movement during chewing.

Conclusions

Posteriorly placed oral implants can modify the Kennedy classification of partially edentulous arches by converting Class I (tooth- and tissue-supported) to Class III (tooth- and implant-supported). ISRPD/IARPD seems to overcome the numerous problems associated with CRPD in addition to achieving a higher level of

patient satisfaction. However, there is still no evidence-based research that validated the use of such treatment modality in managing bilateral distal-extension partial edentulism, or supported the use of implants with healing abutment or resilient attachment as means of providing support and retention to the RPD. Long-term randomized controlled studies are needed.

References

- Dye B, Tan S, Smith V, Lewis B. Trends in oral health status: United States, 1988-1994 and 1999-2004. National Centre for Health Statistics. *Vital Health Stat.* 2007;11:1-92.
- Kelly M, Steele J, Nuttall N, Bradnock G, Morris J, Nunn J *et al.* Adult dental health survey: oral health in the United Kingdom in 1998. London: TSO; 2000.
- Micheelis W, Schiffner U. Fourth German Oral Health Study (DMS IV). Institut der Deutschen Zahnärzte (IDZ, Materialienreihe Band 31; 2006). Cologne: Deutscher Zahnärzte Verlag (in German).
- Slade G, Spencer A, Roberts-Thomson K. Australia's dental generations. The National Survey of Adult Oral Health 2004-06. Canberra: Australia Institute of Health and Welfare; 2007.
- Steele JG, Treasure E, Pitts NB, Morris J, Bradnock G. Total tooth loss in the United Kingdom in 1998 and implications for future. *Br Dent J.* 2000;189:598-603.
- Douglass CW, Watson AJ. Future needs for fixed and removable partial dentures in the United States. *J Prosthet Dent.* 2002;87:9-14.
- Bergman B, Hugoson A, Olsson CO. Caries, periodontal and prosthetic findings in patients with removable partial dentures: a ten-year longitudinal study. *J Prosthet Dent.* 1982;48:506-514.
- Bergman B, Hugoson A, Olsson CO. A 25 year longitudinal study of patients treated with removable partial dentures. *J Oral Rehabil.* 1995;22:595-599.
- Kapur KK. Veterans Administration Cooperative Dental Implant Study - comparisons between fixed partial dentures supported by blade-vent implants and removable partial dentures. Part III: comparisons of masticatory scores between two treatment modalities. *J Prosthet Dent.* 1991;65:272-283.
- Kapur KK. Veterans Administration Cooperative Dental Implant Study - comparisons between fixed partial dentures supported by blade-vent implants and removable partial dentures. Part IV: comparisons of patient satisfaction between two treatment modalities. *J Prosthet Dent.* 1991;66:517-530.
- Rissin L, Feldman RS, Kapur KK, Chauncey HH. Six-year report of the periodontal health of fixed and removable partial denture abutment teeth. *J Prosthet Dent.* 1985;54:461-467.
- Kennedy E. Partial denture construction. *Dental Items of Interest.* 1923;47:23.
- Brudvik JS. Implants and removable partial dentures. In: Brudvik JS, ed. *Advanced removable partial dentures.* Chicago: Quintessence Publishing Co; 1999: p. 153-159.
- Jepson NJ, Thomason JM, Steele JG. The influence of denture design on patient acceptance of partial dentures. *Br Dent J.* 1995;178:296-300.
- Vermeulen AH, Keljens HM, van't Hof MA, Kayser AP. Ten-year evaluation of removable partial dentures: survival rates based on retreatment, not wearing and replacement. *J Prosthet Dent.* 1996;76:267-272.
- Wetherell JD, Smales RJ. Partial denture failures: a long-term clinical survey. *J Dent.* 1980;8:333-340.
- Wöstmann B, Budtz-Jørgensen E, Jepson N, Mushimoto E, Palmqvist S, Sofou A *et al.* Indications for removable partial dentures: a literature review. *Int J Prosthodont.* 2005;18:139-145.
- Kelly E. Changes caused by a mandibular removable partial denture opposing a maxillary complete denture. *J Prosthet Dent.* 1972;27:140-150.
- Saunders TR, Gillis RE, Desjardins RP. The maxillary complete denture opposing the mandibular bilateral distal extension partial denture: treatment considerations. *J Prosthet Dent.* 1979;41:124-128.
- Shen K, Gongloff RK. Prevalence of the combination syndrome among denture patients. *J Prosthet Dent.* 1989;62:642-644.
- Carlsson GE. Clinical morbidity and sequelae of treatment with complete dentures. *J Prosthet Dent.* 1998;79:17-23.
- Palmqvist S, Carlsson GE, Öwall B. The combination syndrome: a literature review. *J Prosthet Dent.* 2003;90:270-275.
- Moher D, Liberati A, Tetzlaff J, Altman DG; PRISMA Group. Preferred reporting items for systematic reviews and meta-analyses: the PRISMA statement. *Ann Intern Med.* 2009;151:264-269.
- Miller SA, Forrest JL. Enhancing your practice through evidence-based decision making: PICO, learning how to ask good questions. *J Evid Based Dent Pract.* 2001;1:136-141.
- Australian Government, NHMRC: How to use the evidence: assessment and application of scientific evidence. Available at http://www.nhmrc.gov.au/_files_nhmrc/file/publications/synopses/cp69.pdf, accessed 16 December 2009.
- Ganz SD. Combination natural tooth and implant-borne removable partial denture: a clinical report. *J Prosthet Dent.* 1991;66:1-5.
- de Carvalho WR, Barboza EP, Caúla AL. Implant-retained removable prosthesis with ball attachments in partially edentulous maxilla. *Implant Dent.* 2001;10:280-284.
- Giffin KM. Solving the distal extension removable partial denture base movement dilemma: a clinical report. *J Prosthet Dent.* 1996;76:347-349.
- Mijiritsky E, Karas S. Removable partial denture design involving teeth and implants as an alternative to unsuccessful fixed implant therapy: a case report. *Implant Dent.* 2004;13:218-222.
- Calbianca M. Combination syndrome: treatment with dental implants. *Implant Dent.* 2003;12:300-305.
- Chronopoulos V, Sarafianou A, Kourtis S. The use of dental implants in combination with removable partial dentures. A case report. *J Esthet Restor Dent.* 2008;20:355-365.

32. Grossmann Y, Levin L, Sadan A. A retrospective case series of implants used to restore partially edentulous patients with implant-supported removable partial dentures: 31-month mean follow-up results. *Quintessence Int.* 2008;39:665–671.
33. Jadad AR, Moher D, Klassen TP. Guides for reading and interpreting systematic reviews: II. How did the authors find the studies and assess their quality? *Arch Pediatr Adolesc Med.* 1998;152:812–817.
34. Fields H Jr, Campfield RW Jr. Removable partial prosthesis partially supported by an endosseous blade implant. *J Prosthet Dent.* 1974;31:273–278.
35. Grossmann Y, Nissan J, Levin L. Clinical effectiveness of implant-supported removable partial dentures – A review of the literature and retrospective case evaluation. *J Oral Maxillofac Surg.* 2009;67:1941–1946.
36. Halterman SM, Rivers JA, Keith JD, Nelson DR. Implant support for removable partial overdentures: a case report. *Implant Dent.* 1999;8:74–78.
37. Keltjens HM, Kayser AP, Hertel R, Battistuzzi PG. Distal extension removable partial dentures supported by implants and residual teeth: considerations and case reports. *Int J Oral Maxillofac Implants.* 1993;8:208–213.
38. Kuzmanovic DV, Payne AGT, Purton DG. Distal implants to modify the Kennedy classification of a removable partial denture: a clinical report. *J Prosthet Dent.* 2004;92:8–11.
39. Mijiritsky E, Ormianer Z, Klinger A, Mardinger O. Use of dental implants to improve unfavorable removable partial denture design. *Compend Contin Educ Dent.* 2005;26:744–6, 748, 750 passim.
40. Mitrani R, Brudvik JS, Philips KM. Posterior implants for distal extension removable prostheses: a retrospective study. *Int J Periodontics Restorative Dent.* 2003;23:353–359.
41. Ohkubo C, Kobayashi M, Suzuki Y, Hosoi T. Effect of implant support on distal-extension removable partial dentures: *in vivo* assessment. *Int J Oral Maxillofac Implants.* 2008;23:1095–1101.
42. Payne A, Kuzmanovic DV, De Silva-Kumara R, van Staden IP. Mandibular removable partial dentures supported by implants: one-year prosthodontic outcomes. *J Dent Res.* 2006; 85(Spec Iss B):2570, (<http://www.dentalresearch.org>).
43. Chikunov I, Doan P, Vahidi P. Implant-retained partial overdenture with resilient attachments. *J Prosthodont.* 2008;17:141–148.
44. Schneider AL, Kurtzman GM. Bar overdentures utilizing the Locator attachment. *Gen Dent.* 2001;49:210–214.
45. Cho HW. Load transfer by distal extension RPD with implant assisted support. *J Dent Res.* 2002; 80:1095, (<http://www.dentalresearch.com>).
46. Itoh H, Sasaki H, Nakahara H, Katsube T, Satoh M, Matyas J *et al.* Load transmission by distal extension RPD with implant assisted support. *J Dent Res.* 2007 86(Spec Iss A):1476, (<http://www.dentalresearch.com>).
47. Cunha LD, Pellizzer EP, Verri FR, Pereira JA. Evaluation of the influence of location of osseointegrated implants associated with mandibular removable partial dentures. *Implant Dent.* 2008;17:278–287.
48. Ohkubo C, Kurihara D, Shimpo H, Suzuki Y, Kokubo Y, Hosoi T. Effect of implant support on distal extension removable partial dentures: *in vitro* assessment. *J Oral Rehabil.* 2007;34:52–56.
49. Verri FR, Pellizzer EP, Rocha EP, Pereira JA. Influence of length and diameter of implants associated with distal extension removable partial dentures. *Implant Dent.* 2007;16:270–280.
50. Mijiritsky E. Implants in conjunction with removable partial dentures: a literature review. *Implant Dent.* 2007;16:146–154.
51. Budtz-Jørgensen E, Bochet G. Alternate framework designs for removable partial dentures. *J Prosthet Dent.* 1998;80:58–66.
52. Becker W, Becker BE, Alsawwied A, Al-Mubarak S. Long-term evaluation of implants in maxillary and mandibular molar positions. A prospective study. *J Periodontol.* 1999;70:896–901.
53. Parein AM, Eckert SE, Wollan PC, Keller EE. Implant reconstruction in the posterior mandible: a retrospective long term study. *J Prosthet Dent.* 1997;78:34–42.
54. Budtz-Jørgensen E, Isidor P. A 5-year longitudinal study of cantilevered fixed partial dentures compared with removable partial dentures in a geriatric population. *J Prosthet Dent.* 1990;64:42–67.
55. Witter DJ, De Haan AP, Käyser AF, Van Rossum GM. A 6-year follow-up study of oral function in shortened dental arches. Part II: craniomandibular dysfunction and oral comfort. *J Oral Rehabil.* 1994;21:353–366.
56. Kanno T, Carlsson GE. A review of the shortened dental arch concept focusing on the work by Käyser/Nijmegen group. *J Oral Rehabil.* 2006;33:850–862.
57. Armellini D, von Fraunhofer JA. The shortened dental arch: a review of the literature. *J Prosthet Dent.* 2004;92:531–535.

Correspondence: Reza A. Shahrhiri, Sir John Walsh Research Institute, School of Dentistry, University of Otago, PO Box 647, Dunedin, New Zealand. E-mail: reza_shahrhiri2006@yahoo.com

Appendix 2



A SIMPLE METHOD TO TRANSFER THE SELECTED PATH OF INSERTION OF A REMOVABLE PARTIAL DENTURE INTRAORALLY

Vincent Bennani, DDS, PhD,^a and Reza Shahmiri, CDT^b
University of Otago School of Dentistry, Dunedin, New Zealand

The treatment of choice for a partially edentulous patient is placement of a fixed partial denture supported by either teeth or implants.¹ However, when implants are contraindicated or when the remaining abutment teeth cannot support a fixed prosthesis, a removable partial denture (RPD) may be an alternative.² In designing an RPD, selecting the most appropriate path of insertion to promote ease of placement, esthetics, retention, stability, and support is a challenging aspect for many clinicians.³ Despite the fact that several different techniques for transferring the path of insertion intraorally have been described, this crucial step remains technically demanding.^{4,5}

This article describes a method for making an index to transfer the selected path of insertion from the diagnostic cast intraorally. This simple technique assists the dentist to more ideally modify the contours of each abutment tooth.

PROCEDURE

1. Select the appropriate path of insertion on the diagnostic cast.

2. Fabricate a silicone index (President heavy body; Coltène/Whaledent, Inc, Cuyahoga Falls, Ohio) on the diagnostic cast, on the remaining teeth, excluding the abutment teeth. Do not cover any soft tissue with the index.

3. When the silicone is polymerized, use a permanent marker to mark the selected path of insertion on the



1 Buccal view of silicone index on diagnostic cast. Note line identifying preselected path of insertion.



2 Buccal clinical view. Note orientation of bur parallel to preselected path of insertion to ease teeth modification.

buccal and lingual aspect of the index (Fig. 1).

4. Remove the index from the cast and trim it with a scalpel to provide an intimate fit intraorally.

5. Align the bur parallel to the mark on the silicone index, and make modifications on the abutment teeth

following the preselected path of insertion (Fig. 2).

REFERENCES

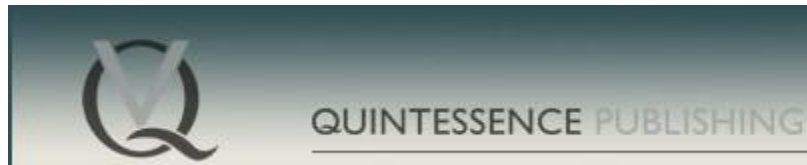
1. Phoenix RD, Cagna DR, Defreest CF, Stewart KL. *Stewart's clinical removable partial prosthodontics*. 3rd ed. Chicago: Quintessence; 2003. p. 1-18.

^aSenior Lecturer, Department of Oral Rehabilitation.

^bStudent, Master Dental Technology program, Department of Oral Rehabilitation. (*J Prosthet Dent* 2009;101:73-74)



Appendix 3



Int Poster J Dent Oral Med • ISSN 1612-7749

International Poster Journal of Dentistry and Oral Medicine

International Poster Journal of Dentistry and Oral Medicine

Int Poster J Dent Oral Med 13 ([2011](#)), No. 1 (15.03.2011)

Int Poster J Dent Oral Med 2011, Vol 13 No 1, Poster 515

Attachments in Implant-Assisted Removable Partial Dentures: A Design Dilemma

Authors:

Reza A. Shahmiri, Dr Momen A. Atieh,
Sir John Walsh Research Institute, School of dentistry, [University](#) of Otago, New Zealand

Date/Event/Venue:

15-17 April 2010
ITI World Symposium
Geneva, Switzerland

Introduction

The placement of two distal implants has been recommended to transform Kennedy class I to a Kennedy class III situation. Different types of attachment were used in implant-assisted removable partial denture (IARPD). However, there is currently no available evidence to

suggest the most effective attachment system¹; The aim of this study was to assess the stress and strain behaviour of ball attachment systems with two different matrix designs (titanium vs. elliptical) incorporated into an existing removable partial denture using a three dimensional finite element analysis (FEA).

Material and Methods

A Faro Arm (Faro Technologies Inc, USA) was used to extract the geometrical data of a replicated partially edentulous human mandible. Standard plus regular neck (4.8 x 12 mm) Straumann® implant and attachment with two different matrix designs, tooth roots and periodontal ligaments were modeled using a combination of reverse engineering processes in Rapidform XOR2 and solid modeling processes in a FEA program Solidworks 2008 (Solidworks Corporation, Concord, MA, USA) (Figure 1, a & b).

Two models were generated:

1. Model A, An IARPD with ball attachment system with titanium matrix (Figure 1, c).
2. Model B, An IARPD with ball attachment system with elliptical matrix (Figure 1, d).

The Models were loaded with a vertical force of 120 N. ANSYS Workbench 11.0 (Swanson Analysis, Huston, PA, USA) was used to analyze the stress and strain patterns.

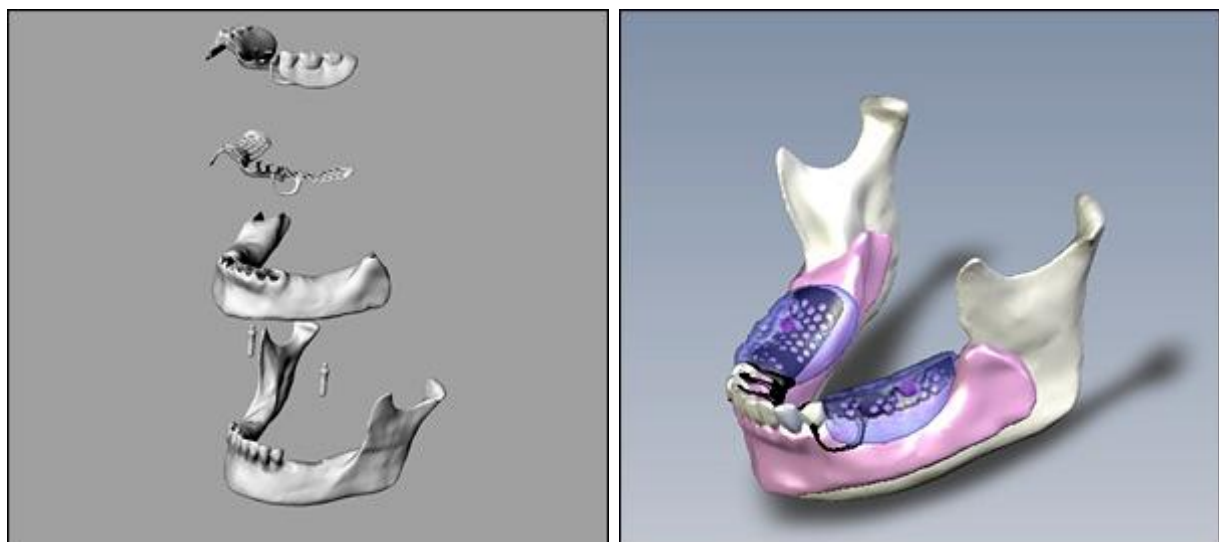


Figure 1(a): All components in the same orientation
Figure 1(b): All body parts and components are assembled



Figure 1(c): Model B with elliptical matrix

Figure 1(d): Model A with titanium matrix

Results

- Model A: maximum stress was concentrated around the neck of ball attachment (male part) (Figure 2),
- Model B: maximum stress was located on the lamella retention insert (female part) (Figure 3).
- In addition, more strain values were observed at the outer surface of titanium matrix (Figure 4).

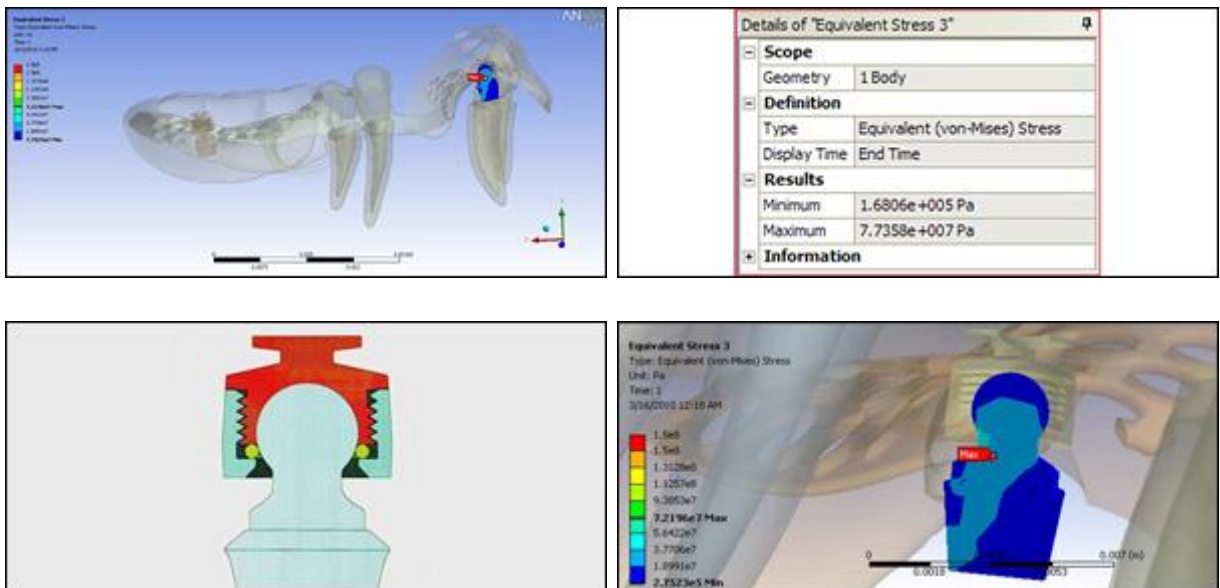


Figure 2: Model A: Stress concentration on the neck of ball attachment

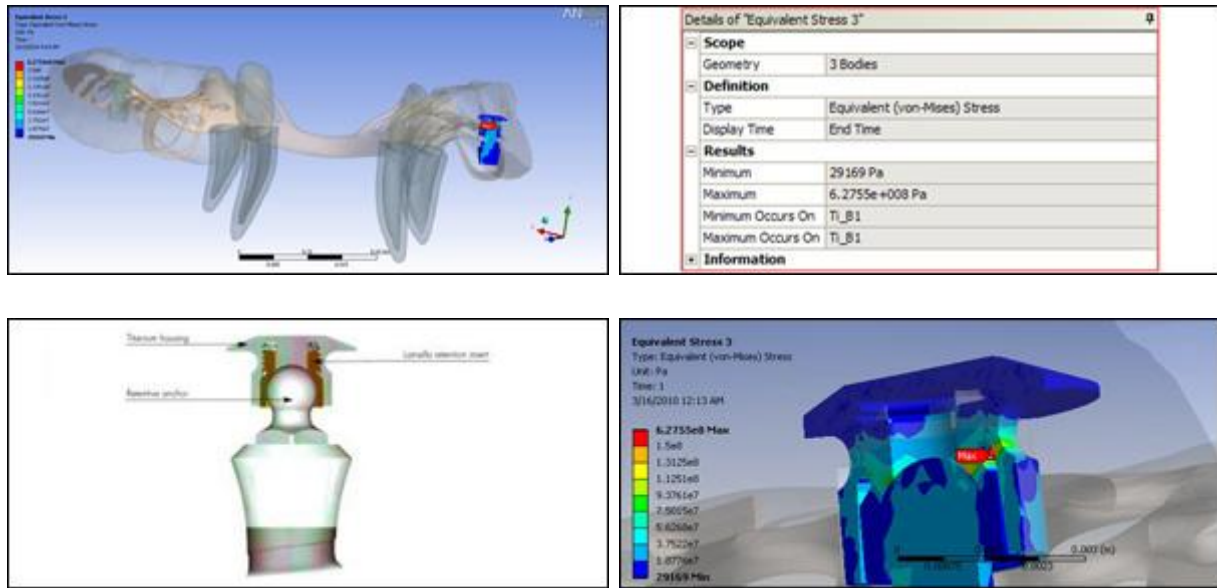


Figure 3: Model B: Stress concentration on the lamella retention insert

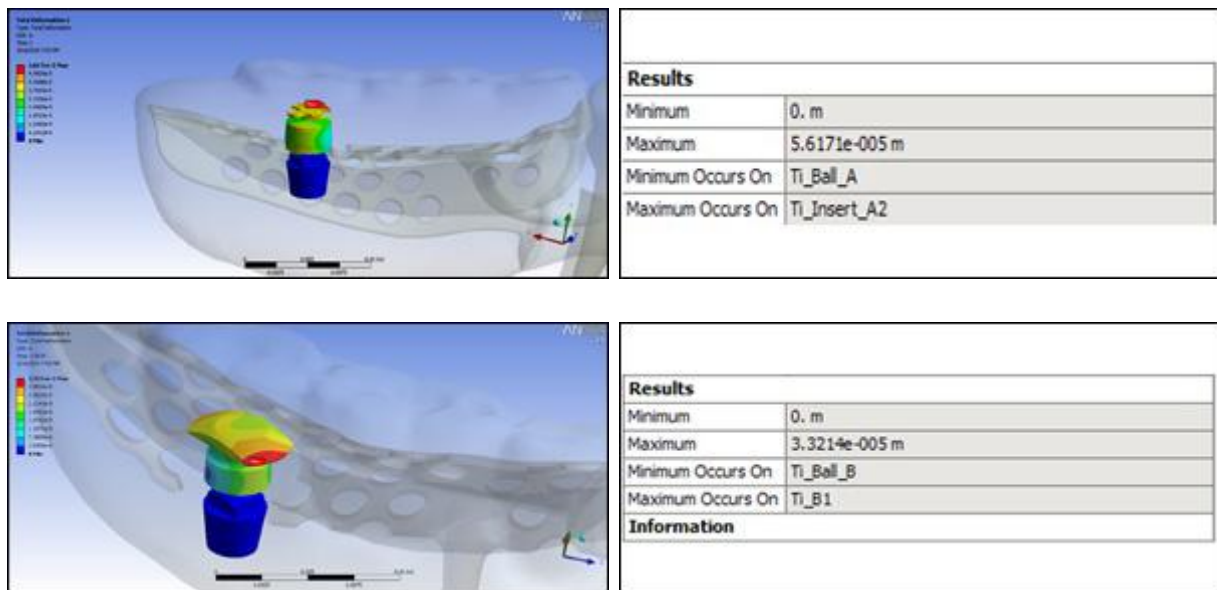


Figure 4: Higher strain value were observed on Ti matrix (Model A)

Discussion

Ball attachments has been used to provide retention and support of IARPD² as well as reducing stress concentration around implants and abutment teeth. However, acrylic fracture of IARPD bases was one of the most commonly reported complications³. In this study, FEA was used to evaluate the stress-strain patterns of two matrix designs incorporated into the same acrylic base. Elliptical matrix showed a more favourable stress-strain behaviour compared to the titanium matrix. The maximum stress concentration of the elliptical matrix was located on the lamella retention insert, which acted as a stress breaker. Hence, the stress transfer to the ball attachment

and underlying structure was reduced. Additionally, less strain values were observed at the outer surface of the attachment which was embedded into the acrylic base. Nevertheless, there is still currently no available clinical evidence to suggest one design over the other in terms of retention and support¹.

Conclusions

Within the limitation of this study, the embedded elliptical matrix in acrylic may achieve a more favourable stress/strain distribution during functional loading compared to the titanium matrix. Further long-term randomized controlled studies are needed.

References

1. Shahmiri, R. A. ; Atieh, M. A. Mandibular Kennedy class I implant-tooth-borne removable partial denture: a systematic review. *Journal of Oral Rehabilitation* 2010;37:225-234.
2. Kuzmanovic, D. V. ; Payne, A. G. T. ; Purton, D. G. Distal implants to modify the Kennedy classification of a removable partial denture: A clinical report. *Journal of Prosthetic Dentistry* 2004; 92:8-11.
3. Payne, A. ; Kuzmanovic, D. V. ; De Silva-kumara, V. ; Van Staden, I. P. Mandibular removable partial dentures supported by implants: one-year prosthodontic outcomes. *Journal of Dental Research* 2006; 85 (Spec Iss B):2570.

Abbreviations

IARPD = Implant Assisted Removable Partial Denture

This Poster was submitted by [Reza A. Shahmiri](#).

Correspondence address:

[Reza A. Shahmiri](#)

University of Otago

Sir John Walsh Research Institute, School of dentistry

900 Cumberland St.

Dunedin North, Dunedin 9012

New Zealand

[© 2002-2011 Quintessence Publishing Group](#)

Appendix 4



4218 Mandibular Kennedy Class I Implant-Assisted RPD: Different Loading Condition

Saturday, July 17, 2010: 3:30 p.m. - 4:45 p.m.

Location: Exhibit Hall (CCIB)

[R. SHAHMIRI](#), J. AARTS, V. BENNANI, and M. SWAIN, [University](#) of Otago, Dunedin,
New Zealand

4218 Mandibular Kennedy Class I Implant-Assisted RPD: Different Loading Condition

Saturday, July 17, 2010: 3:30 p.m. - 4:45 p.m.

Location: Exhibit Hall (CCIB)

R. SHAHMIRI, J. AARTS, V. BENNANI, and M. SWAIN, University of Otago, Dunedin, New Zealand

Objectives: The placement of two implants on distal of Kennedy class I RPD can provide extra support and retention and will result in, improvement of chewing efficiency and biting forces. However, increasing bite force can jeopardize to prostheses if inappropriate occlusal scheme was selected. Objective of this study is to compare two occlusal scheme Kennedy class I implant-assisted RPD: group function vs. generalized balanced occlusion. **Methods:** A model of partially edentulous mandible (Kennedy class I) was constructed with missing of two molar and second premolar. Conventional RPD manufactured according to design of Kennedy class I RPD with Implant were incorporated into RPD. Straumann® Implants were placed on second molar regions. Strain gauges were used to measure strain on framework and acrylic structures. The Implant-assisted RPD was loaded to 120N Uni-laterally and Bi-laterally in three different areas and data extracted from universal testing machine's software and transferred to Excel to identify maximum strain value in each region. **Results:** same tension and compression behavior were observed in all conditions of bi-lateral loading between framework and acrylic structure of implant-assisted RPD. In contrast, an opposite strain behavior was observed between Framework and acrylic structure with uni-lateral loading. **Conclusion:** with limitation of this study it is suggested that generalized balanced occlusion scheme can minimize destructive strain in structure of mandibular Kennedy class I implant-assisted RPD.

Appendix 5

Journal of Oral Implantology

The evaluation of optimal taper of immediately loaded wide-diameter implants: A finite element analysis

Manuscript Number: AAID-JOI-D-11-00104R1

Full Title: The evaluation of optimal taper of immediately loaded wide-diameter implants:
A finite element analysis

Short Title: Taper angle of immediately loaded wide implants

Article Type: Research

Keywords: oral implants, finite element analysis, immediate loading, stress distribution,
tapering angle

Corresponding Author: Momen Atieh, BDS, MSc

Sir John Walsh Research Institute

Dunedin, Otago NEW ZEALAND

Corresponding Author Secondary

Information:

Corresponding Author's Institution: Sir John Walsh Research Institute

Corresponding Author's Secondary

Institution:

First Author: Momen Atieh, BDS, MSc

First Author Secondary Information:

All Authors: Momen Atieh, BDS, MSc

Reza A Shahmiri

All Authors

Abstract:

Objectives:

The study aimed at evaluating the effects of different tapering angles of an immediately loaded wide-diameter implant on the stress/strain distribution in bone and implant following implant insertion in either healed or fresh molar extraction sockets.

Methods:

A total of 10 finite element (FE) implant-bone models, including 8.1 mm diameter implant, superstructure and mandibular molar segment, were created to investigate the biomechanical behaviour of different implant taper angles in both immediate and delayed placement conditions. The degrees of implant taper ranged from 2° to 14° and the contact conditions between the immediately loaded implants and bone were set with frictional coefficients (μ) of 0.3 in the healed models and 0.1 in the extracted models. Vertical and lateral loading forces of 189.5 N were applied in all models.

Results:

Regardless of the degree of implant tapering, immediate loading of wide-diameter implants placed in molar extraction sockets generated higher stress/strain levels than implants placed in healed sockets. In all models, the von-Mises stresses and strains at the implant surfaces, cortical and cancellous bone have increased with increasing the taper angle of the implant body, except for the buccal cancellous bone in the healed models. The maximum von-Mises strains were highly concentrated on the buccal cortical struts in the extracted models and around the implant neck in the healed models. The maximum von-Mises stresses on the implant threads were more concentrated in the non-tapered coronal part of the 11° and 14° tapered implants particularly in the healed models, while the stresses were more evenly dissipated along the implant threads in other models.

Conclusions:

Under immediate loading conditions, the present study indicates that minimally tapered implants generated the most favourable stress and strain distribution patterns in both extracted and healed molar sites.

Powered by Editorial Manager® and Preprint Manager® from Aries Systems Corporation

The evaluation of optimal taper of immediately loaded widiameter

implants: A finite element analysis

Momen A. Atieh^{1*}

Reza A. Shahmiri

¹Sir John Walsh Research Institute, School of Dentistry, University of Otago, Dunedin,
New
Zealand.

Short title: Taper angle of immediately loaded wide implants

***Correspondence to:**

Dr. Momen A. Atieh

Sir John Walsh Research institute

School of Dentistry, University of Otago

310 Great King Street

Dunedin 9016

New Zealand

Email: maatieh@gmail.com

Keywords: oral implants, finite element analysis, immediate loading, stress distribution,
tapering

angle

*Article File

The evaluation of optimal taper of immediately loaded wide-diameter implants: A finite element analysis

Introduction

Over the last decade, the primary stability of implants was tremendously improved through modifying the surgical protocol, implant surface characteristics and design. The ability to achieve and maintain a high primary stability has caused a paradigm shift in the way implants were traditionally placed and loaded. Shortening the treatment time have introduced new terms in the oral implant vocabulary. Terms such as “Immediate” or “Early” placement and loading were used to describe the different treatment modalities that attempted to meet the patients’ demands for a shorter period of intervention.¹⁻⁴ One of the most popular protocols is the one that combines the immediate implant placement with immediate restoration/loading (the “bimodal” approach, Fig 1).³ The immediate placement was defined as placing the implant in fresh extraction socket on the same day of surgery,¹ while the immediate restoration/loading referred to placing the implant restoration within the first 48 hours following implant placement.⁴ The bimodal approach offered the shortest treatment time, optimal soft tissue outcomes, and high short-term success rates.⁵⁻¹¹ However, meta-analytic studies showed a higher failure risk associated with immediate placement/loading of single implants compared with the conventional protocol and advised practitioners to remain cautious in embracing the “immediate” concept.^{2,3}

Implant design is one of the factors that may influence the biomechanical behaviour of an oral implant and hence its primary implant.¹² The earliest traditional implant was cylindrically parallel in design. The paralleled shape was, however, not applicable in all clinical situations.

Therefore, other implant designs and thread geometries were introduced to achieve a better

stability in different anatomical and bone conditions. The tapered (root-analogue) implant was initially marketed by Friatec Corporation to be inserted immediately into an extraction socket.^{13,14} The tapered implant design has a wide diameter coronally and a tapered implant body resembling the shape of an extraction socket. Such design may enhance the immediate placement by offering an implant surface that engages the walls of the tapered socket and minimizes the need for bone graft. In addition, tapered implants can be placed in nonextraction sites where wide-diameter implants offer a more favourable distribution of loading forces.¹⁵ Moreover, it has been suggested that tapered implants may improve aesthetics, allow implant insertion between two adjacent teeth,¹⁶ and avoid the risk of perforation due to anatomical concavities.¹⁷

The tapered design was modelled to enhance the primary implant stability in poor bone quality by transferring the compressive forces to the cortical bone, as the cortical bone is expected to handle higher stress/strain values than cancellous bone.^{18,19} Likewise, wide implants have also been reported to improve the primary stability by increasing the surface area of contact between the bone and the implant.²⁰ However, the surgical technique of placing tapered wide implant can be sensitive and mainly influenced by the degree of implant taper and bone density as excessive compression of bone can be created during implant insertion. Such compressive forces, if exceeded the physiological limits of bone, can lead to osseous necrosis and compromised stability.^{21,22}

The tapering angle can be one of the basic design features that differentiate between the increasing number of commercially available tapered implants in the market. From a biomechanical point of view, the optimal design for immediate loading is the one that has a tapering angle that can enhance the primary stability by allowing an even bone compaction, favourable magnitude and distribution of strains along the cortical and cancellous bone levels, and uniform stresses at the implant surface, without any

detrimental compressive or wedging effects. It is now well accepted that a certain level of intraosseous strain can enhance early osteogenesis at the bone-implant interface.²³⁻²⁵ Thus, an implant configuration that can achieve the desired level of microstrains may have a profound influence on the early phase of periimplant osteogenesis, which is crucial for the long-term success of immediately loaded implants. In implant biomechanics, finite element (FE) method has been extensively used to simulate clinical scenarios that would be more complicated to examine using other methods. The majority of the previous FE studies have extensively evaluated implant design parameters in a fully osseointegrated implant model.²⁶⁻²⁸ However, the biomechanical role of these parameters in immediate/early placement and loading scenarios has not been adequately studied in the literature. The aim of this study was therefore to analyse, using a non-linear FE approach, the influence of the implant tapering angle on the strain values in the cortical and cancellous bone and the stress distribution in immediately loaded wide-diameter implants placed in the molar sites under two different placement protocols (healed ridges *versus* extraction sockets).

Materials and Methods

FE model design

Three-dimensional models of posterior mandibular segment with wide-diameter implant and superstructure were created using a personal computer (AMD Athlon 64 x2 processor) and a computer aided design program (SolidWorks 2009, SolidWorks Corporation, Concord, MA). The dimensions of the mandibular bone segment were 27 mm in height and 12 mm in buccolingual width, and consisted of a spongy centre of cancellous bone surrounded by a 2 mm layer of cortical bone.²⁹ A molar extraction socket was modelled to simulate the immediate placement protocol. The socket dimensions were based on the anatomy and geometry of the roots of mandibular molars. The bone-implant models were

created according to tapering angle of the implant body (2°, 5°, 8°, 11°, and 14°) and the type of implant insertion (healed *versus* extraction site). Roman numbers (I-V) were used to describe the different tapering angles (Fig. 2) and either “h” or “e” was used to designate a healed or extraction site respectively. Thus, a total of 10 different implant models were available for analysis. Each implant had an 8.1 mm diameter, a length of 11 mm, and a thread pitch of 0.8 mm. For simplicity, a 5-mm high abutment was assembled to the implant as one piece unit and all-ceramic provisional crown was modelled over the titanium abutment. A rigid bond was assumed along the prosthesis-abutment interface and the thickness of the cement was excluded from the model.³⁰⁻³²

Material properties and interface conditions

The material properties of the bone, implant and prosthetic crown (Table 1) were presumed to be linear, elastic, homogenous and isotropic.^{33,34} A non-linear face-to-face contact model with coefficient of friction (μ) of 0.3 was used to simulate the contact condition in the healed ridges between the surface of immediately loaded implant and bone prior to osseous integration.^{35,36} A lower coefficient of friction (μ) of 0.1 was selected in the extracted models to account for the blood interface which acts as a lubricant between the immediately loaded implant and bone. The frictional contact elements were used to allow for contact pressure and shear movement.³⁷

Constraints and loads

The analysis was performed using FE software (SolidWorks Simulation version 2009 for windows). A loading force of 189.5N³⁸ was applied vertically and obliquely (45 degrees) to every node of the cusp to simulate immediate masticatory condition in the molar region. The direction of the load applied in all the models is shown in Fig. 3. An automatic mesh was generated and the models consisted of 42274 to 62087 elements and 9665 to 13263

nodes, depending on the implant taper and placement protocol. The boundary conditions were applied by constraining the three degrees of freedom at each node located at the mesial and distal aspects of the bone segment. The maximum von-Mises stress at the implant and the maximum displacement in bone were reported. All the stress/strain distribution patterns were illustrated using contour maps.

Results

The influence of the tapering design of an immediately loaded oral implant inserted in either a healed or extracted molar models was evaluated by calculating the maximum von-Mises stresses at the implant and the maximum von-Mises strains on the adjacent bone. The maximum von-Mises stress/strain values at the implant, cortical and cancellous levels are summarized in Table 2.

The tapered implants generated more stress/strain values at the implant, cortical and cancellous bone in the simulated extracted sites than the healed sites. At each tapering angle, the maximum von-Mises stress values at the immediately loaded implants in the extracted models were almost doubled compared to those in the healed models. Moreover, the increase in the implant taper angle resulted in higher stress values in both the extraction and non-extraction models. Hence, the lowest stress value was recorded in the 2° tapered implant in the healed model (9.9 MPa; Fig. 4, a), while the highest stress value was recorded in the most tapered implant in the extracted model (35.3 MPa; Fig. 4, b). At the abutment-implant interface, the maximum von-Mises stress values were considerably high when the taper angle was more than 8°. In the healed model, the peak values of von-Mises stresses occurred at the first three threads of the tapered implants in models IV and V, while the stress values were more evenly distributed along the implant threads in other models. In the cortical bone, the maximum von-Mises strains were generated at the cortical

bone around the implant neck in the healed model V (0.0003679ϵ ; Fig. 5, a) and at the cortical buccal strut adjacent to the implant neck in the extracted model V (0.003383ϵ ; Fig. 5, b). In the cancellous bone, the healed models showed a different behaviour in the strain distribution, as the highest von-Mises strain value occurred in the buccal side of the cancellous bone around the least tapered implant (0.001654ϵ ; Fig. 6, a), while the strain distribution in the cancellous bone in the extracted models followed the stress/strain patterns along the implant surface and the cortical bone, with the highest von-Mises strain value being generated around the apical part of the most tapered implant (0.007120ϵ ; Fig. 6, b).

In the healed models, reducing the tapering angle from 14° to 2° decreased both the maximum von-Mises stress at the oral implant and the maximum von-Mises strain at the cortical bone around the implant by 50.7% and 32.2% respectively. Alternatively, the value of maximum von-Mises strain at the cancellous bone decreased by 54.2% by increasing the tapering angle to 14° (Fig. 7, a). In the extracted models, the reduction in maximum von-Mises stress at the implant was less with only 39.1% reduction as the implant taper angle decreased to 2° , whereas the strain values along cortical and cancellous bone were reduced by 68.9% and 55.2% respectively (Fig. 7, b). Thus, the degree of implant tapering may have more influence on the strain patterns along the simulated extracted sockets than the healed sites. The plotting of the maximum von-Mises stress values at the implant threads for each model showed that the maximum values were more located in the coronal parallel-sided part of the implant. The first three threads of the tapered implants in the healed models IV and V showed a considerably higher stress values than the rest of the implant threads (Fig. 8, a). A similar pattern was observed in the extracted models. However, the difference between the stress values along the threads was small with more gradual change between the coronal and apical (Fig. 8, b).

Discussion

The current FE study estimated the influence of different tapering angles on the stress/strain profiles of immediately loaded wide-diameter implants and the simulated bone models that represented either a healed or a fresh molar extraction socket. FE analysis was carried out to examine the optimal implant tapering angle that can provide a beneficial and uniform stress/strain distribution at the bone-implant interface. The von-Mises values were used in

calculating the stresses and strains in both the bone and the implant models, which is often the most commonly reported in FE studies as it summarizes the overall stress profile at a point.^{39,40}

This study demonstrated that increasing the degree of implant taper can result in higher stress/strain values in an immediate loading scenario in both healed and extracted molar models.

The only exception was the cancellous bone in the healed sites in which increasing the implant taper angle reduced the strain values. As the implant tapering increased in the healed models, the area of maximum von-Mises stress is more concentrated at the parallel coronal part of the implant particularly at the implant-abutment interface and the strain values are more coronally shifted towards the adjacent cortical bone. It is worth to note that the anatomical shape of the extracted molar sockets may not allow uniform contact between the tapered implant body and the bony socket walls. Thus, the maximum contacts were observed at the most coronal part and around the apical part of the oral implant. This explains the stress/strain distribution patterns at the implant, cortical and cancellous regions in the extracted models.

The results of the current analysis suggest that a tapering angle of 2° can provide a significantly lower strain level at the cortical and cancellous bone in the extraction site indicating a better biomechanical behaviour of minimally tapered implants inserted in molar extraction sockets (Fig. 7, a), while in the healed socket, a tapering angle of 8° can result in more favourable strain distribution in both cortical and cancellous bone (Fig. 7, b). The high stress/strain patterns caused by use of high tapered implants can be attributed to the increased wedging effect that may ultimately lead to micro-cracks and bone damage.⁴¹ The use of a relatively small tapered angle ($\leq 108^\circ$) may direct the maximum stress levels away from the abutment-implant interface, which is the most susceptible area to loading as excessive loading forces can cause joint opening, and thus jeopardizing implant survival regardless of the implant diameter.⁴²

Although an optimal implant taper angle under immediate loading condition has not been proposed in the literature, Previous FE studies^{27,43} have investigated the effect of implant taper in models where complete osseointegration and fully bonded bone-implant interface were assumed.

Petrie and Williams²⁷ created 16 FE models to examine the influence of three implant parameters (implant diameter, length and taper). The implant tapering angles employed in the models ranged from 0 - 14° . The authors predicted that wide, long and non-tapered implants can provide the most favourable strain patterns at the peri-implant crestal bone. Siegele and Soltesz⁴³ evaluated four implant shapes (cylindrical, tapered, screw and conical). The FE analysis suggested that conical or tapered implant design produced higher crestal stresses than the cylindrical one. Likewise, this study showed that implants with small tapered angles have also offered a favourable stress distribution along the implant threads and reduced displacement of the surrounding bone in an immediate placement loading scenario. It has been suggested that wide implants increase the contacted surfaces

between implant and adjacent bone and thus minimize the micromovements and enhance the implant stability.

Nevertheless, wide-diameter tapered implants are not necessarily the optimal choice in certain anatomical sites such as molar extraction sockets, where bone may be damaged due to the high degree of compression that take place on the buccal strut during insertion and subsequent immediate loading. This is evident in the high insertion torque generated as tapered implants engage the cortical bone layer. The resultant compressive forces may lead to osseous necrosis and bone resorption limited to the cortical bone layer.^{21,22}

The FE analyses have been extensively used to assist both researchers and clinicians in modifying implant designs and solving complicated problems. However, there are several limitations of the FE study that need to be acknowledged: (1) Homogenous and isotropic material properties were assumed. (2) The complicated geometry of implant and bone was difficult to be accurately modelled. Hence an arbitrary model was created based on actual dimensions of mandibular bone cross-section. (3) The study was limited to one tapering design in which the implant had a coronal non-tapered part and an apical tapered part with different tapering angles. There was no attempt to study an opposite geometry of a coronally tapered implant with parallel-sided apical part. (4) The effect of implant tapering angle in immediate protocols was analysed independently of other factors (i.e. bone quality, implant length and diameter). Nevertheless it provided more insight analysis on a particular design parameter in an immediate loading model. (5) A time-dependent model⁴⁴ of immediate loading was not considered. The current FE analysis, however, offered several advantages including the use of three-dimensional FE models instead of two-dimensional models to represent two common modalities of implant placement (extracted *versus* healed sites) and the adoption of non-linear contact analysis to simulate the

complicated relationship between the prepared osteotomy and the oral implant under immediate loading.

Conclusions

Despite the limitations due to the assumptions used in the FE models, the following clinically relevant conclusions can still be drawn from this analysis:

- The von-Mises strains caused by immediate loading of immediately placed wide tapered implants were mainly concentrated in the cortical buccal strut around the implant neck where bone is at high risk of resorption.
- An approximately 8° and less tapered implants may provide the most favourable choice in the healed molar sites in terms of minimizing stresses around the implant neck and strains in the peri-implant alveolar bone.
- An implant taper angle of 2° allowed the maximum anatomical contact between the implant threads and the molar extraction socket walls and showed the lowest stress and strain levels among all tapered implant designs.
- In immediate implant placement, tapered implant was designed to duplicate the shape of natural single rooted anterior tooth. However, a strongly tapered implant may not be biomechanically advantageous in multi-rooted extraction socket even when a wide diameter is considered. Therefore, it would seem advisable to avoid the use of strongly tapered implants for immediate placement/loading in molar sites.
- Further studies are still needed to evaluate other implant geometries that allow even and

minimal stress/strain distribution along the implant surface and adjacent bone in different implant placement and loading protocols.

Conflict of interest

None.

References

1. Hammerle CH, Chen ST, Wilson TG, Jr. Consensus statements and recommended clinical procedures regarding the placement of implants in extraction sockets. *Int J Oral Maxillofac Implants* 2004;19 Suppl:26-8.
2. Atieh MA, Atieh AH, Payne AG, Duncan WJ. Immediate loading with single implant crowns: a systematic review and meta-analysis. *Int J Prosthodont* 2009;22(4):378-87.
3. Atieh MA, Payne AG, Duncan WJ, Cullinan MP. Immediate restoration/loading of immediately placed single implants: is it an effective bimodal approach? *Clin Oral Implants Res* 2009;20(7):645-59.
4. Cochran DL, Morton D, Weber HP. Consensus statements and recommended clinical procedures regarding loading protocols for endosseous dental implants. *Int J Oral Maxillofac Implants* 2004;19 Suppl:109-13.
5. Schnitman PA, Wohrle PS, Rubenstein JE, DaSilva JD, Wang NH. Ten-year results for Branemark implants immediately loaded with fixed prostheses at implant placement. *Int J Oral Maxillofac Implants* 1997;12(4):495-503.
6. Chiapasco M, Gatti C, Rossi E, Haefliger W, Markwalder TH. Implant-retained mandibular overdentures with immediate loading. A retrospective multicenter study on 226 consecutive cases. *Clin Oral Implants Res* 1997;8(1):48-57.
7. Kan JY, Rungcharassaeng K, Liddelw G, Henry P, Goodacre CJ. Periimplant tissue response following immediate provisional restoration of scalloped implants in the esthetic

zone: a one-year pilot prospective multicenter study. *J Prosthet Dent* 2007;97(6 Suppl):S109-18.

8. Andersen E, Haanaes HR, Knutsen BM. Immediate loading of single-tooth ITI implants in the anterior maxilla: a prospective 5-year pilot study. *Clin Oral Implants Res* 2002;13(3):281-7.

9. Drago CJ, Lazzara RJ. Immediate provisional restoration of Osseotite implants: a clinical report of 18-month results. *Int J Oral Maxillofac Implants* 2004;19(4):534-41.

10. Degidi M, Piattelli A. Immediate functional and non-functional loading of dental implants: a 2- to 60-month follow-up study of 646 titanium implants. *J Periodontol* 2003;74(2):225-41.

11. Ribeiro FS, Pontes AE, Marcantonio E, Piattelli A, Neto RJ, Marcantonio E, Jr. Success rate of immediate nonfunctional loaded single-tooth implants: immediate versus delayed implantation. *Implant Dent* 2008;17(1):109-17.

12. Meredith N. Assessment of implant stability as a prognostic determinant. *Int J Prosthodont* 1998;11(5):491-501.

13. Schulte W. [Tubingen implant made of Frialit: 5 years of experience]. *Dtsch Zahnarztl Z* 1981;36(9):544-50.

14. d'Hoedt B, Lukas D, Schulte W. [The Tubingen implant as immediate and late implant, a statistical comparison]. *Dtsch Zahnarztl Z* 1986;41(10):1068-72. 15. Pilliar RM, Deporter DA, Watson PA, Valiquette N. Dental implant design--effect on bone remodeling. *J Biomed Mater Res* 1991;25(4):467-83.

16. Shapoff CA. Clinical advantages of tapered root form dental implants. *Compend Contin Educ Dent* 2002;23(1):42-4, 46, 48 passim.

17. Garber DA, Salama H, Salama MA. Two-stage versus one-stage--is there really a controversy? *J Periodontol* 2001;72(3):417-21.

18. Misch CE. Density of bone: effect on treatment plans, surgical approach, healing, and progressive boen loading. *Int J Oral Implantol* 1990;6(2):23-31.
19. Martinez H, Davarpanah M, Missika P, Celletti R, Lazzara R. Optimal implant stabilization in low density bone. *Clin Oral Implants Res* 2001;12(5):423-32.
20. Ivanoff CJ, Sennerby L, Johansson C, Rangert B, Lekholm U. Influence of implant diameters on the integration of screw implants. An experimental study in rabbits. *Int J Oral Maxillofac Surg* 1997;26(2):141-8.
21. Bashutski JD, D'Silva NJ, Wang HL. Implant compression necrosis: current understanding and case report. *Journal of Periodontology* 2009;80(4):700-4.
22. Piattelli A, Scarano A, Balleri P, Favero GA. Clinical and histologic evaluation of an active "implant periapical lesion": a case report. *The International journal of oral & maxillofacial implants* 1998;13(5):713-6.
23. Simmons CA, Meguid SA, Pilliar RM. Mechanical regulation of localized and appositional bone formation around bone-interfacing implants. *J Biomed Mater Res* 2001;55(1):63-71.
24. Meyer U, Joos U, Mythili J, Stamm T, Hohoff A, Fillies T, Stratmann U, Wiesmann HP. Ultrastructural characterization of the implant/bone interface of immediately loaded dental implants. *Biomaterials* 2004;25(10):1959-67.
25. Degidi M, Scarano A, Piattelli M, Perrotti V, Piattelli A. Bone remodeling in immediately loaded and unloaded titanium dental implants: a histologic and histomorphometric study in humans. *J Oral Implantol* 2005;31(1):18-24.
26. Anitua E, Tapia R, Luzuriaga F, Orive G. Influence of implant length, diameter, and geometry on stress distribution: a finite element analysis. *Int J Periodontics Restorative Dent* 2010;30(1):89-95.

27. Petrie CS, Williams JL. Comparative evaluation of implant designs: influence of diameter, length, and taper on strains in the alveolar crest. A three-dimensional finite element analysis. *Clin Oral Implants Res* 2005;16(4):486-94.
28. Himmlova L, Dostalova T, Kacovsky A, Konvickova S. Influence of implant length and diameter on stress distribution: a finite element analysis. *J Prosthet Dent* 2004;91(1):20-5.
29. Schwartz-Dabney CL, Dechow PC. Edentulation alters material properties of cortical bone in the human mandible. *J Dent Res* 2002;81(9):613-7.
30. Brunski JB. Biomechanical factors affecting the bone-dental implant interface. *Clin Mater* 1992;10(3):153-201.
31. Simsek B, Erkmen E, Yilmaz D, Eser A. Effects of different inter-implant distances on the stress distribution around endosseous implants in posterior mandible: a 3D finite element analysis. *Med Eng Phys* 2006;28(3):199-213.
32. Hojjatie B, Anusavice KJ. Three-dimensional finite element analysis of glass-ceramic dental crowns. *J Biomech* 1990;23(11):1157-66.
33. Albakry M, Guazzato M, Swain MV. Biaxial flexural strength, elastic moduli, and x-ray diffraction characterization of three pressable all-ceramic materials. *J Prosthet Dent* 2003;89(4):374-80.
34. Ciftci Y, Canay S. The effect of veneering materials on stress distribution in implantsupported fixed prosthetic restorations. *Int J Oral Maxillofac Implants* 2000;15(4):571-82.
35. Rubin PJ, Rakotomanana RL, Leyvraz PF, Zysset PK, Curnier A, Heegaard JH. Frictional interface micromotions and anisotropic stress distribution in a femoral total hip component. *J Biomech* 1993;26(6):725-39.

36. Alkan I, Sertgoz A, Ekici B. Influence of occlusal forces on stress distribution in preloaded dental implant screws. *J Prosthet Dent* 2004;91(4):319-25.
37. Viceconti M, Muccini R, Bernakiewicz M, Baleani M, Cristofolini L. Large-sliding contact elements accurately predict levels of bone-implant micromotion relevant to osseointegration. *J Biomech* 2000;33(12):1611-8.
38. Mericske-Stern R, Assal P, Mericske E, Burgin W. Occlusal force and oral tactile sensibility measured in partially edentulous patients with ITI implants. *Int J Oral Maxillofac Implants* 1995;10(3):345-53.
39. Papavasiliou G, Kamposiora P, Bayne SC, Felton DA. Three-dimensional finite element analysis of stress-distribution around single tooth implants as a function of bony support, prosthesis type, and loading during function. *J Prosthet Dent* 1996;76(6):633-40.
40. Holmes DC, Loftus JT. Influence of bone quality on stress distribution for endosseous implants. *J Oral Implantol* 1997;23(3):104-11.
41. O'Sullivan D, Sennerby L, Meredith N. Influence of implant taper on the primary and secondary stability of osseointegrated titanium implants. *Clin Oral Implants Res* 2004;15(4):474-80.
42. Hoyer SA, Stanford CM, Buranadham S, Fridrich T, Wagner J, Gratton D. Dynamic fatigue properties of the dental implant-abutment interface: joint opening in wide diameter versus standard-diameter hex-type implants. *J Prosthet Dent* 2001;85(6):599-607.
43. Siegele D, Soltesz U. Numerical investigations of the influence of implant shape on stress distribution in the jaw bone. *Int J Oral Maxillofac Implants* 1989;4(4):333-40.
44. Winter W, Heckmann SM, Weber HP. A time-dependent healing function for immediate loaded implants. *J Biomech* 2004;37(12):1861-7.

Table 1 Mechanical parameters of materials used in the finite element model^{35,36}

Material	Young's modulus (MPa)	Poisson's ratio (ν)
Cortical bone	13800	0.30
Cancellous bone	1380	0.30
Titanium	110000	0.35
Lithium disilicate glass ceramic	91000	0.23

Table 2 Maximum von-Mises stress/strain values on the implant and surrounding bone in the finite element model

Model	Maximum von-Mises stress on implant (MPa)	Maximum von-Mises strain in cortical bone	Maximum von-Mises strain in cancellous bone
<u>Healed site</u>			
Model I-h	9.9	0.0002497	0.001654
Model II-h	10.6	0.0002607	0.001346
Model III-h	11.7	0.0002610	0.0009558
Model IV-h	16.0	0.0003558	0.0008971
Model V-h	20.1	0.0003679	0.0007445
<u>Extraction site</u>			
Model I-e	21.5	0.001052	0.003190
Model II-e	22.3	0.001371	0.003291
Model III-e	28.2	0.002203	0.004237
Model IV-e	33.6	0.002715	0.004677
Model V-e	35.3	0.003383	0.007120

Fig. 1 Time frame of different implant placement and loading protocols³

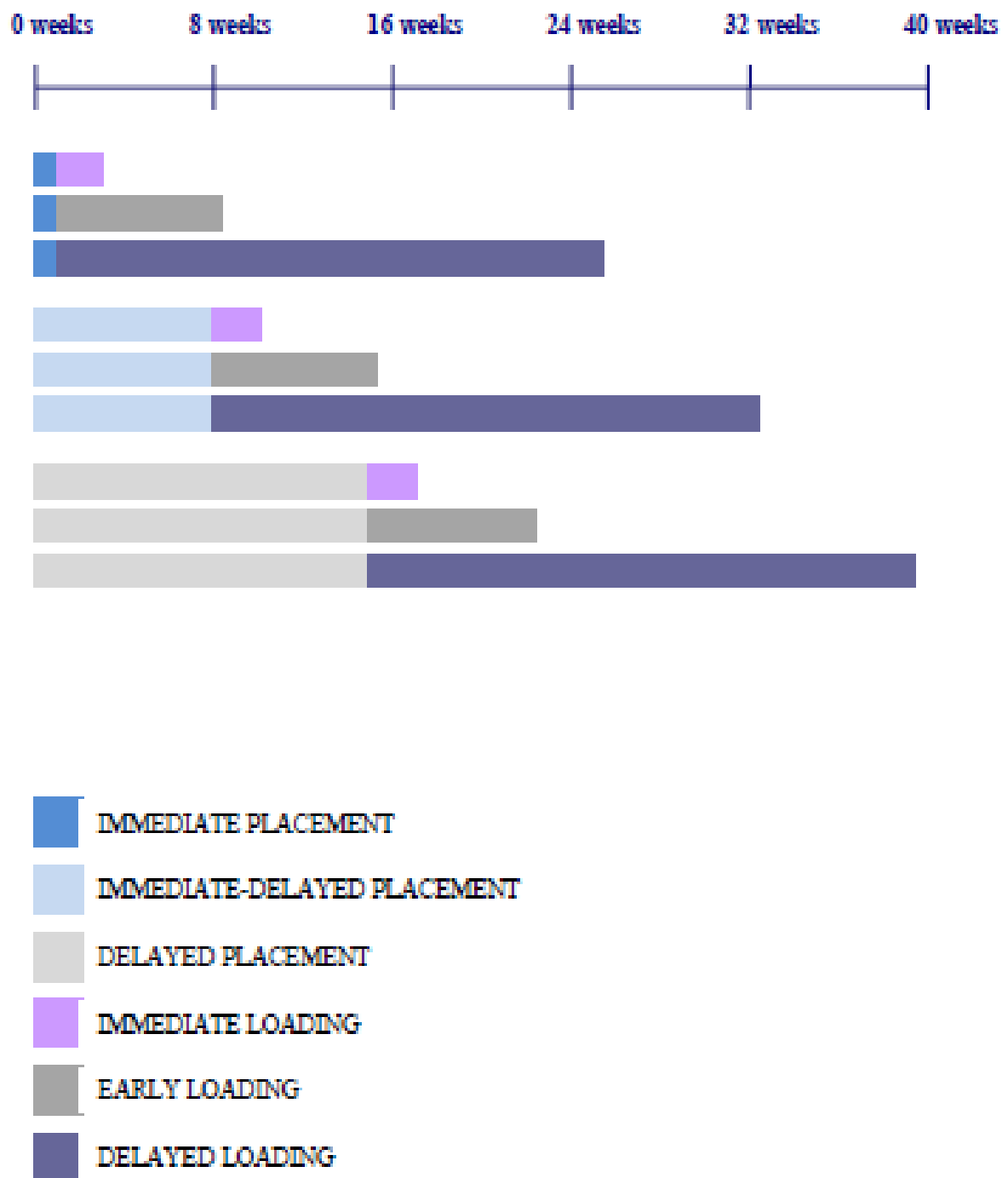


Fig. 2 Geometry of the tapered implant models (I-V)

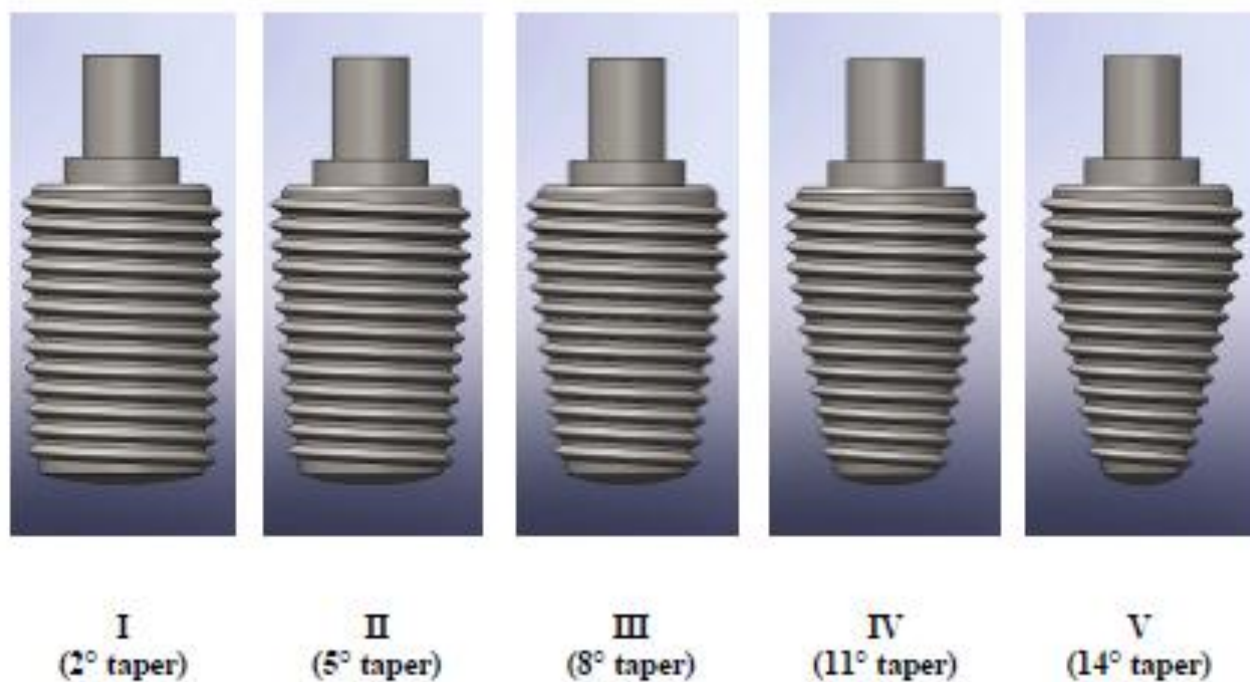


Fig. 3 Implant-bone model under loading force of 189.5 N



(b) Extracted models

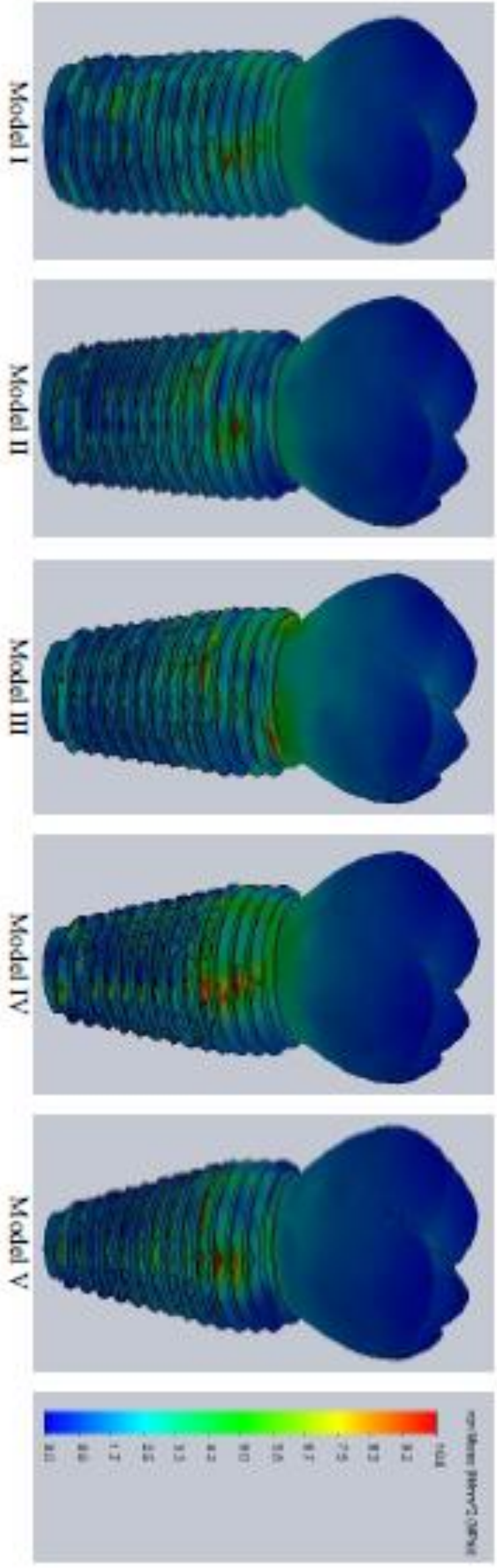


Fig. 4 von-Mises stress distribution on wide-diameter implants at different implant tapering angles

(a) Healed models

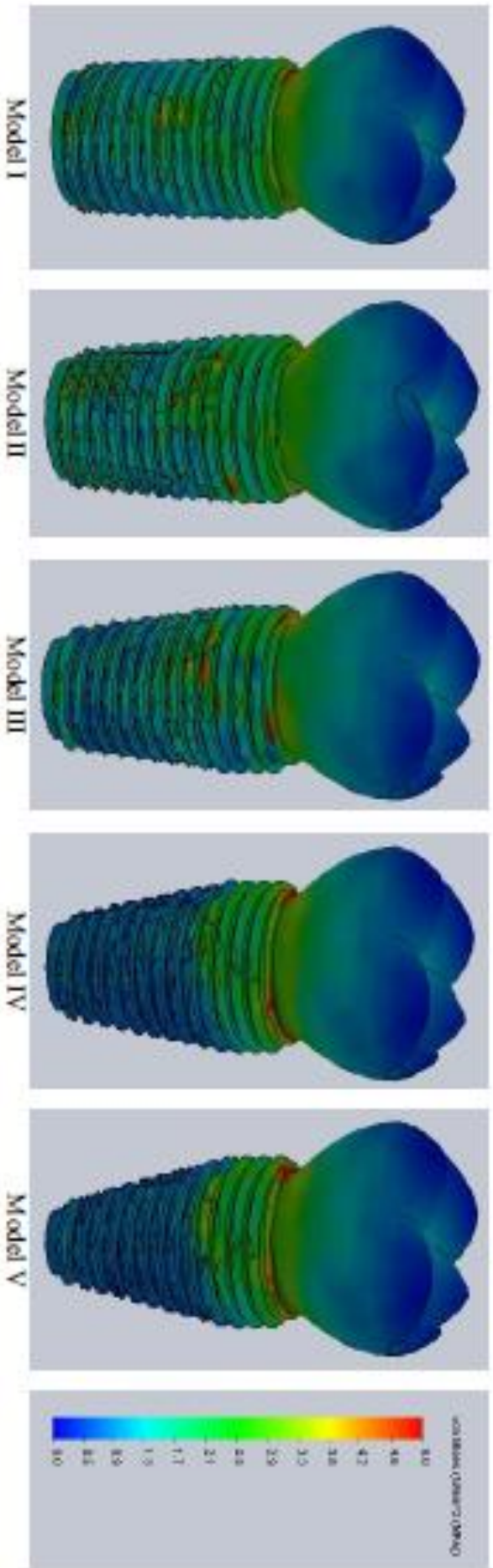
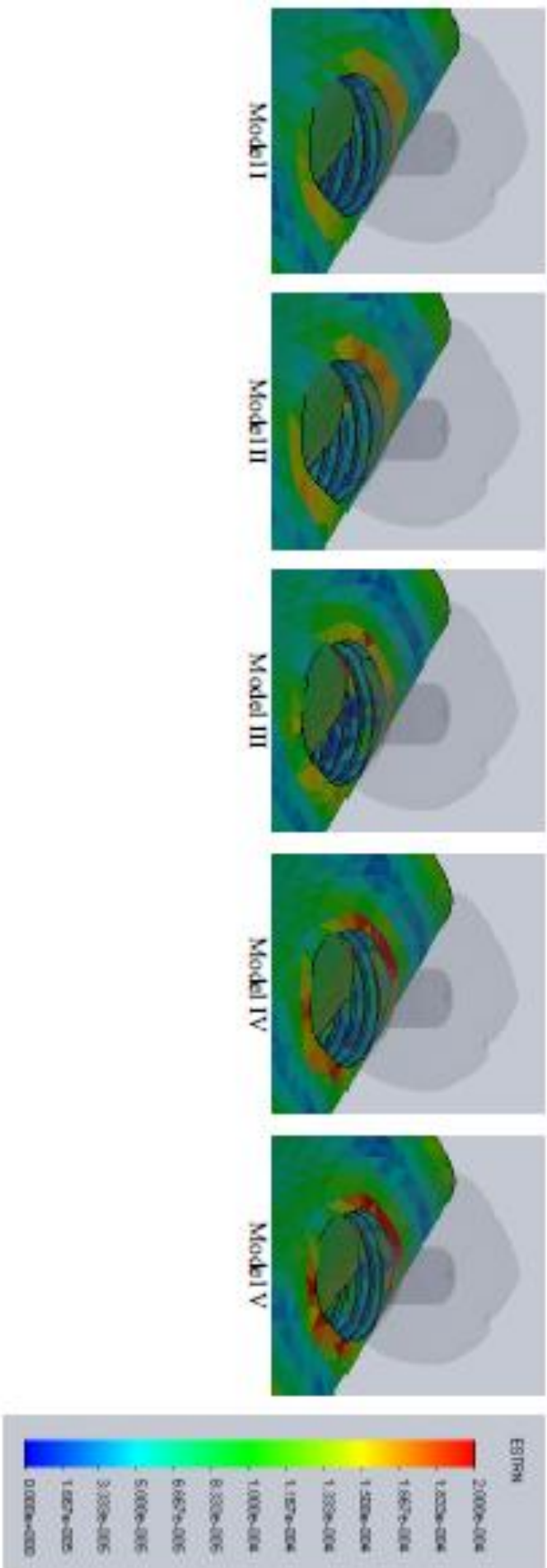


Fig. 5 von-Mises strain distribution on the cortical bone around the implant neck at different implant tapering angles

(a) Healed models



(b) Extracted models

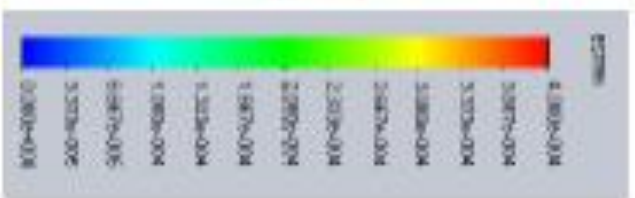
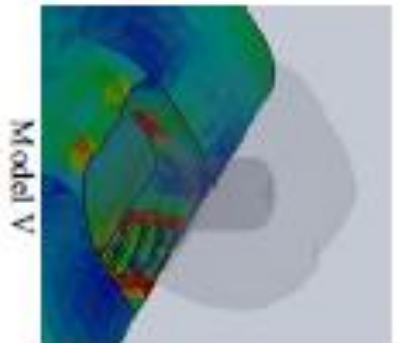
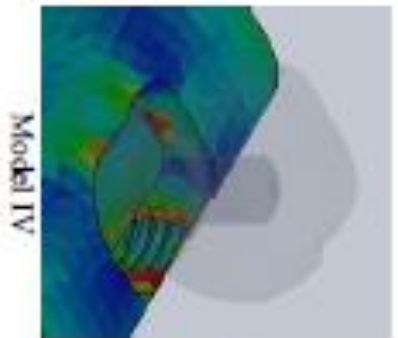
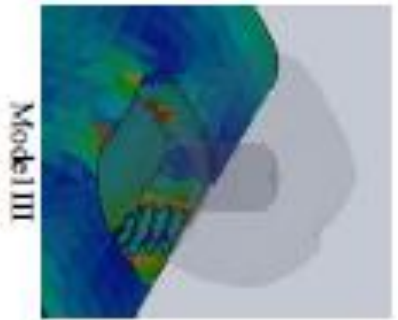
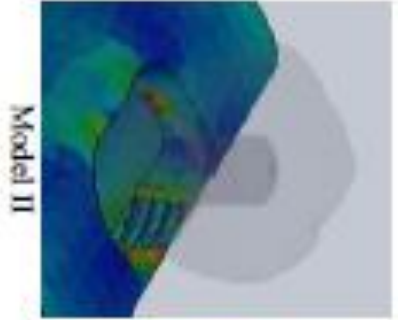
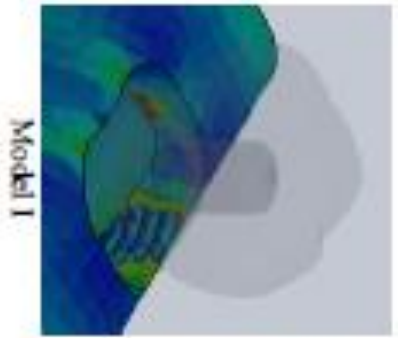
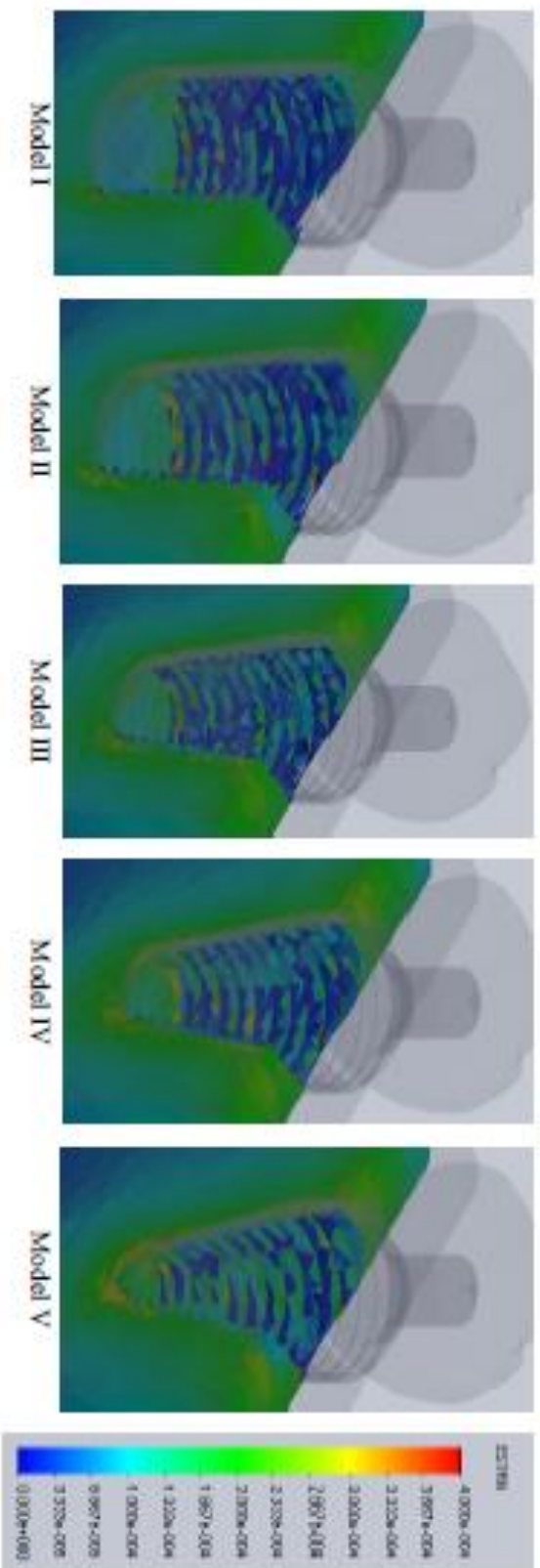


Fig. 6 von-Mises strain distribution on the cancellous bone at different implant tapering angles

(a) Healed models



(b) Extracted models

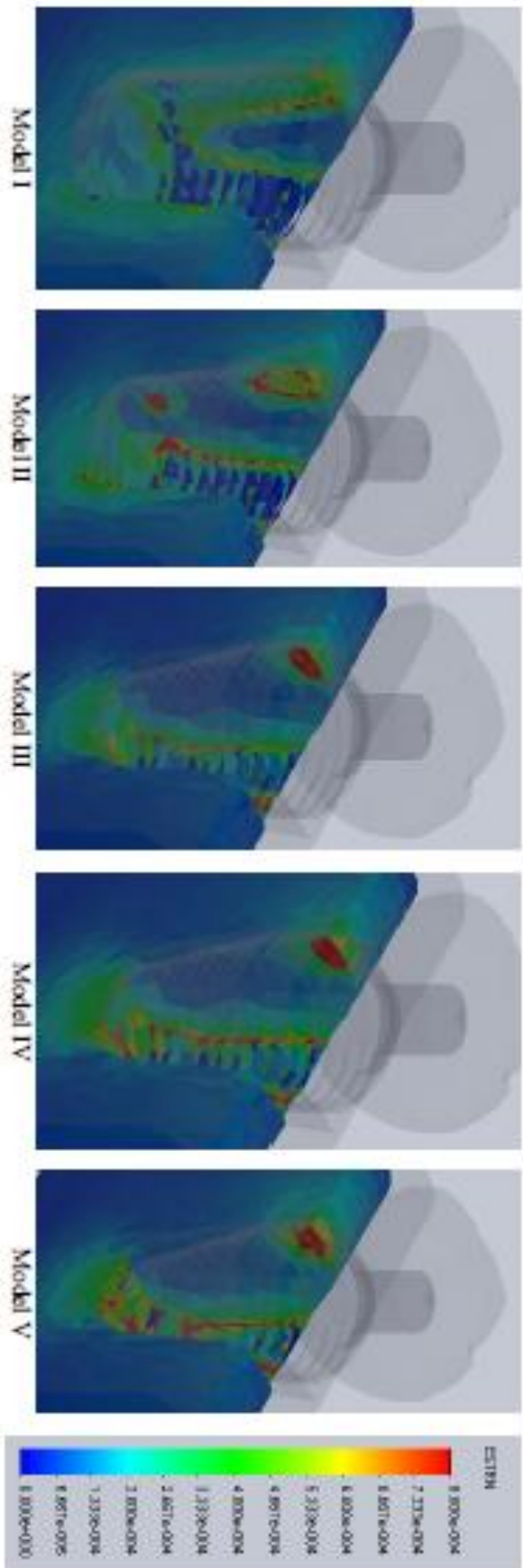
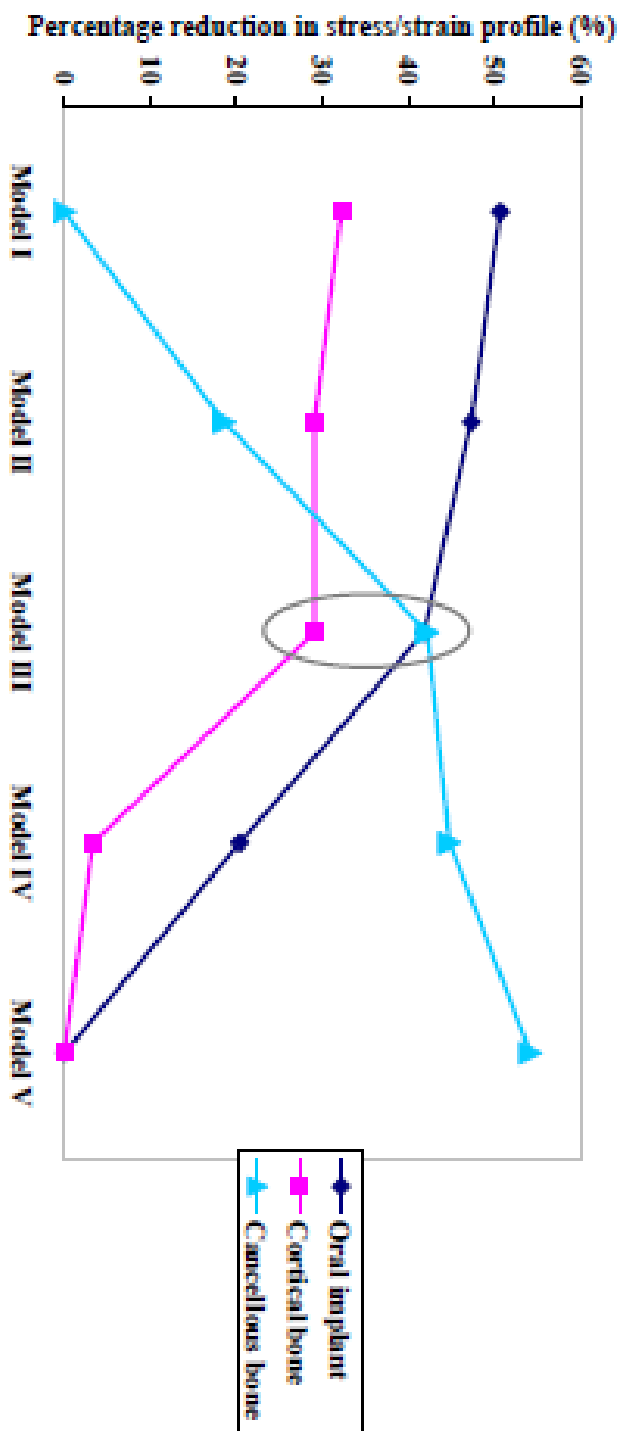


Fig. 7 The percentage decrease in the stress / strain profile caused by different tapered implant designs

(a) Healed models



(b) Extracted models

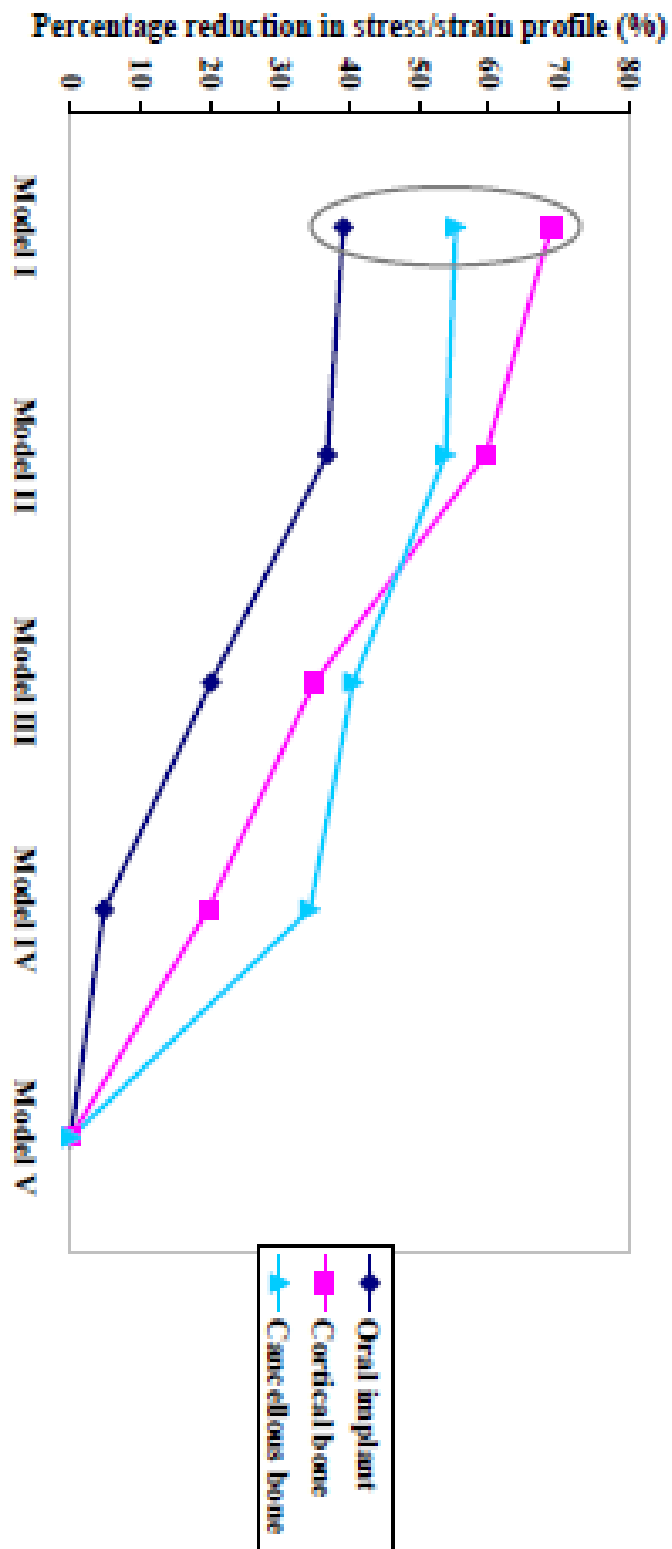
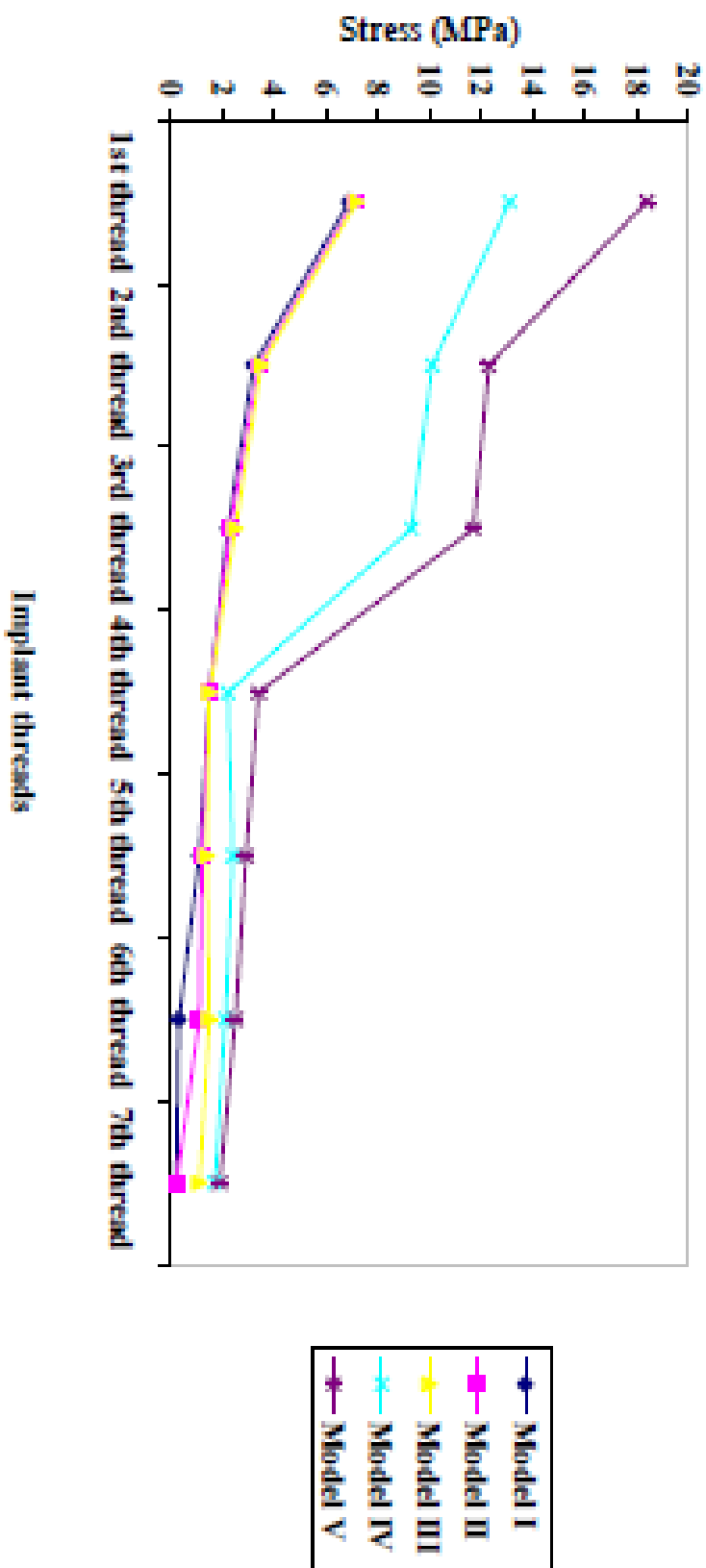
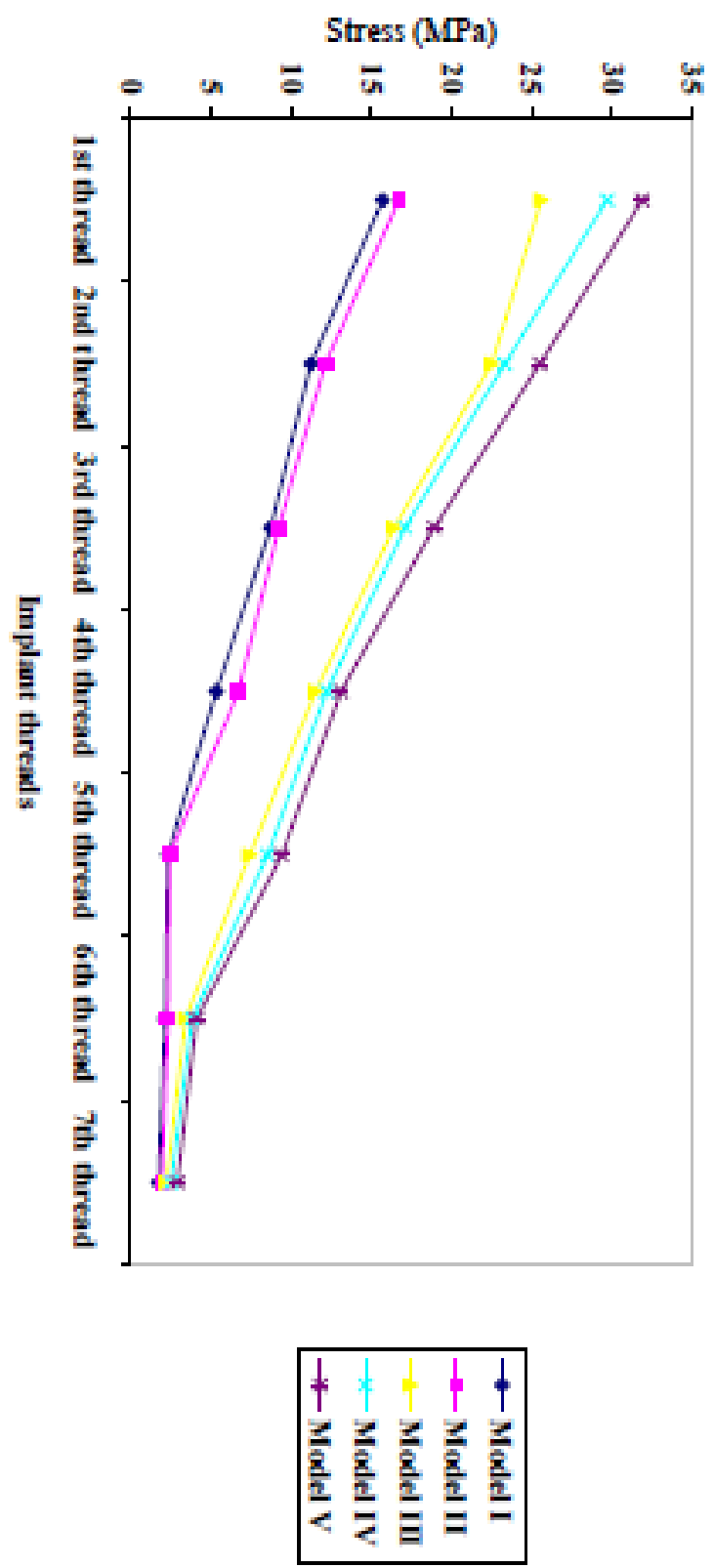


Fig. 8 Influence of implant taper angle on the von-Mises stress distribution along the oral implant threads

(a) Healed models



(b) Extracted models



Micro-strain value of all strain gauges

	G8-BL	G6-BL	G7-MD	G5-MD	G11-MDI	G4-MDI	G12-BLI	G3-BLI	G9-MDI	G2-MDI	G10-BLI	G1-BLI
Bi-U-Acrylic	-25.4	11.5	-21	-28.8	72.8	34.6	138.2	83.1	6.2	4.2	281.5	74
	-24.9	3.2	-14.5	-10.3		37.6	138.3	72.2	2.7	5	245.1	51.6
	-22.6	6.6	-13.1	-20.4	75.9	35.7	140.7	75.5	3.8	10.5	247.9	50.8
	-27.7	12.1	-23.6	-6.4	69.6	28.4	142.6	74.9	-3.3	4.6	248.8	49.6
Ave	-25.2	8.4	-22.6	-16.5	74.5	28.1	140	61.7	2.4	5.3	255.8	45.4
SD	2.09	4.23	6.87	10.1	4.36	3.98	2.11	4.68	4.04	2.76	15.19	11.7
Bi-M-Acrylic												
	152.7	88.8	-2.4	-13.3	55.5	12.2	80	50.6	31.4	42.3	176.5	23.5

Appendix 4

	150.7	89.3	-2.2	-14.4	59.1	14.1	77.3	52.7	28.3	43.5	175.1	27.9
	142.3	88	-1.5	-12.1	61.1	15.7	75.9	50.1	34.4	47.5	172.6	25.7
	147.9	87.7	-1.9	-12.8	59.4	14.5	74.6	51.4	30.8	41.3	173.5	25
Ave	148.4	88.5	-2	-13.2	58.8	14.1	77	51.2	31.2	43.7	174.4	25.5
SD	4.51	0.73	0.39	2.51	4.52	39	2.31	97	145	1.13	2.72	1.83
Bi-P- Acrylic												
	228.2	129.3	4.5	-18.1	42.3	9.6	52.4	47.7	12.6	20.6	129.5	29.5
	229.3	127.4	5.7	-13.9	48.5	7	49.5	54.2	15.8	21.2	132.3	27.6
	227.1	127.7	6.5	-13.3	43.4	12.1	51.5	46	15.6	22.8	132.4	30
	230	127	9.1	-13.5	50.1	7.5	51.4	51.3	13.2	18.9	134.4	28.6

Ave	228.7	127.9	6.5	-14.7	46.1	9.05	51.2	49.8	14.3	20.9	132.2	28.6
SD	1.27	1.01	1.95	2.28	3.81	2.32	1.22	3.67	1.64	1.61	2.01	1.06
<i>Bi-U-Metal</i>												
	57.3	107.9	13.4	-47	0.2	-8.3	-59.9	23	1.7	-7.8	16.3	9
	62.7	110.6	13.7	-46.2	0.4	-6.1	-57.6	23.3	0.7	-5.7	18.1	10
	57	107.5	10.3	-44.6	0.4	-6.2	-60	24.5	3.3	-3.7	15.4	9
	61.5	111.8	14.4	-46.7	0.5	-3.7	-65.2	22.2	1	-4.4	26.5	10.9
Ave	59.6	109.5	13	-46.1	0.4	-4.2	-60.7	23.5	1.7	-5.4	3.9	9.7
SD	2.9	2.09	1.82	1.07	0.11	1.88	2.78	0.98	1.16	1.8	1.92	0.91

Bi-M-Metal

66.8 88.1 6 -31.4 0.3 -3.3 -72.1 26.6 4.5 25 15.1 15.8

68.8 91.6 5.9 -29.9 0.1 1.3 -71.8 31.5 6 31.5 14.8 17.5

74.4 92.1 7.6 -26.9 0.2 1.9 -68.9 25.8 3.1 25.8 14.1 11.9

71 93.4 6.7 -28.3 0 2 -74.9 25 4.2 25 15 12.8

***Ave* 70.3 91.3 6.6 -29.1 0.2 2.1 -79.1 27.2 4.5 26 14.8 14.5**

***SD* 2.82 1.96 0.68 1.69 0.11 2.2 2.12 2.53 1.04 47 0.39 2.25**

Bi-P-Metal

	92.9	132.2	12.6	-32.1	-0.3	-1.6	-75.6	13.4	-0.4	-22.9	4.6	2.9
	90.2	132.3	10.9	-34	0.9	-1.1	-76.7	16.5	-1.5	-20.9	5	4.2
	95.5	138.6	12	-36.7	1.6	-2.9	-74.8	18.5	0.4	-24.5	4.8	1.1
	91.2	131	9.9	-29.9	1.8	-5.3	-79.1	15.9	1.4	-25.9	4.2	3.1
Ave	92.5	133.5	11.4	-33.2	1	-2.7	-76.6	16.1	-0.03	-23.6	4.7	2.8
SD	2.32	3.43	1.2	2.89	0.95	1.88	1.87	2.1	1.23	2.15	0.34	1.28
Uni-U-Acrylic												
		58		-12.6		35.3		93.6		50		53.4
		59.6		-5		39.1		91.5		46		53.2

	60.3	-7.9	37.8	91.2	46.8	50.9
	58.8	-7	37.6	90.3	42.5	51
Ave	59.1	-8.13	37.4	91.6	46.3	52.1
SD	0.99	3.22	1.58	1.4	3.08	1.36
Uni-M-Acrylic						
	234	-36	16.3	95.3	71.8	33.4
	233.1	-36.7	20.4	97.1	75.3	38
	232.9	-36.6	22.7	98.2	79	37.9
	238.4	-29.1	24.6	99.6	79.9	41.2

Ave	234.6	-34.6	21	97.6	76.5	37.6
SD	2.58	3.68	3.57	1.82	3.71	3.21
Uni-P-Acrylic						
	-1.7	-50.8	14.5	88.7	0.9	46.6
	-0.7	-47.1	11	86.1	1	43.2
	-1.2	-43.4	15	89.8	0.4	49.4
	-1	-43.1	13.5	86.2	0.3	47.1
Ave	-1.1	-46.1	13.6	87.7	0.65	46.5
SD	0.42	3.62	1.59	1.85	0.35	2.56

**Uni-U-
Metal**

-17.8 14.9 6.5 -11.9 -1.2 -6.6

-24.1 12.3 4 -12 -0.6 -8.3

-18.8 17.7 3.6 -10.3 -2.2 -5.6

-18.7 16.5 1.7 -7.3 1.1 -4.3

Ave -19.9 15.4 4 -10.4 0.7 -6.2

SD 2.87 2.33 1.97 2.19 1.38 1.69

**Uni-M-
Metal**

	-47.6	32.4	5.8	-22.2	7.8	-3.5
	-45.4	33.9	7.6	-19.7	6.2	-2.3
	-48.8	30.5	7.2	-21	7.4	-3.5
	-46.4	32.8	4.4	-23.2	6.6	-3.3
Ave	-47.1	32.4	6.3	-21.5	7	-3.2
SD	1.47	1.42	1.45	1.51	0.73	0.57
Uni-P-Metal						
	-55.5	37.8	9.3	-32.4	11.1	-3.5
	-56.7	44.8	9.4	-33.9	11.9	-2.1
	-56.3	47.8	10.3	-32.6	11	-1.7

	-57.5	43.4	9.2	-29.7	12.4	-1.1
Ave	-56.5	43.4	9.05	-32.1	11.6	-2.1
SD	0.83	4.9	0.51	1.76	0.67	1.02